

LIBRARY  
CALIFORNIA AIR RESOURCES BOA  
P. O. BOX 2815  
Sacramento, CA 95812

A STUDY OF NITRATE AIR QUALITY  
IN THE SOUTH COAST AIR BASIN

by

Glen R. Cass  
Gregory J. McRae  
Armistead G. Russell  
John H. Seinfeld  
Arthur W. Stelson

with

Shohreh Gharib  
Mary Peterson  
James W. Tilden

EQL Open File Report 83-2

July 30, 1983

Environmental Quality Laboratory  
California Institute of Technology  
Pasadena, California 91125

TD 883.5  
C2  
C377  
1983

Final Report to the

STATE OF CALIFORNIA  
AIR RESOURCES BOARD

in

completion of research under  
ARB Contract No. A7-169-30

#### Disclaimer

The statements and conclusions in this report are those of the authors and not necessarily those of the California Air Resources Board. The mention of commercial products, their source or their use in connection with material reported herein is not to be construed as either an actual or implied endorsement of such products.

## TABLE OF CONTENTS

ABSTRACT		
TABLE OF CONTENTS		iii
LIST OF FIGURES		iv
LIST OF TABLES		vii
CHAPTER I	Executive Summary	1
CHAPTER II	Relative Humidity and Temperature Dependence of the Ammonium Nitrate Dissociation Constant	8
CHAPTER III	Relative Humidity and pH Dependence of the Vapor Pressure of Ammonium Nitrate-Nitric Acid Solutions at 25°C	19
CHAPTER IV	Mathematical Modeling of the Formation and Transport of Ammonium Nitrate Aerosol	28
APPENDIX A	The Origin of Ammonia Emissions to the Atmosphere in an Urban Area	45
APPENDIX B	Chemical Mass Accounting of Urban Aerosol	90

## LIST OF FIGURES

CHAPTER	NUMBER		PAGE
I	1	$\text{NH}_4\text{NO}_3$ Dissociation Constant Temperature and Relative Humidity Dependence	4
	2	Concentration Profiles at El Monte on 28 June 1974.	7
II	1	$\text{NH}_4\text{NO}_3$ Relative Humidity of Deliquescence Temperature	11
	2	$\text{NH}_4\text{NO}_3$ Solubility Temperature Dependence	11
	3	$\text{NH}_4\text{NO}_3$ Dissociation Constant Temperature and Relative Humidity Dependence	13
	4	Temperature and Concentration Dependence of $\text{NH}_4\text{NO}_3$ Solution Relative Humidity	14
	5	Experimental Diurnal $\text{NH}_3$ - $\text{HNO}_3$ Product and Aerosol Nitrate Trends at Pittsburgh, CA	15
	6	Experimental Relative Humidity and Temperature Dependence of the $\text{NH}_3$ - $\text{HNO}_3$ Product at Claremont, CA	16
	7	Diurnal $\text{NH}_3$ - $\text{HNO}_3$ Product Trend Calculated from FT-IR Measurements at Riverside, CA	16
III	1	Molar Ammonium and Nitrate Losses from High Volume Gas Fiber Filters Stored at Room Temperature	20
	2	Effect of Relative Humidity on Ammonia-Nitric Acid Partial Pressure Product	22
	3	Ionization of Nitric Acid	23
	4	Effect of pH on the Ammonia and Nitric Acid Partial Pressures	24
	5	Effect of Ionic Strength on Calculated Ammonium/Hydrogen Ion Mean Molal Activity Coefficient Ratio	25
IV	1	Schematic Representation of (a) Vertically Resolved Lagrangian Trajectory Model and (b) the Computational Grid Cell Convention	30
	2	(a) $\text{NH}_4\text{NO}_3$ Equilibrium Dissociation Constant as a Function of Temperature (Relative Humidity 50%) and (b) $\text{NH}_4\text{NO}_3$ Equilibrium Dissociation Constant as a Function of Relative Humidity (Temperature 25%)	31

## LIST OF FIGURES (continued)

3	Flow Diagram of $\text{NH}_4\text{NO}_3$ Formation Mechanism Illustrating Three Basic Steps in Calculation Procedure	32
4	Predicted Ammonium Nitrate Concentration Surfaces at 15, 25 and 35°C and 45, 65 and 85% RH for Total Ammonia and Total Nitric Acid Concentrations up to 20 and 40 ppb, Respectively	34
5	Gridded Map of the South Coast Air Basin Used for Constructing Ammonia Emissions Inventory. Superimposed on the Map is the Trajectory Path that Reaches El Monte at 3pm (PDT) on 28 June 1974	34
6	Spatial Representation of Daily Emissions of Ammonia ( $\text{NH}_3$ ), Nitrogen Oxides ( $\text{NO}_x$ ), Reactive Hydrocarbons (RHC) and Carbon Monoxide (CO) in the South Coast Air Basin (Inventory Period June 1974)	37
7	Concentration Profiles at El Monte on 28 June 1974	38
8	Predicted Concentrations and Observed Meteorological Variables for the Air Parcel Reaching El Monte at 2pm (PDT) 28 June 1974	41
9	Evolution of Vertical Concentration Profiles of $\text{NH}_3$ , $\text{HNO}_3$ and $\text{NH}_4\text{NO}_3$ in the Air Parcel that Reaches El Monte at 2pm (PDT) 28 June 1974.	42
APPENDIX A		
1	The South Coast Air Basin Showing the Grid System Used	49
2	The Spatial Distribution of Ammonia Emissions in the South Coast Air Basin - 1974	50
APPENDIX B		
1	Time-Averaged Normalized Aerosol Volume Distributions and Sampler Upper Effective Size Limit	93
2	Relation Between Aerosol Carbon and Aerosol Lead	95
3	Relation Between Aerosol Carbonaceous Material and Aerosol Lead	95
4	Measured Nitrate vs Calculated Nitrate	95

## LIST OF FIGURES (continued)

5	Water Activities for Typical Electrolytes as a Function of Ionic Strength	97
6	Aerosol Water vs. Electrolyte Concentration	97
7	Filtration Efficiencies for Whatman 41, Gelman A, and Gelman GA-1	98

## LIST OF TABLES

NUMBER		PAGE
CHAPTER II		
1	Thermodynamic Data for the Ammonium Nitrate System at 298 K	10
CHAPTER III		
1	Free Energy Data for the $\text{NH}_3\text{-HNO}_3\text{-H}_2\text{O}$ System at 298 K	21
2	Equilibrium Constants for the $\text{NH}_3\text{-HNO}_3\text{-H}_2\text{O}$ System at 298 K	21
CHAPTER IV		
1	Sensitivity of Ammonium Nitrate Formation Model to Input Parameters	33
2	Summary of Ammonia Emissions by Source Category in the South Coast Air Basin	35
APPENDIX A		
1	Emission Factors for Ammonia from Combustion Sources	51
2	Emission Factors for Ammonia from Highway Vehicles	59
3	Ammonia Emission Estimates for Stationary Combustion Sources	63
4	Ammonia Emission Estimates for Mobile Combustion Sources	65

## LIST OF TABLES (continued)

5	Emissions from Industrial Process Sources	66
6	Emission Factors for Ammonia Release from Soil Surface	67
7	Ammonia Estimates for Release from Soil Surfaces	68
8	Dry and Liquid Fertilizers for Farm Plus Non-Farm Use	70
9	Percentage of N Applied, Apportioned Between Farm and Non-Farm Use	71
10	Fertilizer Nitrogen Applied	72
11	Partition of Farm Fertilizer Use Between Crops and Orchards	73
12	Nitrogen Applied on Crops, Orchards, and Non-Farm Areas	74
13	Percentage of Land Use in Each County Located Within the Grided Inventory Map Area and Within the South Coast Air Basin	75
14	Fertilizer Nitrogen Applied Inside the South Coast Air Basin	76
15	Ammonia Loss Due to Fertilizer Application by County - 1974	77
16	Loss of Anhydrous Ammonia Due to Handling and Field Application	78
17	Summary of NH <sub>3</sub> Emissions from Fertilizer Application and Handling	79
18	Summary of Animal Waste Data	80
19a	1974 Livestock Inventory - Cattle	81
19b	1974 Livestock Inventory - Continued	82
19c	1974 Livestock Inventory - Continued	83
20	Fraction of Animals Located Inside South Coast Air Basin Portion of Each County	84
21	Total NH <sub>3</sub> Emissions from Livestock in the Modeling Region of the South Coast Air Basin - 1974	85
22	Emission Factors for Ammonia Loss Due to Non-Farm Animals	86

## LIST OF TABLES (continued)

23	NH <sub>3</sub> Emissions from Human and Domestic Animal Populations	87
24	Ammonia Emission Estimates for Refrigerants and Household Cleaning Chemicals	88
25	Summary of Ammonia Emissions by Source Category in the South Coast Air Basin - 1974	89
APPENDIX B		
1	ACHEX Sampling Time and Location Summary	92
2	Summary of Measured and Calculated Los Angeles Aerosol Concentrations	93
3	Aerosol Metal Oxides	93
4	Equilibrium Analysis of Hydroxide Formation	93
5	Solubility of Inorganic Salts	94
6	Calculated and Measured Total Mass ( $\mu\text{g m}^{-3}$ )	96
7	Least-Squares Analysis of Measured and Calculated Total Mass	96
8	Calculated Electrolyte-to-Water Mass Ratios and Ionic Strengths for Los Angeles Aerosol	97

CHAPTER I

EXECUTIVE SUMMARY

## Chapter I

## Executive Summary

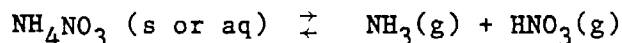
Aerosol nitrates are important contributors to the visibility reduction experienced in the Los Angeles area. This problem is particularly severe in the eastern portion of the South Coast Air Basin near the city of Riverside, where up to 40% of the light scattering observed during the ACHEX experiment was attributed to particulate nitrates.

At the beginning of the research effort reported here it was known that aerosol nitrates are formed in the atmosphere during chemical reactions involving precursor emissions of gaseous oxides of nitrogen and ammonia. The ability to closely define the cause and effect relationship between emission sources and resulting nitrate air quality was hidden by the chemical complexity of the system. The purpose of this research was to explore the feasibility of constructing a mathematical air quality model that could be used for testing control measures directed at gas phase precursor emissions for their effect on downwind aerosol nitrate air quality.

In pursuit of that objective, the chemistry of aerosol ammonium nitrate formation has been established. This description of atmospheric  $\text{NH}_4\text{NO}_3$  chemistry has been embedded within the Caltech photochemical trajectory model, and model predictions have been verified by comparison to atmospheric measurements in the Los Angeles area. In the course of this research, the sources and spatial

distribution of ammonia emissions to the atmosphere of the South Coast Air Basin have been quantified for the first time.

Field experiments suggest that ammonium nitrate, nitric acid, and ammonia are in equilibrium in the atmosphere:



The partition between gas phase and aerosol phase constituents is described by the equilibrium dissociation constant, K, where:

$$[\text{NH}_3][\text{HNO}_3] \leq K \quad (1)$$

If the concentration product of gas phase  $\text{NH}_3$  times  $\text{HNO}_3$  increases to equal K, then any further addition of  $\text{NH}_3$  or  $\text{HNO}_3$  into the air parcel will be manifested by formation of enough  $\text{NH}_4\text{NO}_3$  to reduce the gas phase concentration product of  $[\text{NH}_3][\text{HNO}_3]$  to equal the value of K. Conversely, at  $[\text{NH}_3][\text{HNO}_3]$  concentration products below the value of K, no  $\text{NH}_4\text{NO}_3$  will be formed. Given a method for calculating the value of K, it is possible to predict the amount of  $\text{NH}_4\text{NO}_3$  that will be formed from a known amount of atmospheric nitric acid and ammonia.

In Chapter II of this report, it is shown that the  $\text{NH}_4\text{NO}_3$  equilibrium dissociation constant, K, is a thermodynamic parameter that can be calculated theoretically from fundamental thermochemical data. As seen in Figure 1, the equilibrium dissociation constant K is a strong function of temperature and relative humidity, varying from circa  $10^3$  ppb<sup>2</sup> at low humidity and 40°C temperature to below  $10^{-1}$  ppb<sup>2</sup>

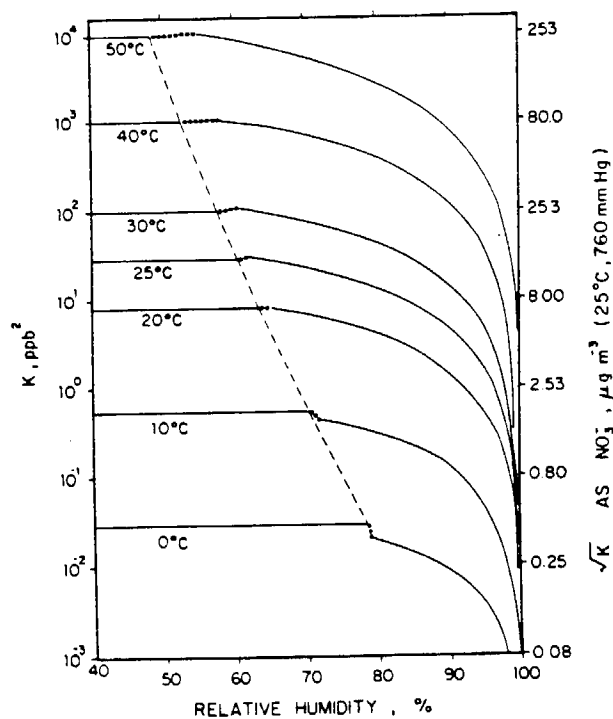


FIGURE 1

$\text{NH}_4\text{NO}_3$  dissociation constant temperature and relative humidity dependence: (---) solid  $\text{NH}_4\text{NO}_3$  to aqueous  $\text{NH}_4\text{NO}_3$  solution transition predicted from Ch. II; (—) Isothermal prediction of  $\text{NH}_4\text{NO}_3$  dissociation constant for solid  $\text{NH}_4\text{NO}_3$  and non-ideal  $\text{NH}_4\text{NO}_3$  solutions at indicated temperatures. Extrapolation between predicted solid and maximum calculable aqueous  $\text{NH}_4\text{NO}_3$  dissociation constant.

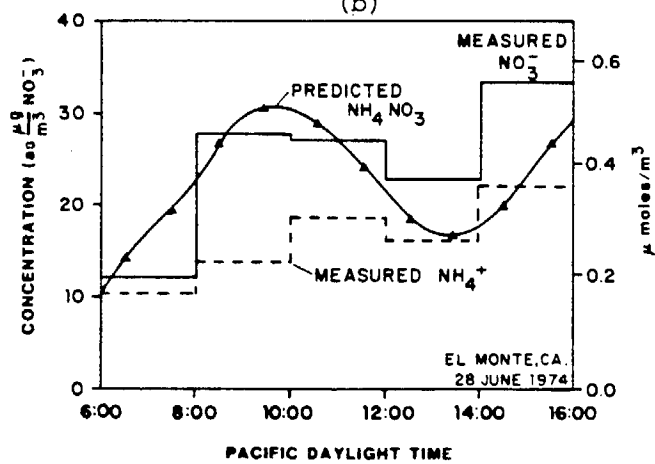
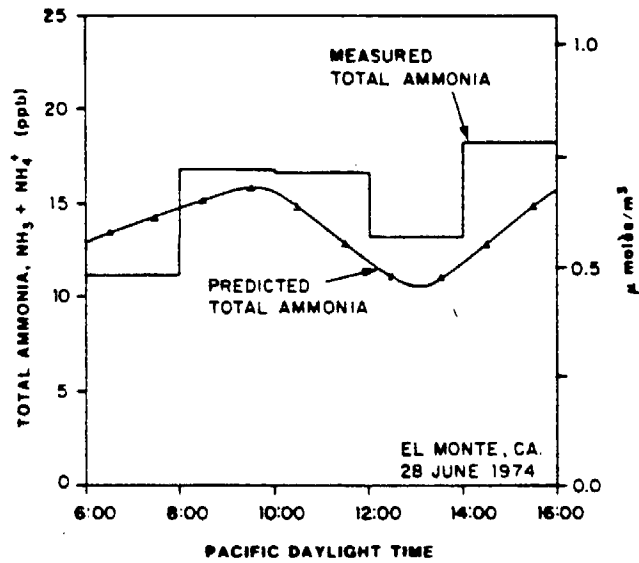
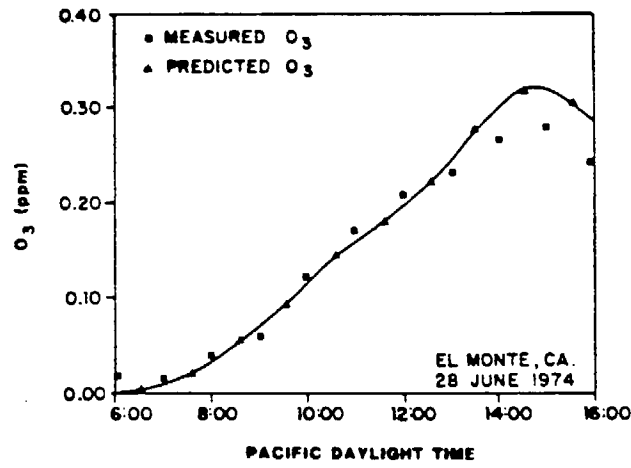
at either very low temperatures or very high relative humidity. This means that 25 ppb of  $\text{NH}_3$  and 25 ppb of  $\text{HNO}_3$  would produce no aerosol on a very hot dry day in the eastern Los Angeles basin, while on a cooler day with lower relative humidity more than  $70 \mu\text{g}/\text{m}^3$  of  $\text{NH}_4\text{NO}_3$  aerosol could be formed from the same gas phase precursor constituents.

Material balance calculation procedures developed in Appendix B to this report show that Los Angeles area aerosols during the ACHEX experiment contained solution droplets with concentrations between 8 and 26 molar. At ionic strengths implied by these concentration data, solution chemistry is highly non-ideal, and aerosol liquid water content is strongly dependent on relative humidity. In Chapter III of this report, the relative humidity dependence of the  $\text{NH}_4\text{NO}_3$  dissociation constant,  $K$ , is examined for highly concentrated non-ideal solutions. A smooth transition in values of  $K$  is demonstrated as relative humidity changes pass through the deliquescence point that marks the dividing line between solid  $\text{NH}_4\text{NO}_3$  and solution droplets containing  $\text{NH}_4^+$  and  $\text{NO}_3^-$  ions. The value of the equilibrium dissociation constant,  $K$ , as a function of relative humidity is shown to not vary significantly between pH 1 and 7.

A mathematical model describing the transport and formation of aerosol ammonium nitrate is presented in Chapter IV. The ammonium nitrate formation chemistry developed in Chapters II and III is inserted into a photochemical trajectory model capable of computing  $\text{HNO}_3$  and  $\text{NH}_3$  concentrations in the atmosphere directly from data on pollutant source emissions. Sensitivity analysis shows that  $\text{NH}_4\text{NO}_3$

concentration predictions are strongly influenced by ambient temperature and  $\text{NH}_3$  levels. An inventory of ammonia emissions in the South Coast Air Basin is developed as documented in Appendix A to this report. The  $\text{NH}_3$  emission inventory is combined with inventories for reactive hydrocarbons and oxides of nitrogen, then inserted into the nitrate formation model.

The air quality model is tested by comparison to ambient  $\text{NH}_3$ ,  $\text{NH}_4^+$  and  $\text{NO}_3^-$  concentrations measured at El Monte, California during June 1974. Results are shown in Figure 2. Ambient ozone concentrations and the level of total ammonia-derived pollutant concentrations are reproduced quite closely. The time history and average level of  $\text{NH}_4\text{NO}_3$  concentrations predicted by the model matches the measured  $\text{NO}_3^-$  aerosol concentration at El Monte to within the uncertainty of the atmospheric measurement methods available for nitrates in 1974. Future applications of this air quality modeling procedure are discussed at the end of Chapter IV, along with the need for further model verification tests using atmospheric monitoring data taken by recently developed low artifact sampling procedures.



(c)

FIGURE 2

Concentration profiles at El Monte on 28 June 1974. (a) Predicted and measured  $O_3$  concentrations, (b) Predicted total ammonia ( $NH_3 + NH_4^+$ ) and measured total ammonium, (c) Predicted  $NH_4NO_3$ , measured  $NH_4^+$  and measured  $NO_3^-$ .

CHAPTER II

RELATIVE HUMIDITY AND TEMPERATURE DEPENDENCE OF  
THE AMMONIUM NITRATE DISSOCIATION CONSTANT

A.W. Stelson and J.H. Seinfeld

## RELATIVE HUMIDITY AND TEMPERATURE DEPENDENCE OF THE AMMONIUM NITRATE DISSOCIATION CONSTANT

A. W. STELSON and J. H. SEINFELD

Department of Chemical Engineering, California Institute of Technology, Pasadena, CA 91125, U.S.A.

(First received 16 March 1981 and in final form 27 May 1981)

**Abstract**—Expressions for predicting the temperature and relative humidity dependence of the  $\text{NH}_4\text{NO}_3$  dissociation constant are derived from fundamental thermodynamic principles. The general trends predicted by the theory agree with the atmospheric data of Appel *et al.* (1979, 1980), Pitts (1978, 1979) and Tuazon *et al.* (1980).

### INTRODUCTION

Ammonium nitrate has been identified in atmospheric aerosol (Lundgren, 1970; Stephens and Price, 1972; Gordon and Bryan, 1973; Mamane and Pueschel, 1980). An understanding of the temperature and relative humidity dependence of the relationship between  $\text{NH}_4\text{NO}_3$  and its precursors,  $\text{NH}_3$  and  $\text{HNO}_3$ , is desirable.

Stelson *et al.* (1979) and Doyle *et al.* (1979) showed that measured atmospheric ammonia-nitric acid partial pressure products scattered about the thermodynamically predicted solid  $\text{NH}_4\text{NO}_3$  dissociation constant, indicating the likelihood of chemical equilibrium existing in this system. Stelson and Seinfeld (1981) demonstrated that Los Angeles aerosols contain ionic solids or concentrated solutions, 8–26 molal, indicating that any thermodynamic analysis must account for non-idealities present in concentrated solutions. Stelson and Seinfeld (1982) calculated the ammonia and nitric acid partial pressures over ammonium nitrate-nitric acid solutions accounting for nitrate, hydrogen and ammonium ion non-idealities. Their analysis showed the ammonia-nitric acid partial pressure product is sensitive to relative humidity but insensitive to pH(1–7). Thus, the aqueous  $\text{NH}_4\text{NO}_3$  dissociation constant at a specific temperature and relative humidity should typify the ammonia-nitric acid partial pressure product of a slightly acidic ammonium nitrate solution.

Atmospheric gas phase ammonia and nitric acid and particulate nitrate measurements demonstrate important trends. Significant amounts of ammonium nitrate precursors, ammonia and nitric acid, have been found in urban air accompanied by strong diurnal trends (Spicer, 1974; Pitts, 1978, 1979; Appel *et al.*, 1979; Tuazon *et al.*, 1980). Stelson *et al.* (1979) and Doyle *et al.* (1979) explained these observations through temperature dependence of the solid  $\text{NH}_4\text{NO}_3$  dissociation constant. Appel *et al.* (1979) observed that measured ammonia-nitric acid partial pressure products were less than the predicted dissociation constant even though aerosol nitrate was present. Forrest

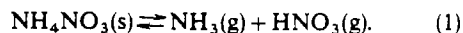
*et al.* (1980) spiked filters with  $\text{NH}_4\text{NO}_3$  and drew ambient air through the filters for 3–5 h. The greatest  $\text{NH}_4\text{NO}_3$  losses occurred at relative humidities below 60%, whereas at 100% relative humidity, no  $\text{NH}_4\text{NO}_3$  was lost. Stelson and Seinfeld (1982) were able to explain the results of Appel *et al.* (1979) and Forrest *et al.* (1980) by the relative humidity dependence of the  $\text{NH}_4\text{NO}_3$  dissociation constant at 25°C. Appel *et al.* (1980) observed a temperature and relative humidity dependence of measured ammonia-nitric acid partial pressure products.

The object of this work is to derive expressions for the temperature and relative humidity dependence of the  $\text{NH}_4\text{NO}_3$  dissociation constant based on fundamental thermodynamic principles. The temperature dependence of the solid  $\text{NH}_4\text{NO}_3$  dissociation constant will be calculated using the method developed by Stelson *et al.* (1979). The regions where ammonium nitrate is in the solid form or in aqueous solution will be determined from expressions for the  $\text{NH}_4\text{NO}_3$  relative humidity of deliquescence and solubility. For aqueous ammonium nitrate, the  $\text{NH}_4\text{NO}_3$  dissociation constant and solution relative humidity will be calculated by non-ideal aqueous solution thermodynamics. Using appropriate expressions for the  $\text{NH}_4\text{NO}_3$  dissociation constant, a diagram can be constructed for the temperature and relative humidity dependence of the  $\text{NH}_4\text{NO}_3$  dissociation constant. Finally, the thermodynamic predictions are compared with ambient measurements of Appel *et al.* (1979, 1980), Pitts (1978, 1979) and Tuazon *et al.* (1980).

### THEORY AND THERMODYNAMIC DATA FOR THE AMMONIUM NITRATE SYSTEM

#### Solid $\text{NH}_4\text{NO}_3$ dissociation constant

At temperatures below 170°C, solid ammonium nitrate exists in equilibrium with ammonia and nitric acid:



The equilibrium constant for this reaction,  $K_p'$ , is

related to the partial pressures of  $\text{NH}_3$  and  $\text{HNO}_3$  by  $K'_p = p_{\text{NH}_3} p_{\text{HNO}_3}$ , and  $K'_p$  is related to the standard Gibbs free energy change for reaction,  $\Delta G_T^0$ , by

$$\Delta G_T^0 = -RT \ln K'_p \quad (2)$$

Since the thermodynamic data for  $\text{NH}_4\text{NO}_3$  are limited, an extrapolation formula for the equilibrium constant as a function of temperature can be derived by integrating the van't Hoff equation,

$$\ln K'_p = \alpha - \frac{\Delta H_o}{RT} + \int_{298}^T \frac{1}{RT'^2} (C_{p_{\text{NH}_3}} + C_{p_{\text{HNO}_3}} - C_{p_{\text{NH}_4\text{NO}_3}}) dT' \quad (3)$$

where  $\alpha$  = integration constant,  $\Delta H_o$  = change in enthalpy at 298 K, and  $C_{p_{\text{NH}_3}}$ ,  $C_{p_{\text{HNO}_3}}$ ,  $C_{p_{\text{NH}_4\text{NO}_3}}$  = the heat capacities of  $\text{NH}_3$ ,  $\text{HNO}_3$  and  $\text{NH}_4\text{NO}_3$ , respectively. Using the data in Table 1 and assuming the heat capacities are independent of temperature, we obtain from Equation (3),

$$\ln K = 84.6 - \frac{24220}{T} - 6.1 \ln \left( \frac{T}{298} \right) \quad (4)$$

where  $K$  is the equilibrium constant in units of  $\text{ppb}^2$ .

#### Relative humidity of deliquescence and solubility

Up to the relative humidity of deliquescence, ammonium nitrate should be present as a solid. The results of Tang (1980) indicate  $\text{NH}_4\text{NO}_3$  aerosol is quite hygroscopic at  $\sim 30\%$  relative humidity vs  $\sim 62\%$  observed for bulk  $\text{NH}_4\text{NO}_3$  at  $25^\circ\text{C}$  (Dingemans, 1941; Adams and Merz, 1919; Edgar and Swan, 1922; Prideaux, 1920). Whether the observation of Tang (1980) is the result of a property unique to the size of the  $\text{NH}_4\text{NO}_3$  aerosol or the presence of an impurity is difficult to ascertain. Prideaux (1920) observed that the presence of a small amount of sodium nitrate in ammonium nitrate significantly reduced the relative humidity of deliquescence. Since we cannot adequately evaluate the observations of Tang (1980), we will assume  $\text{NH}_4\text{NO}_3$  exhibits tradi-

tional deliquescence as implied by the majority of the literature.

An expression can be derived for the saturated solution relative humidity

$$\ln(\text{RHD}) = -\frac{L}{R} \left( \frac{1}{T} - \frac{1}{298} \right) + \ln(\text{RHD})_{298} \quad (5)$$

where RHD = per cent relative humidity of deliquescence and  $L$  = water heat of fusion (Denbigh, 1971). Using the water heat of fusion from Weast (1973) and the relative humidity of a saturated  $\text{NH}_4\text{NO}_3$  solution at 298.15 K from Hamer and Wu (1972),

$$\ln(\text{RHD}) = \frac{723.7}{T} + 1.7037 \quad (6)$$

Equation (6) agrees well with the least square expression derived from the data of Dingemans (1941),

$$\ln(\text{RHD}) = \frac{856.23 \pm 13.25}{T} + 1.2306 \pm 0.0439 \quad (7)$$

Equations (6) and (7) are shown with experimental data in Fig. 1.

For an ideal solution, the solubility temperature dependence is

$$\left[ \frac{\partial \ln(m^2)}{\partial T} \right]_p = \frac{H^0 - h^s}{RT^2} \quad (8)$$

where  $m$  =  $\text{NH}_4\text{NO}_3$  molality,  $H^0$  = the  $\text{NH}_4\text{NO}_3$  partial molal enthalpy at infinite dilution and  $h^s$  = enthalpy of crystalline  $\text{NH}_4\text{NO}_3$ . By integrating Equation (8),

$$\ln m = -\frac{(H^0 - h^s)}{2R} \left( \frac{1}{T} - \frac{1}{298} \right) + \ln(m)_{298} \quad (9)$$

is obtained. Using the thermodynamic data in Table 1 and noting that  $(m)_{298} = 25.954$  from Hamer and Wu (1972),

$$\ln m = -\frac{1600}{T} + 8.6228 \quad (10)$$

Equation (10) agrees well with the least squares expression for the data of Stephen and Stephen (1963),

Table 1. Thermodynamic data for the ammonium nitrate system at 298 K

Species	$\frac{\Delta G}{R} (\text{K}^{-1})$	$\frac{\Delta H}{R} (\text{K}^{-1})$	$\frac{C_p}{R}$	Reference
$\text{NH}_3(\text{g})$	-1977*	-5526*	4.285	Parker <i>et al.</i> (1976)* JANAF (1971)
$\text{HNO}_3(\text{g})$	-8903	-16,155	6.416	JANAF (1971)
$\text{NH}_4\text{NO}_3(\text{c, IV})$	-22,220*	-44,080*	16.8	Parker <i>et al.</i> (1976)* Wagman <i>et al.</i> (1968)
$\text{NH}_4\text{NO}_3(\text{aq, } m = 1)$	-22,940†	-40,880†	-0.505	Wagman <i>et al.</i> (1968)† Roux <i>et al.</i> (1978)

$\Delta G$  = Standard free energy of formation.

$\Delta H$  = Heat of formation.

$C_p$  = Heat capacity.

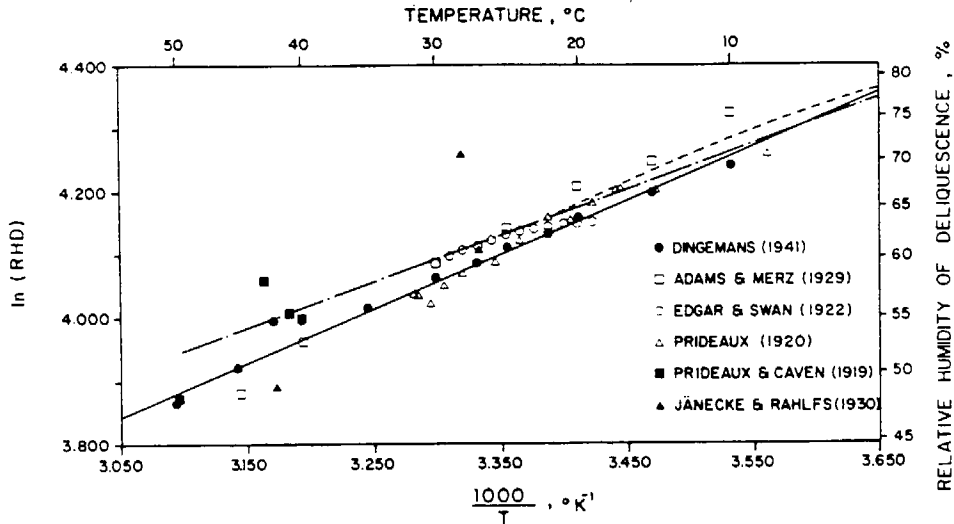


Fig. 1.  $\text{NH}_4\text{NO}_3$  relative humidity of deliquescence temperature dependence: (---) Equation (6); (—) Equation (7); (-·-) Equations (11), (15), (21) and (22).

$$\ln m = -\frac{1837.3 \pm 18.0}{T} + 9.4235 \pm 0.0602. \quad (11)$$

Equations (10) and (11) are shown with the data of Stephen and Stephen (1963) in Fig. 2.

Figures 1 and 2 show the strong temperature dependence of the relative humidity of deliquescence and the solubility of ammonium nitrate. This temperature dependence is an unfortunate complication when attempting to extrapolate aqueous ammonium nitrate thermodynamic data to temperatures above 25°C.

*Aqueous  $\text{NH}_4\text{NO}_3$  dissociation constant*

Analogous to the solid  $\text{NH}_4\text{NO}_3$  dissociation constant derivation, an expression for the equilibrium constant over aqueous  $\text{NH}_4\text{NO}_3$  can be derived

$$\ln K_p^* = \alpha - \frac{\Delta H_o}{RT} + \int_{298}^T \frac{1}{RT'^2} \int_{298}^{T'} (C_{\text{PNH}_3} - C_{\text{PHNO}_3} - C_{\text{PNH}_4\text{NO}_3}^0) dT' dT'', \quad (12)$$

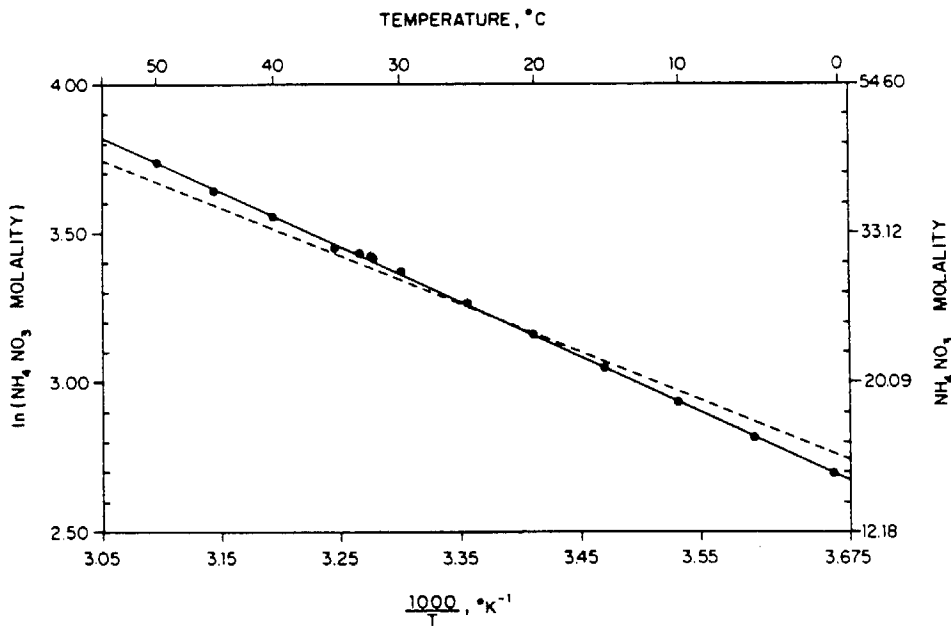


Fig. 2.  $\text{NH}_4\text{NO}_3$  solubility temperature dependence: (—) Equation (11); (---) Equation (10); Data from Stephen and Stephen (1963).

where  $K_p^* = p_{\text{NH}_3} p_{\text{HNO}_3} / a_{\text{NH}_4\text{NO}_3} = K_p' / a_{\text{NH}_4\text{NO}_3}$ ,  $a_{\text{NH}_4\text{NO}_3} = \gamma_{\text{NH}_4\text{NO}_3}^{\pm 2} m^2$ ,  $\bar{C}_p^0$  =  $\text{NH}_4\text{NO}_3$  partial heat capacity at infinite dilution, and  $\gamma_{\text{NH}_4\text{NO}_3}^{\pm}$  = mean molal ionic activity coefficient of dissolved  $\text{NH}_4\text{NO}_3$ . Using the data in Table 1 and assuming the heat capacities are independent of temperature, we obtain from Equation (12),

$$\ln K^* = \ln \frac{K}{a_{\text{NH}_4\text{NO}_3}} = 54.18 - \frac{15,860}{T} + 11.206 \ln \left( \frac{T}{298} \right) \quad (13)$$

where  $K^*$  has units of  $\text{ppb}^2 \text{ molal}^{-2}$ . The temperature variation of  $\gamma_{\text{NH}_4\text{NO}_3}^{\pm}$  can be calculated from

$$\left( \frac{\partial \ln \gamma_{\text{NH}_4\text{NO}_3}^{\pm}}{\partial T} \right)_p = \frac{\bar{H}^0 - \bar{H}}{RT^2} \quad (14)$$

where  $\bar{H}$  = the  $\text{NH}_4\text{NO}_3$  partial molal enthalpy at  $m$  (Denbigh, 1971, p. 279). By integrating (14),

$$\left( \ln \gamma_{\text{NH}_4\text{NO}_3}^{\pm} \right)_T = \left( \ln \gamma_{\text{NH}_4\text{NO}_3}^{\pm} \right)_{298} + \left( \frac{\bar{H} - \bar{H}^0}{R} \right)_{298} + \left( \frac{1}{T} - \frac{1}{298} \right) - \left( \frac{\bar{C}_p - \bar{C}_p^0}{R} \right) \left( \ln \frac{T}{298} + \frac{298}{T} - 1 \right) \quad (15)$$

is obtained, where  $\bar{C}_p^0$ ,  $\bar{C}_p$  =  $\text{NH}_4\text{NO}_3$  partial molal heat capacities at infinite dilution and  $m$ , respectively,

and  $\left( \frac{\bar{H} - \bar{H}^0}{R} \right)_{298}$  = the normalized  $\text{NH}_4\text{NO}_3$  relative partial molal enthalpy difference between infinite dilution and  $m$  at 298.15 K. To evaluate  $(\ln \gamma_{\text{NH}_4\text{NO}_3}^{\pm})_T$ , the concentration dependence of  $(\ln \gamma_{\text{NH}_4\text{NO}_3}^{\pm})_{298}$ ,

$\left( \frac{\bar{H} - \bar{H}^0}{R} \right)_{298}$  and  $\left( \frac{\bar{C}_p - \bar{C}_p^0}{R} \right)$  must be known. The

expression of Hamer and Wu (1972) can be used to represent the concentration dependence of  $(\ln \gamma_{\text{NH}_4\text{NO}_3}^{\pm})_{298}$  to 25.954 molal. Obtaining ex-

pressions for  $\left( \frac{\bar{H} - \bar{H}^0}{R} \right)_{298}$  and  $\left( \frac{\bar{C}_p - \bar{C}_p^0}{R} \right)$  is more

complicated.

Relative apparent molal heat content data can be obtained from Wagman *et al.* (1968) and Vanderzee *et al.* (1980). Since the data of Vanderzee *et al.* (1980) are more recent and span a larger concentration range, they will be used to represent the variation in enthalpy with concentration. A polynomial regression can be calculated using ideal gas constant normalized relative apparent molal heat content data of Vanderzee *et al.* (1980) between 0.1 and 25 molal. The partial molal enthalpy was derived using Equation (8-2-7) from Harned and Owen (1958), as

$$(\bar{H} - \bar{H}^0) = \phi_L + m \frac{\partial(\phi_L)}{\partial m} \quad (16)$$

where  $\phi_L$  = relative apparent molal heat content at  $m$ . The resulting polynomial regression is

$$\left( \frac{\bar{H} - \bar{H}^0}{R} \right)_{298} = 297.85 m^{1/2} - 983.98 m + 508.08 m^{3/2} - 133.86 m^2 + 19.328 m^{5/2} - 1.2071 m^3 \quad (17)$$

where the standard deviation for the normalized relative apparent molal heat content polynomial regression is  $\pm 3.54 \text{ K}^{-1}$ . The error in the relative partial molal enthalpy polynomial regression is unknown since it was obtained using the normalized relative apparent molal heat content polynomial regression and (16).

Roux *et al.* (1978) measured the apparent molal heat capacity,  $\phi_{c_p}$ , of aqueous ammonium nitrate at 25° C to 22.4 molal. Their expression for their data,

$$\frac{\phi_{c_p}}{R} = -0.505 + 3.482 m^{1/2} + 3.159 m - 1.605 m^{3/2} + 0.274 m^2 - 0.0161 m^{5/2}, \quad (18)$$

agrees well with the measurements of Gucker *et al.* (1936) and Sorina *et al.* (1977). Using Equation (8-4-7) from Harned and Owen (1958),

$$\bar{C}_p = \phi_{c_p} + m \frac{\partial \phi_{c_p}}{\partial m} \quad (19)$$

the partial molal heat capacity can be calculated from (18) as,

$$\frac{\bar{C}_p}{R} = -0.505 + 5.223 m^{1/2} + 6.318 m - 4.013 m^{3/2} + 0.822 m^2 - 0.0564 m^{5/2}. \quad (20)$$

The data of Sorina *et al.* (1977) extend to 50 molal, supersaturation at 25° C. With relative apparent molal heat content and solute activity data to 50 molal, the temperature extrapolation of  $\gamma_{\text{NH}_4\text{NO}_3}^{\pm}$  could be performed to saturation at 50° C. Unfortunately, the relative apparent molal heat content data are limited to 25 molal (Vanderzee *et al.*, 1980). Even though (20) is based on data to 22.4 molal, it will be used to 25 molal. Within the region 22.4–25 molal, (20) is a smoothly continuous extrapolation of the data below 22.4 molal and represents the data of Gucker *et al.* (1936) and Sorina *et al.* (1977) fairly well.

Once  $(\ln \gamma_{\text{NH}_4\text{NO}_3}^{\pm})_T$  has been calculated, the osmotic coefficient of the solution,  $\phi_T$ , can be derived from the Gibbs-Duhem equation,

$$\phi_T = 1 + \frac{1}{m} \int_0^m m d(\ln \gamma_{\text{NH}_4\text{NO}_3}^{\pm})_T. \quad (21)$$

The per cent relative humidity at temperature  $T$ ,  $RH_T$ , can be calculated from

$$RH_T = 100 \exp \left( - \frac{vmM\phi_T}{1000} \right) \quad (22)$$

where  $v$  = the number of moles of ions formed by the ionization of one mole of solute and  $M$  = molecular weight of water.

RESULTS

By using appropriate expressions for the temperature dependence of solid or aqueous phase  $\text{NH}_4\text{NO}_3$  thermodynamic properties, the dissociation constant can be calculated at a specific temperature and relative humidity. With (7), the form of ammonium nitrate, solid or aqueous, can be determined. At a specific temperature the  $\text{NH}_4\text{NO}_3$  dissociation constant is invariant below the relative humidity of deliquescence and can be obtained from (4). Above the relative humidity of deliquescence, the  $\text{NH}_4\text{NO}_3$  dissociation constant relative humidity dependence can be calculated from (13), (15), (21) and (22) to 25 molal. Equation (11) is used to calculate the solubility temperature dependence. Figure 3 has been constructed using the previously mentioned techniques. Notice discontinuities exist between the solid  $\text{NH}_4\text{NO}_3$  dissociation constant and the dissociation constant for a saturated solution at 25°C and below.

The possible sources of these discontinuities at temperatures below 25°C are manifold and the relative error from each source is difficult to evaluate. First, the temperature extrapolations for the solid  $\text{NH}_4\text{NO}_3$  and the aqueous  $\text{NH}_4\text{NO}_3$  dissociation constants are based on different thermodynamic data sets so an inconsistent value in one data set can cause

discontinuity. Second, the relative humidity of deliquescence is obtained by different methods for solid  $\text{NH}_4\text{NO}_3$  and aqueous  $\text{NH}_4\text{NO}_3$ . The relative humidity of deliquescence for solid  $\text{NH}_4\text{NO}_3$  was calculated from (7) and aqueous  $\text{NH}_4\text{NO}_3$  from (11), (15), (21) and (22). The relative error can be seen by comparing the solid and dashed curves in Fig. 1. Third, error is introduced by differentiating the polynomial regressions obtained for the relative apparent molal heat content and the apparent molal heat capacity to get expressions for the partial molal enthalpy and heat capacity. The amount of error is known for the original polynomial regressions but not for the derived regressions. Finally, the error must be introduced by the enthalpy, heat capacity, relative humidity of deliquescence or solubility data or the temperature extrapolation technique, since the free energy data are consistent at 298 K (Stelson and Seinfeld, 1982).

Above 25°C, an interpolation must be performed between the relative humidity corresponding to 25 molal and saturation. Since the curves are fairly flat in the region between 25 molal and saturation, a linear interpolation between the dissociation constant at 25 molal and at saturation should approximate the dissociation constant in this region.

The temperature dependence of the saturated solution relative humidity can be calculated using (11).

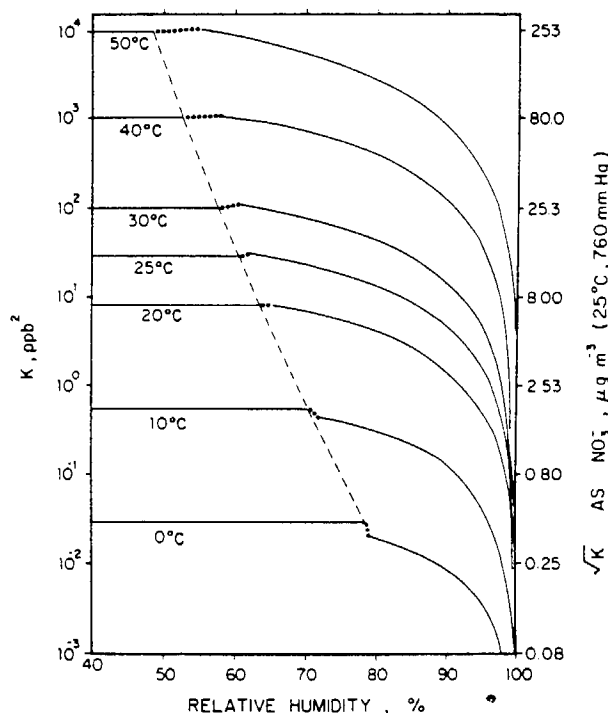


Fig. 3.  $\text{NH}_4\text{NO}_3$  dissociation constant temperature and relative humidity dependence: (----) solid  $\text{NH}_4\text{NO}_3$  to aqueous  $\text{NH}_4\text{NO}_3$  solution transition predicted from Equation (7); (—) Isothermal prediction of  $\text{NH}_4\text{NO}_3$  dissociation constant for solid  $\text{NH}_4\text{NO}_3$  and non-ideal  $\text{NH}_4\text{NO}_3$  solutions at indicated temperatures; (---) Extrapolation between predicted solid and maximum calculable aqueous  $\text{NH}_4\text{NO}_3$  dissociation constant.

(15), (21) and (22) for temperatures below 25° C. A curve calculated using this method is shown in Fig. 1.

Data for the molal variation of the solution relative humidity at various temperatures are shown in Fig. 4. The data scatter is considerable and shows no definite temperature variation trend. Curves for the relative humidity concentration dependence were calculated at 0, 25 and 50° C using (15), (21) and (22) and are shown in Fig. 4. The predictions coincide with the general area of the data but do not show agreement with any particular data set. Also shown in Fig. 4 is the relative humidity concentration dependence for an ideal  $\text{NH}_4\text{NO}_3$  solution which poorly predicts the non-ideal  $\text{NH}_4\text{NO}_3$  behavior.

Figure 4 illustrates the infeasibility of attempting to use water activities at higher temperatures, 25–50° C, and the Gibbs–Duhem equation to calculate solute activities. The data have too much scatter and are too sparse at any particular temperature. Furthermore, the maximum concentration of existing water activity data is 29.2 molal and saturation is 42 molal at 50° C.

#### DISCUSSION

Atmospheric measurements of simultaneous ammonia, nitric acid, temperature, relative humidity,

aerosol ammonium and aerosol nitrate are very limited. With partial data sets, the merit of the thermodynamic calculations can be demonstrated.

Figure 5 shows diurnal variation of the measured ammonia–nitric acid partial pressure product and the respirable aerosol nitrate at Pittsburg, CA (Appel *et al.*, 1979). The trends of the curves are very similar. If the similarity between the diurnal variation of the ammonia–nitric acid partial pressure product and the respirable aerosol nitrate resulted strictly from atmospheric dilution effects, these data when cross plotted, should result in a single curve. The data were analysed by this method and the test failed. Thus, the similar trend between the observed ammonia–nitric acid partial pressure product and the respirable aerosol nitrate cannot be merely attributed to atmospheric dilution. Also shown are the daily maximum bulk  $\text{NH}_4\text{NO}_3$  dissociation constants calculated from the daily maximum temperature and (4). Ammonia–nitric acid partial pressure products below the daily maximum bulk  $\text{NH}_4\text{NO}_3$  dissociation constant can result from the lack of aerosol ammonium nitrate, the presence of an unreactive solute, the temperature being less than the daily maximum or the relative humidity being greater than the deliquescence point. Ammonia–nitric acid partial pressure products above the daily maximum bulk  $\text{NH}_4\text{NO}_3$  dissociation constant could be ex-

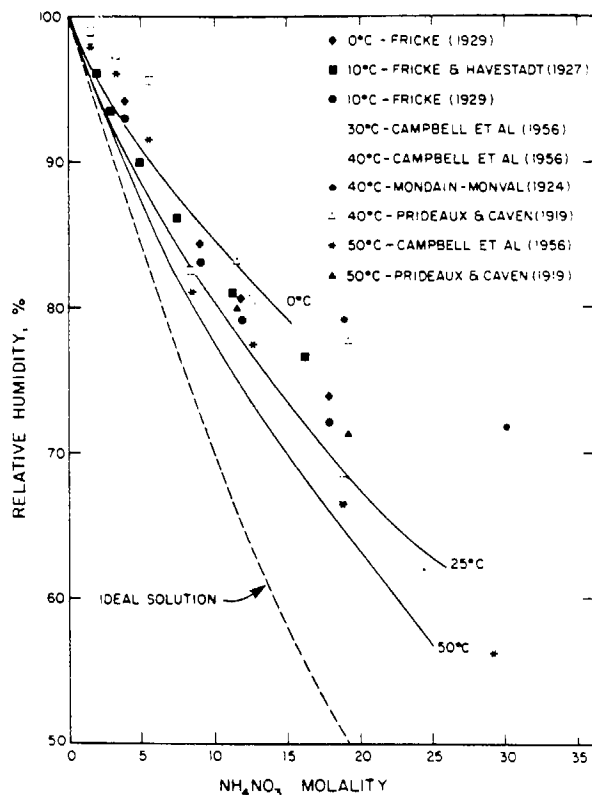


Fig. 4. Temperature and concentration dependence of  $\text{NH}_4\text{NO}_3$  solution relative humidity: (----) Ideal solution prediction; (—) non-ideal solution predictions at 0, 25 and 50° C.

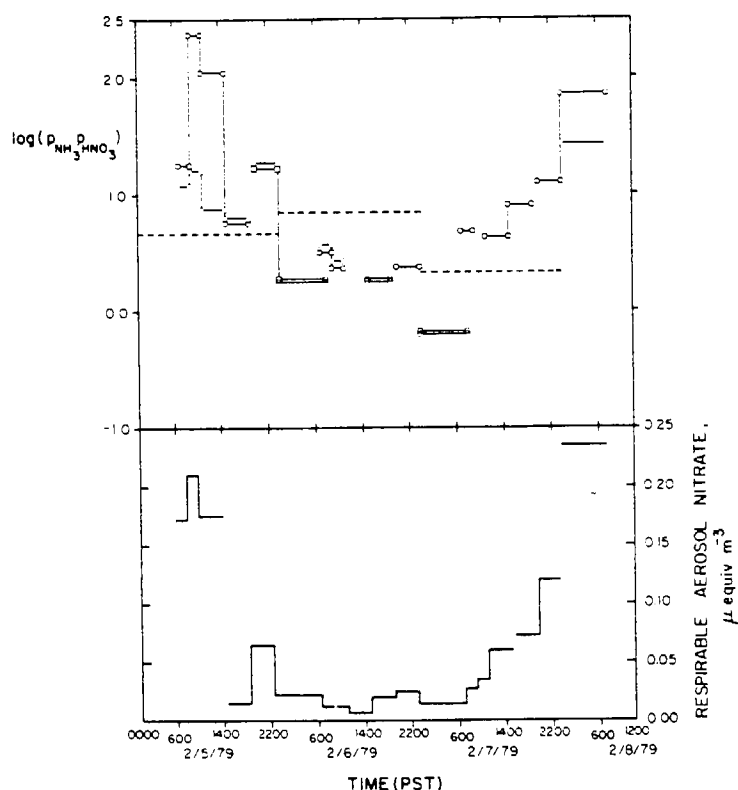


Fig. 5. Experimental diurnal  $\text{NH}_3\text{-HNO}_3$  product and aerosol nitrate trends at Pittsburg, CA (Appel *et al.*, 1979): (o-o) Product calculated from NaCl impregnated Whatman 41 filter gaseous  $\text{HNO}_3$  measurements; (□-□) Product calculated from Duralon nylon filter gaseous  $\text{HNO}_3$  measurements; (----) Maximum  $\text{NH}_4\text{NO}_3$  dissociation constant based on the daily maximum temperature and Equation (4);  $p_{\text{NH}_3}p_{\text{HNO}_3}$  in  $\text{ppb}^2$ .

plained by kinetic limitations or Kelvin effects. Kinetic limitations are doubtful since the ammonia-nitric acid reaction is very fast (Kaiser and Japar, 1978; Morris and Niki, 1971). Experimental errors could result in positive or negative deviations.

The effect of an unreactive solute in solution with ammonium nitrate on the ammonia-nitric acid partial pressure can be evaluated qualitatively. From the Gibbs-Duhem equation,

$$RH = 100 \exp \left( \frac{-M}{1000} \left[ \int_0^m m \, d \ln a_{\text{NH}_4\text{NO}_3} + \int_0^{m_i} m_i \, d \ln a_i \right] \right) \quad (23)$$

where  $m_i$  = molality of inert solute and  $a_i$  = activity of inert solute. Assuming the inert solute is ideal and undissociated,

$$RH = 100 \exp \left( \frac{-M}{1000} \left[ \int_0^m m \, d \ln a_{\text{NH}_4\text{NO}_3} + m_i \right] \right) \quad (24)$$

Equation (24) shows the addition of an ideal inert solute would decrease the relative humidity above an ammonium nitrate solution for a specific ammonium

nitrate molality. Since the additional solute is assumed to be non-interactive with the dissolved ammonium nitrate, the ammonia-nitric acid partial pressure product would be the same as the situation without any inert solute. Thus, the presence of an inert solute results in an ammonia-nitric acid partial pressure being observed at a lower relative humidity than would be predicted from the pure ammonium nitrate-water system.

The Kelvin effect for solid  $\text{NH}_4\text{NO}_3$  can be evaluated using an expression derived by Banic and Iribarne (1980),

$$d_p = \frac{4\sigma M}{\rho RT \ln S} \quad (25)$$

where  $\sigma$  =  $\text{NH}_4\text{NO}_3$  surface tension,  $d_p$  = particle diameter,  $M$  =  $\text{NH}_4\text{NO}_3$  molecular weight,  $\rho$  =  $\text{NH}_4\text{NO}_3$  density and  $S$  = the saturation ratio which equals  $K$  for curved surface/ $K$  for flat surface. The  $\text{NH}_4\text{NO}_3$  surface tension was approximated as  $108.4 \text{ dyn cm}^{-1}$  at  $25^\circ \text{C}$  by the approach of Rehinder (1926). The surface tension is approximate because it required extrapolation from  $168.5^\circ \text{C}$  across three different  $\text{NH}_4\text{NO}_3$  crystalline structures (Nagatani *et al.*, 1967). With the  $\text{NH}_4\text{NO}_3$  density and molecular

weight from Weast (1973), (25) simplifies to

$$d_p = \frac{8.1 \times 10^{-3}}{\ln S} \quad (26)$$

In Fig. 5, saturation ratios greater than 5 are observed. (Compare observed ammonia-nitric acid partial pressure products and the daily maximum bulk  $\text{NH}_4\text{NO}_3$  dissociation constants in Fig. 5.) Can these supersaturations be attributed to the Kelvin effect? For a saturation ratio of 5, the calculated particle diameter is  $0.005 \mu\text{m}$  which is too small to be atmospherically realistic since  $0.005 \mu\text{m}$  particles would be readily scavenged by larger particles.

The relative humidity dependence of the ammonia-nitric acid product at Claremont, CA, is displayed in Fig. 6 (Appel *et al.*, 1980). Next to each datum is the temperature in Centigrade at the time of measurement. Underlined temperatures refer to points positively deviating from the dissociation constant calculated at the temperature and relative humidity of each measurement. Also shown are  $\text{NH}_4\text{NO}_3$  dissociation constant isotherms, 20, 25 and  $30^\circ\text{C}$ , calculated using the procedures developed in this work. The data show scatter but are in general agreement with the predictions of this work.

Figure 7 shows the diurnal variation of the

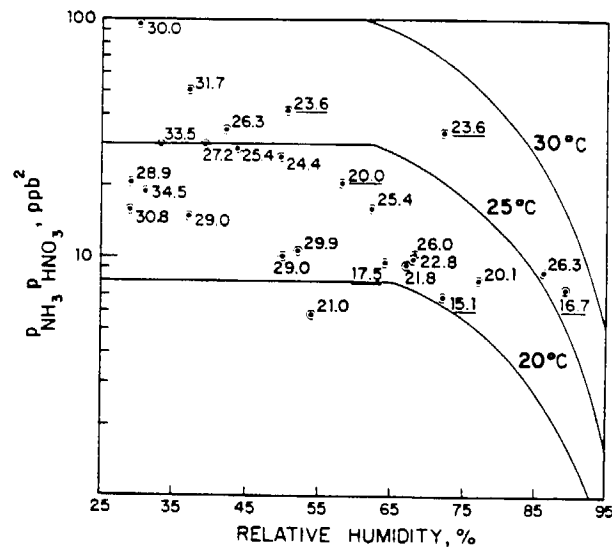


Fig. 6. Experimental relative humidity and temperature dependence of the  $\text{NH}_3\text{-HNO}_3$  product at Claremont, CA (adapted from Appel *et al.*, 1980): (—) Predicted  $\text{NH}_4\text{NO}_3$  dissociation constant relative humidity dependence at 20, 25 and  $30^\circ\text{C}$ : Values next to data from Appel *et al.* (1980) are the temperatures in  $^\circ\text{C}$ .

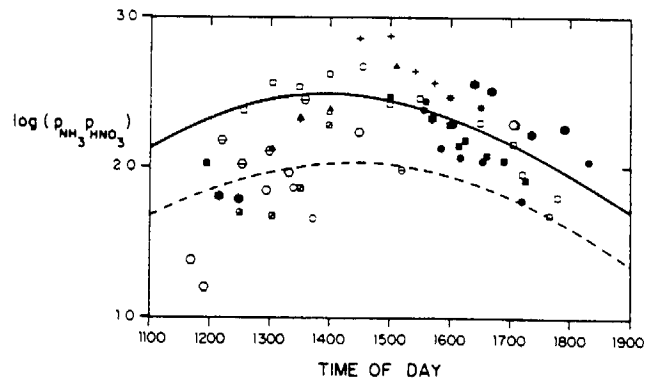


Fig. 7. Diurnal  $\text{NH}_3\text{-HNO}_3$  product trend calculated from FT-IR measurements at Riverside, CA (Pitts, 1978; 1979; Tuazon *et al.*, 1980): (—) solid  $\text{NH}_4\text{NO}_3$  dissociation constant diurnal trend calculated from Equation (4) and the average temperature profile for episode days (maximum  $\text{O}_3 > 0.2 \text{ ppm}$ ), May–October 1976 (Pitts, 1978); (----) solid  $\text{NH}_4\text{NO}_3$  dissociation constant diurnal trend calculated from Equation (4) and the average temperature profile for all days, May–October 1976 (Pitts, 1978); Different data symbols refer to different days of measurement;  $P_{\text{NH}_3}P_{\text{HNO}_3}$  in  $\text{ppb}^2$ .

ammonia-nitric acid product calculated from measurements at Riverside, CA (Pitts, 1978, 1979; Tuazon *et al.*, 1980). Also shown are the diurnal variations of the solid  $\text{NH}_4\text{NO}_3$  dissociation constant calculated from (4) and the average temperature profiles for all days and episode days (maximum  $\text{O}_3 > 0.2$  ppm) between May and October 1976 (Pitts, 1978). Note the strong diurnal pattern with the peak occurring between 1400 and 1600 which corresponds to the daily maximum temperature and minimum relative humidity region.

Finally, some comments on how this work should be applied are in order. Figures 6 and 7 show the trends predicted by the thermodynamics generally follow the atmospheric data trends though positive and negative deviations from the pure  $\text{NH}_4\text{NO}_3$  thermodynamics are apparent. Negative deviations can be explained by the presence of additional solutes in solution. Positive deviations cannot be explained with current theoretical development. The polluted atmospheric aerosol can be multicomponent or supersaturated which leads to deviations from the pure  $\text{NH}_4\text{NO}_3$  theoretical predictions. Thus, this work should be used as guidance to identify important parameters in aerosol measurement and to give a relative feeling for what the distribution of nitrate is between the gas and aerosol phases and a basis for assembling more detailed multicomponent theories.

Additionally, Fig. 3 merits comment. The right ordinate of Fig. 3 is  $\sqrt{K}$ , expressed as nitrate,  $\mu\text{g m}^{-3}$ , at 25 C and 760 mm Hg. Typical aerosol nitrate values range between 0 and 40  $\mu\text{g m}^{-3}$  (Stelson *et al.*, 1979). This range is spanned by the ordinate of Fig. 3. Thus, the importance of accurately monitoring temperature and relative humidity during aerosol nitrate measurement is apparent.

### CONCLUSIONS

Some important conclusions are evident from this work:

(1) A thermodynamic extrapolation method was developed to predict the temperature and relative humidity variation of the  $\text{NH}_4\text{NO}_3$  dissociation constant.

(2) The approach of using existing water activity data at temperatures other than 25 C to calculate solute activities is shown to be infeasible.

(3) The general trends predicted by the thermodynamic model agree with the atmospheric observations of Appel *et al.* (1979, 1980), Pitts (1978, 1979), and Tuazon *et al.* (1980).

(4) Positive deviations of measured ammonia-nitric acid partial pressure products from the solid  $\text{NH}_4\text{NO}_3$  dissociation constant at the temperatures of measurement cannot be readily explained other than on the basis of experimental error.

**Acknowledgements**—This work was supported by Environmental Protection Agency grant R806844 and State of California Air Resources Board contract A7-169-30.

### REFERENCES

- Adams J. R. and Merz A. R. (1929) Hygroscopicity of fertilizer materials and mixtures. *Ind. Engng Chem.* **21**, 305-307.
- Appel B. R., Tokiwa Y., Hoffer E. M., Kothny E. L., Haik M. and Wesolowski J. J. (1980) Evaluation and development of procedures for determination of sulfuric acid, total particle-phase acidity and nitric acid in ambient air—Phase II. Calif. Air Res. Board A8-111-31 Final Report.
- Appel B. R., Tokiwa Y., Wall S. M., Haik M., Kothny E. L. and Wesolowski J. J. (1979) Determination of sulfuric acid, total particle-phase acidity and nitric acid in ambient air. Calif. Air Res. Board A6-209-30 Final Report.
- Banic C. M. and Iribarne J. V. (1980) Nucleation of ammonium chloride in the gas phase and the influence of ions. *J. geophys. Res.* **85**, 7459-7464.
- Campbell A. N., Fishman J. B., Rutherford G., Schaefer T. P. and Ross L. (1956) Vapor pressures of aqueous solutions of silver nitrate, of ammonium nitrate, and of lithium nitrate. *Can. J. Chem.* **34**, 151-159.
- Denbigh K. (1971) *The Principles of Chemical Equilibrium*. 3rd Edn. Cambridge University Press, London.
- Dingemans P. (1941) The vapor pressure of saturated solutions of ammonium nitrate. *Recl Trav. chim pays-Bas Belg.* **60**, 317-328.
- Doyle G. J., Tuazon E. C., Graham R. A., Mischke T. M., Winer A. M. and Pitts J. N. Jr. (1979) Simultaneous concentrations of ammonia and nitric acid in a polluted atmosphere and their equilibrium relationship to particulate ammonium nitrate. *Envir. Sci. Technol.* **13**, 1416-1419.
- Edgar G. and Swan W. O. (1922) The factors determining the hygroscopic properties of soluble substances. I. The vapor pressures of saturated solutions. *J. Am. chem. Soc.* **44**, 570-577.
- Forrest J., Tanner R. L., Spandau D., D'Ottavio T. and Newman L. (1980) Determination of total inorganic nitrate utilizing collection of nitric acid on NaCl-impregnated filters. *Atmospheric Environment* **14**, 137-144.
- Fricke R. (1929) The thermodynamic behavior of concentrated solutions. *Z. Elektrochem.* **35**, 631-640.
- Fricke R. and Havestadt L. (1927) Work of dilution and heat of dilution in the sphere of concentrated solutions. *Z. Elektrochem. angew. phys. Chem.* **33**, 441-455.
- Gordon R. J. and Bryan R. J. (1973) Ammonium nitrate in airborne particles in Los Angeles. *Envir. Sci. Technol.* **7**, 645-647.
- Gucker F. T. Jr., Ayres F. D. and Rubin T. R. (1936) A differential method employing variable heaters for the determination of the specific heats of solutions, with results for ammonium nitrate at 25 C. *J. Am. chem. Soc.* **58**, 2118-2126.
- Hamer W. J. and Wu Y. C. (1972) Osmotic coefficients and mean activity coefficients of uni-univalent electrolytes in water at 25 C. *J. phys. chem. Ref. Data* **1**, 1047-1099.
- Harned H. S. and Owen B. B. (1958) *The Physical Chemistry of Electrolytic Solutions*. ACS Monograph Series No. 137. 3rd Edn., Chap. 8. Reinhold, New York.
- JANAF Thermochemical Tables. 2nd Edn. (1971). NSRDS-NBS 37.
- Jänecke E. and Rahlfs E. (1930) The system:  $\text{NH}_4\text{NO}_3 - \text{H}_2\text{O}$ . *Z. anorg. allg. Chem.* **192**, 237-244.
- Kaiser E. W. and Japar S. M. (1978) Upper limit to the gas phase reaction rates of HONO with  $\text{NH}_3$  and  $\text{O}(^3\text{P})$  atoms. *J. phys. Chem.* **82**, 2753-2754.

CHAPTER III

RELATIVE HUMIDITY AND pH DEPENDENCE OF THE  
VAPOR PRESSURE OF AMMONIUM NITRATE-NITRIC  
ACID SOLUTIONS AT 25°C

A. W. Stelson and J. H. Seinfeld

- Lundgren D. A. (1970) Atmospheric aerosol composition and concentration as a function of particle size and of time. *J. Air Pollut. Control Ass.* **20**, 603-608.
- Mondain-Monval P. (1924) Law of the solubility of salts. *C.r. hebdom. Séanc. Acad. Sci., Paris* **178**, 1164-1166.
- Mamane Y. and Pueschel R. F. (1980) A method for the detection of individual nitrate particles. *Atmospheric Environment* **14**, 629-639.
- Morris E. D. Jr. and Niki H. (1971) Mass spectrometric study of the reactions of nitric acid with O atoms and H atoms. *J. phys. Chem.* **75**, 3193-3194.
- Nagatani M., Seiyama T., Sakiyama M., Suga H. and Seki S. (1967) Heat capacities and thermodynamic properties of ammonium nitrate crystal: Phase transitions between stable and metastable phases. *Bull. Chem. Soc. Jap.* **40**, 1833-1844.
- Parker V. B., Wagman D. D. and Garvin D. (1976) Selected thermochemical data compatible with the CODATA recommendations. NBSIR 75-968.
- Pitts J. N., Jr. (1978) Detailed characterization of gaseous and size-resolved particulate pollutants at a South Coast Air Basin smog receptor site: levels and modes of formation of sulfate, nitrate and organic particulates and their implications for control strategies. Calif. Air Res. Board ARB-5-384 and A6-171-30 Final Report.
- Pitts J. N., Jr. (1979) Chemical consequences of air quality standards and of control implementation programs: roles of hydrocarbons, oxides of nitrogen, oxides of sulfur and aged smog in the production of photochemical oxidant and aerosol. Calif. Air Res. Board A6-172-30 Final Report.
- Prideaux E. B. R. (1920) The deliquescence and drying of ammonium and alkali nitrates and a theory of the absorption of water vapour by mixed salts. *J. Soc. chem. Ind.* **39**, 182-185T.
- Prideaux E. B. R. and Caven R. M. (1919) The evaporation of concentrated and saturated solutions of ammonium nitrate, vapour pressures, heats of solution, and hydrolysis. *J. Soc. chem. Ind.* **38**, 353-355T.
- Rehinder P. (1926) Surface activity and adsorptive power. II. Water as a surface-active material. *Z. phys. Chem.* **121**, 103-126.
- Roux A., Musbally G. M., Perron G. and Desnoyers J. E. (1978) Apparent molal heat capacities and volumes of aqueous electrolytes at 25°C: NaClO<sub>3</sub>, NaClO<sub>4</sub>, NaNO<sub>3</sub>, NaBrO<sub>3</sub>, NaIO<sub>3</sub>, KClO<sub>3</sub>, KBrO<sub>3</sub>, KIO<sub>3</sub>, NH<sub>4</sub>NO<sub>3</sub>, NH<sub>4</sub>Cl, and NH<sub>4</sub>ClO<sub>4</sub>. *Can. J. Chem.* **56**, 24-28.
- Sorina G. A., Kozlovskaya G. M., Tsekhanskaya Y. V., Bezlyudova L. I. and Shmakov N. G. (1977) The specific heats of ammonium nitrate solutions and the partial specific heats of their components. *Russ. J. phys. Chem.* **51**, 1226-1227.
- Spicer C. W. (1974) The fate of nitrogen oxides in the atmosphere. Battelle Columbus Rep. to Coordinating Res. Council and U.S. Environ. Protection Agency Rep. 600/3-76-030.
- Stelson A. W., Friedlander S. K. and Seinfeld J. H. (1979) A note on the equilibrium relationship between ammonia and nitric acid and particulate ammonium nitrate. *Atmospheric Environment* **13**, 369-371.
- Stelson A. W. and Seinfeld J. H. (1981) Chemical mass accounting of urban aerosol. *Envir. Sci. Technol.* **15**, 671-679.
- Stelson A. W. and Seinfeld J. H. (1982) Relative humidity and pH dependence of the vapor pressure of ammonium nitrate-nitric acid solutions at 25°C. *Atmospheric Environment* **16**, 993-1000.
- Stephen H. and Stephen T. eds. (1963) *Solubilities of Inorganic and Organic Compounds*. Vol. 1, Part 1, p. 217. Macmillan, New York.
- Stephens E. R. and Price M. A. (1972) Comparison of synthetic and smog aerosols. *J. Coll. Int. Sci.* **39**, 272-286.
- Tang I. N. (1980) Deliquescence properties and particle size change of hygroscopic aerosols. In *Generation of Aerosols* (Edited by K. Willeke), Chap. 7. Ann Arbor Science Publishers, Ann Arbor.
- Tuazon E. C., Winer A. M., Graham R. A. and Pitts J. N. Jr. (1980) Atmospheric measurements of trace pollutants by kilometer pathlength FT-IR spectroscopy. *Adv. envir. Sci. Technol.* **10**, 259-300.
- Vanderzee C. E., Waugh D. H. and Haas N. C. (1980) Enthalpies of dilution and relative apparent molar enthalpies of aqueous ammonium nitrate. The case of a weakly hydrolysed (dissociated) salt. *J. chem. Thermodynamics* **12**, 21-25.
- Wagman D. D., Evans W. H., Parker V. B., Harlow I., Baily S. M. and Schumm R. H. (1968) Selected values of chemical thermodynamic properties; tables for the first thirty-four elements in the standard order of arrangement. NBS technical note 270-3.
- Weast R. C. ed. (1973) *Handbook of Chemistry and Physics*, 54th Edn., p. D-159. Chemical Rubber Publ. Co., Cleveland.

CHAPTER III

RELATIVE HUMIDITY AND pH DEPENDENCE OF THE  
VAPOR PRESSURE OF AMMONIUM NITRATE-NITRIC  
ACID SOLUTIONS AT 25°C

A. W. Stelson and J. H. Seinfeld

## RELATIVE HUMIDITY AND pH DEPENDENCE OF THE VAPOR PRESSURE OF AMMONIUM NITRATE-NITRIC ACID SOLUTIONS AT 25° C

ARTHUR W. STELSON and JOHN H. SEINFELD

Department of Chemical Engineering, California Institute of Technology, Pasadena, CA 91125, U.S.A.

(First received 22 May 1981 and in final form 6 July 1981)

**Abstract**—Quantitative expressions for the ammonia-nitric acid equilibrium product and the partial pressures of ammonia and nitric acid over non-ideal nitric acid-ammonium nitrate solutions are developed. The relative humidity and pH dependence of the equilibrium product and the partial pressures are obtained from free energy thermodynamic data. The thermodynamic predictions show the ammonia-nitric acid equilibrium product is inversely related to relative humidity. The importance of correcting for non-ideality is demonstrated. The assumption of ideality for ammonium nitrate in solution incurs an error of an order of magnitude in the ammonia-nitric acid equilibrium product prediction at the point of deliquescence and of 20% in the relative humidity of deliquescence. The trends indicated by the analysis are consistent with the filter study results of Forrest, Tanner, Spandau, D'Ottavio and Newman (1980, *Atmospheric Environment* 14, 137-144) and Appel, Wall, Tokiwa and Haik (1980, *Atmospheric Environment* 14, 549-554).

### INTRODUCTION

The presence of ammonium nitrate in atmospheric aerosols has been confirmed by a number of investigators (Lundgren, 1970; Stephens and Price, 1972; Gordon and Bryan, 1973; Mamane and Pueschel, 1980). The studies of Doyle, Tuazon, Graham, Mischke, Winer and Pitts (1979) and Stelson, Friedlander and Seinfeld (1979) have inferred the existence of an equilibrium between ammonium nitrate precursors, ammonia and nitric acid, and solid particulate ammonium nitrate. Using the ambient ammonia and nitric acid data of Spicer (1974) at West Covina, CA, Stelson *et al.* (1979) showed that the measured and predicted concentration products,  $K = P_{\text{NH}_3}P_{\text{HNO}_3}$ , were in essential agreement. Doyle *et al.* (1979) demonstrated the same phenomenon at Riverside, CA based on FT-IR ammonia and nitric acid measurements.

Significant problems in the measurement of aerosol nitrate have been experienced. Smith, Grosjean and Pitts (1978) found substantial losses of particulate nitrate and ammonium from high volume glass fiber filter samples taken at Riverside, CA when stored at room temperature. The data of Smith *et al.* (1978) are re-interpreted in Fig. 1, where a least squares fit of the molar ammonium and nitrate losses produces a line with slope 1.094, strongly indicative of  $\text{NH}_4\text{NO}_3$  volatilization. Forrest *et al.* (1980) spiked filters with  $\text{NH}_4\text{NO}_3$  and drew ambient air through the filters for 3-5 h. The greatest  $\text{NH}_4\text{NO}_3$  losses occurred at relative humidities below 60%, whereas at 100% relative humidity, no  $\text{NH}_4\text{NO}_3$  was lost. Appel *et al.* (1980) measured  $\text{NH}_3$  and  $\text{HNO}_3$  concentration products,  $P_{\text{NH}_3}P_{\text{HNO}_3}$ , at Pittsburg, CA using filter techniques and obtained values generally below those needed for

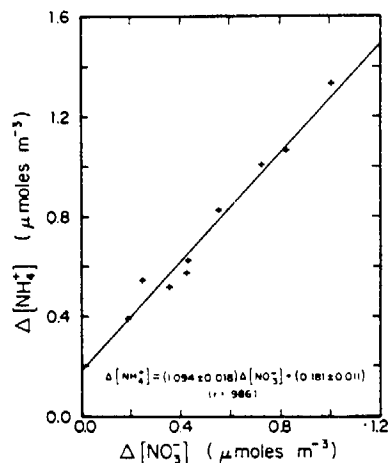


Fig. 1. Molar ammonium and nitrate losses from high volume glass fiber filters stored at room temperature. — Linear least square fit. + Data of Smith *et al.* (1978).

saturation, even though aerosol nitrate was present.

Stelson and Seinfeld (1981) have shown that Los Angeles aerosols contain ionic solids or concentrated solutions, 8-26 M. The ionic strengths corresponding to these concentrations lie in the range where ionic strength is most sensitive to relative humidity, suggesting that relative humidity is an important determinant of aerosol water content.

The object of this work is to further our understanding of the  $\text{NH}_3\text{-HNO}_3\text{-H}_2\text{O}$  system by studying the role of relative humidity and pH on the system's equilibrium. One issue that can be addressed with such a study, for example, is explanation of the filter results

of Appel *et al.* (1980) and Forrest *et al.* (1980). Specifically, we wish to carry out a thermodynamic analysis of the  $\text{NH}_3\text{-HNO}_3\text{-H}_2\text{O}$  system at 25° C for pH varying from 1 to 7 and relative humidity varying between 0 and 100%. In our analysis, no assumptions concerning the ideality of solutions will be made. The results can be compared to those of ideal solution theory as well as to the semi-quantitative ones of Tang (1980a). No corrections will be made for the Kelvin effect, since the aerosols of interest have been shown generally to exceed 0.5  $\mu\text{m}$  dia. (Lundgren, 1970; Mamane and Poeschel, 1980).

A calculation procedure for the ammonia-nitric acid equilibrium product relative humidity dependence over solid and aqueous ammonium nitrate is developed. Then, expressions for the individual ammonia and nitric acid partial pressures over non-ideal ammonium nitrate-nitric acid solutions are derived. Finally, the influence of pH on the partial pressures of ammonia and nitric acid is explored.

#### AMMONIA-NITRIC ACID EQUILIBRIUM PRODUCT OVER SOLID AND AQUEOUS AMMONIUM NITRATE

Below 62% relative humidity at 25° C, ammonium nitrate should be present as a solid, and above this value it should be in solution (Stelson *et al.*, 1979). Although recent work of Tang (1980b) indicates ammonium nitrate does not exhibit traditional deliquescence but is hygroscopic at relative humidities greater than about 30%, we will assume ammonium nitrate deliquesces at 62% relative humidity for the purpose of this work.

Recent available free energy data for the  $\text{NH}_3\text{-HNO}_3\text{-H}_2\text{O}$  system are given in Table 1, from which the equilibrium constants for the  $\text{NH}_3\text{-HNO}_3\text{-H}_2\text{O}$  system in Table 2 can be calculated. The equilibrium constants in Table 2 and throughout this paper are thermodynamic equilibrium constants where pressure is referenced to one atmosphere and aqueous solute concentration to unit molality. The differences between the values for reactions 4-6 and those of Tang (1980a) are < 6%. A 21% difference exists between the equilibrium constant used for reaction 3 by Tang (1980a) and the value in Table 2.

The equilibrium constants listed in Table 2 can be tested for internal consistency in two ways. First,  $K_2$  should equal  $K_5 K_4 K_3 / K_6$ . Based on the values given,  $K_5 K_4 K_3 / K_6 = 2.46 \times 10^{-18}$  vs  $K_2 = 2.71 \times 10^{-18}$ , an error of 9.2%. Second,  $K_1$  should equal  $K_2 a_{\text{NH}_4\text{NO}_3}$ , where  $a_{\text{NH}_4\text{NO}_3}$  = saturated ammonium nitrate solution activity. Using the value of  $a_{\text{NH}_4\text{NO}_3}$  of Hamer and Wu (1972),  $K_1 = 3.14 \times 10^{-17}$ , which agrees well with  $K_1 = 3.03 \times 10^{-17}$  as calculated and given in Table 2.

For ammonium nitrate at 25° C below 62% relative humidity, the equilibrium product is  $K_1$ . Above 62%, the equilibrium product is given by

$$p_{\text{NH}_3} p_{\text{HNO}_3} = K_2 \gamma_{\text{NH}_4^+} \gamma_{\text{NO}_3^-} m_{\text{NH}_4^+} m_{\text{NO}_3^-} = K_2 (\gamma_{\pm})_{\text{NH}_4\text{NO}_3}^2 m_{\text{NH}_4\text{NO}_3}^2 \quad (1)$$

where  $p_{\text{NH}_3}$ ,  $p_{\text{HNO}_3}$  = the partial pressures of ammonia and nitric acid;  $\gamma_{\text{NH}_4^+}$ ,  $\gamma_{\text{NO}_3^-}$  = the molal activity coefficients of the  $\text{NH}_4^+$  and  $\text{NO}_3^-$  ions;  $m_{\text{NH}_4^+}$ ,  $m_{\text{NO}_3^-}$ ,  $m_{\text{NH}_4\text{NO}_3}$  = the molalities of  $\text{NH}_4^+$ ,  $\text{NO}_3^-$  and  $\text{NH}_4\text{NO}_3$  and  $(\gamma_{\pm})_{\text{NH}_4\text{NO}_3}$  = the mean molal activity coefficient for  $\text{NH}_4\text{NO}_3$ . Using the  $\text{NH}_4\text{NO}_3$  solution

Table 1. Free energy data for the  $\text{NH}_3\text{-HNO}_3\text{-H}_2\text{O}$  system at 298 K

Species	$\Delta G/R, K^{-1}$	Reference
$\text{NH}_3(\text{g})$	- 1,977	Parker <i>et al.</i> (1976)
$\text{HNO}_3(\text{g})$	- 8,903	JANAF (1971)
$\text{NH}_4\text{NO}_3(\text{c. IV})$	- 22,220	Parker <i>et al.</i> (1976)
$\text{NH}_4\text{NO}_3(\text{aq}, m = 1)$	- 22,940	Wagman <i>et al.</i> (1968)
$\text{NO}_3^-(\text{aq}, m = 1)$	- 13,410	Parker <i>et al.</i> (1976)
$\text{H}^+(\text{aq}, m = 1)$	0	Parker <i>et al.</i> (1976)
$\text{NH}_4^+(\text{aq}, m = 1)$	- 9,558	Parker <i>et al.</i> (1976)
$\text{H}_2\text{O}(\text{l})$	- 28,530	Parker <i>et al.</i> (1976)
$\text{NH}_3 \cdot \text{H}_2\text{O}(\text{aq})$	- 31,730	Wagman <i>et al.</i> (1968)
$\text{OH}^-(\text{aq}, m = 1)$	- 18,925	Parker <i>et al.</i> (1976)

Table 2. Equilibrium constants for the  $\text{NH}_3\text{-HNO}_3\text{-H}_2\text{O}$  system at 298 K

Reaction	Equilibrium constant*
1 $\text{NH}_4\text{NO}_3(\text{c. IV}) \rightleftharpoons \text{NH}_3(\text{g}) + \text{HNO}_3(\text{g})$	$3.03 \times 10^{-17}$
3 $\text{NH}_4\text{NO}_3(\text{aq}) \rightleftharpoons \text{NH}_3(\text{g}) + \text{HNO}_3(\text{g})$	$2.71 \times 10^{-18}$
3 $\text{NO}_3^-(\text{aq}) + \text{H}^+(\text{aq}) \rightleftharpoons \text{HNO}_3(\text{g})$	$2.72 \times 10^{-7}$
4 $\text{NH}_3 \cdot \text{H}_2\text{O}(\text{aq}) \rightleftharpoons \text{H}_2\text{O}(\text{l}) + \text{NH}_3(\text{g})$	$1.65 \times 10^{-2}$
5 $\text{NH}_4^+(\text{aq}) + \text{OH}^-(\text{aq}) \rightleftharpoons \text{NH}_3 \cdot \text{H}_2\text{O}(\text{aq})$	$5.37 \times 10^4$
6 $\text{H}^+(\text{aq}) + \text{OH}^-(\text{aq}) \rightleftharpoons \text{H}_2\text{O}(\text{l})$	$9.79 \times 10^{13}$

\* Values calculated from the free energy data of Table 1.

activity coefficient data from Hamer and Wu (1972), the equilibrium product can be calculated as a function of  $\text{NH}_4\text{NO}_3$  molality. The relative humidity, r.h., over the solution can be calculated as a function of  $\text{NH}_4\text{NO}_3$  molality from the molal osmotic coefficients in Hamer and Wu (1972),

$$\text{r.h.} = 100.0 a_w = 100.0 \exp(-3.6031 \times 10^{-2} m_{\text{NH}_4\text{NO}_3} \phi_m), \quad (2)$$

where  $a_w$  = the water activity and  $\phi_m$  = the molal osmotic coefficient at  $m_{\text{NH}_4\text{NO}_3}$ . Since the equilibrium product and the relative humidity over solution are both solely dependent on  $m_{\text{NH}_4\text{NO}_3}$ , the equilibrium product -  $m_{\text{NH}_4\text{NO}_3}$  functionality can be replaced by a function relating the equilibrium product directly to the relative humidity, as in Fig. 2. Note that the product,  $p_{\text{NH}_3} p_{\text{HNO}_3}$ , is expressed in units of  $\text{ppb}^2$  in Fig. 2 for convenience in atmospheric applications. The effect of non-ideality can be examined by assuming  $\phi_m$  and  $(\gamma_{\pm})_{\text{NH}_4\text{NO}_3}$  are unity. (See the curve labelled ideal solution in Fig. 2.) The ideal solution curve ends at  $m_{\text{NH}_4\text{NO}_3} = 25.954$ , saturated  $\text{NH}_4\text{NO}_3$  solution at  $25^\circ\text{C}$ , which shows the ideal solution approach grossly mispredicts the deliquescence relative humidity.

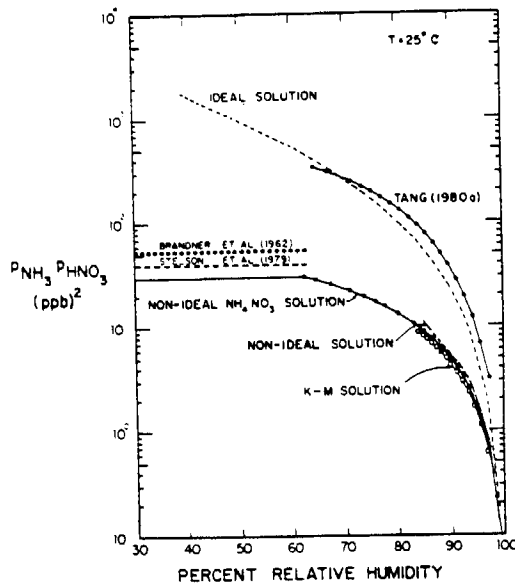


Fig. 2. Effect of relative humidity on ammonia-nitric acid partial pressure product.

The approach of Tang (1980a) can also be used to evaluate the product,  $p_{\text{NH}_3} p_{\text{HNO}_3}$ , for pH, 1-7, and ammonium nitrate concentrations, 1.0-10.5 M. Over this range of hydrogen, ammonium and nitrate concentrations, the amount of undissociated nitric acid predicted by the approach of Tang (1980a) was < 0.3%. Thus, it is appropriate within this regime to consider the amount of undissociated nitric acid to be zero, i.e. purely an ionic solution. For very acidic

solutions,  $\text{pH} < 1$ , the presence of undissociated nitric acid must be taken into account. The  $p_{\text{NH}_3} p_{\text{HNO}_3}$  values shown in Fig. 2 on the curve labelled Tang (1980a) represent the limit as  $\text{pH} \rightarrow 7$ , although the variation between  $\text{pH} = 1$  and 7 is not large. The water activity was determined assuming the solution was purely ammonium nitrate. The molal osmotic coefficient data from Hamer and Wu (1972) were used to calculate the water activity, and the molar to molal concentration conversion was carried out using  $\text{NH}_4\text{NO}_3$  solution density data of Adams and Gibson (1932). The calculated result is shown in Fig. 2.

The solid  $\text{NH}_4\text{NO}_3$  vapor pressure product calculated using a least squares fit of the data of Brandner, Junk, Lawrence and Robins (1962) and the thermodynamic prediction of Stelson *et al.* (1979) are also shown in Fig. 2. The new solid vapor pressure product prediction and the non-ideal  $\text{NH}_4\text{NO}_3$  solution curve at saturation join closely, indicating the improved quality of this prediction for the  $\text{NH}_4\text{NO}_3$  solid vapor pressure product at  $25^\circ\text{C}$  over that of Stelson *et al.* (1979).

Finally, curves labelled non-ideal and K-M solution are shown in Fig. 2. The K-M solution curve was calculated by multiplying ammonia and nitric acid partial pressures determined from equilibria 3-6 in Table 2. The non-ideal solution curve serves as a check of the assumptions used in deriving quantitative expressions for the ammonia and nitric acid partial pressures. The procedure used in calculating the individual nitric acid and ammonia partial pressures will now be developed.

#### NITRIC ACID PARTIAL PRESSURE

The nitric acid partial pressure is determined from the equilibrium of reaction 3 in Table 2,

$$p_{\text{HNO}_3} = K_3 \gamma_{\text{H}} \gamma_{\text{NO}_3} m_{\text{H}} m_{\text{NO}_3}, \quad (3)$$

where  $\gamma_{\text{H}}$  = the molal activity coefficient for  $\text{H}^+$  ion and  $m_{\text{H}} = \text{H}^+$  ion molality. Kusik and Meissner (1978) developed an expression for predicting the activity coefficient of a salt in a multicomponent electrolytic mixture from which the  $\gamma_{\text{H}} \gamma_{\text{NO}_3}$  product can be evaluated,

$$\gamma_{\text{H}} \gamma_{\text{NO}_3} = (\gamma_{\pm})_{\text{H}, \text{NO}_3}^{1+x} (\gamma_{\pm})_{\text{NH}_4^+, \text{NO}_3}^{-x}, \quad (4)$$

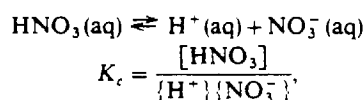
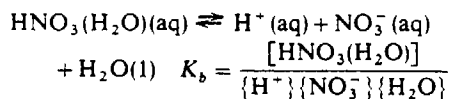
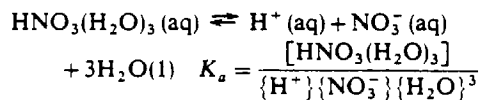
where  $x = m_{\text{H}}/m_{\text{NO}_3}$  and  $(\gamma_{\pm})_{\text{H}, \text{NO}_3}$  = mean molal activity coefficient for dissociated nitric acid. Using the value for  $K_3$  determined from thermodynamic data in Table 1,

$$p_{\text{HNO}_3} = 272 (\gamma_{\pm})_{\text{H}, \text{NO}_3}^{1+x} (\gamma_{\pm})_{\text{NH}_4^+, \text{NO}_3}^{-x} x m_{\text{NO}_3}^2 (\text{ppb}). \quad (5)$$

By specifying  $m_{\text{H}}$ ,  $m_{\text{NO}_3}$  and  $m_{\text{NH}_4^+}$ , the ionic strength,  $I$ , is determined by  $I = m_{\text{NO}_3} + m_{\text{NH}_4^+}$ , and only  $(\gamma_{\pm})_{\text{H}, \text{NO}_3}$  needs to be evaluated to calculate the nitric acid partial pressure. The ionic strength functional dependence of  $(\gamma_{\pm})_{\text{H}, \text{NO}_3}$  must be calculated by an

indirect method which is different from the usual experimental activity coefficient determination methods, vapor pressure, freezing point depression or electrochemical, since nitric acid does not totally dissociate in water.

The degree of dissociation of nitric acid in water as a function of acid concentration can be determined using the approach of Högfeltdt (1963), in which the dissociation of nitric acid is represented by three equilibria:



where [ ] represents molar concentration and { } refers to the activity.  $K_a$ ,  $K_b$  and  $K_c$  are  $3.63 \times 10^{-2}$ ,  $8.13 \times 10^{-3}$  and  $1.66 \times 10^{-4}$ , respectively (Högfeltdt, 1963). Högfeltdt (1963) assumes the molar activity coefficients of the undissociated aqueous nitrate species to be unity. When converting to a molal basis, the undissociated nitric acid species molal activity coefficient,  $\gamma_u$ , is not unity, but rather is given by

$$\gamma_u = \frac{1000d}{d_0(1000 + M_{\text{HNO}_3}m_s)} \quad (6)$$

where  $d$  and  $d_0$  are the nitric acid solution and pure water densities in  $\text{gm ml}^{-1}$ , respectively,  $M_{\text{HNO}_3}$  = the molecular weight of nitric acid, and  $m_s$  = the stoichiometric nitric acid molality. Using Högfeltdt's equilibria and Equation (6), the fraction of nitric acid that is dissociated,  $\alpha$ , can be calculated from

$$\alpha = 1 - \frac{d_0 \gamma_u^2 m_s}{\gamma_u} (K_a a_w^3 + K_b a_w + K_c) \quad (7)$$

where  $\gamma_s$  = the stoichiometric molal nitric acid activity coefficient. The dissociation of nitric acid can be calculated using the stoichiometric molal nitric acid activity and water activity data fit of Hamer and Wu (1972), pure water density and nitric acid molecular weight of Weast (1973), and the nitric acid solution density interpolation formula of Granzhan and Laktionova (1975). The dissociation calculated from Equation (7) is compared to the dissociation data of Krawetz (1955) and Redlich, Duerst and Merbach (1968) in Fig. 3. The agreement, especially with the data of Redlich *et al.* (1968), is good.

The total nitric acid dissociation constant can be expressed in terms of  $K_a$ ,  $K_b$  and  $K_c$  by

$$K_N = \frac{1}{K_a a_w^3 + K_b a_w + K_c} \quad (8)$$

Using Högfeltdt's equilibrium constants and noting that  $a_w = 1.0$  at infinite dilution,  $K_N = 22.4$ , which

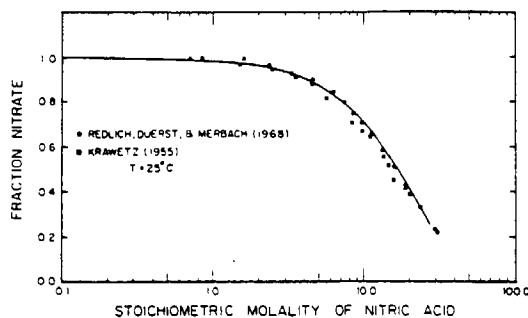


Fig. 3. Ionization of nitric acid.

compares favorably with values of 15.4, 20.0 and 26.8 from Davis and De Bruin (1964), Redlich *et al.* (1968) and Young Maranville and Smith (1959), respectively.

The mean molal ionic activity coefficients for the  $\text{H}^+$  and  $\text{NO}_3^-$  ions,  $(\gamma_{\pm})_{\text{HNO}_3}$ , can be found from

$$(\gamma_{\pm})_{\text{HNO}_3} = \gamma_s / \alpha \quad (9)$$

Using Equations (6), (7) and (9),  $(\gamma_{\pm})_{\text{HNO}_3}$  can be calculated as a function of ionic strength. The maximum ionic strength is about 8.3 M and occurs between 17 and 21 stoichiometric nitric acid molality. The mean molal ionic activity coefficient polynomial regression up to 7.5 M is

$$\ln (\gamma_{\pm})_{\text{HNO}_3} = \frac{-1.17625\sqrt{I}}{1 + 1.44\sqrt{I}} + 2.260 \times 10^{-1} I - 4.722 \times 10^{-2} I^2 + 1.656 \times 10^{-2} I^3 - 2.396 \times 10^{-3} I^4 + 1.384 \times 10^{-4} I^5 \quad (10)$$

where the standard deviation is  $\pm 0.0022$ . Although  $(\gamma_{\pm})_{\text{HNO}_3}$  should also be a function of the undissociated nitric acid concentration, the effect of undissociated nitric acid will be shown to be negligible up to 7.0 ionic strength.

#### AMMONIA PARTIAL PRESSURE

The partial pressure of ammonia over the solution is (Tang, 1980a)

$$p_{\text{NH}_3} = \frac{K_4 K_5}{K_6} \frac{\gamma_{\text{NH}_4} m_{\text{NH}_4}}{\gamma_{\text{H}} m_{\text{H}}} \quad (11)$$

By specifying  $m_{\text{NH}_4}$ ,  $m_{\text{H}}$  and  $m_{\text{NO}_3}$ , the ionic strength is determined, and  $\gamma_{\text{NH}_4}/\gamma_{\text{H}}$  depends on the ionic strength. From the approach of Kusik and Meissner (1978)

$$\frac{\gamma_{\text{NH}_4}}{\gamma_{\text{H}}} = \frac{(\gamma_{\pm})_{\text{NH}_4\text{NO}_3}}{(\gamma_{\pm})_{\text{HNO}_3}} \quad (12)$$

and Equation (11) simplifies to

$$p_{\text{NH}_3} = 9.05 \times 10^{-3} \frac{(\gamma_{\pm})_{\text{NH}_4\text{NO}_3}}{(\gamma_{\pm})_{\text{HNO}_3}} \left( \frac{1-x}{x} \right) (\text{ppb}) \quad (13)$$

with the values for the equilibrium constants from Table 2.

### VARIATION OF AMMONIA AND NITRIC ACID PARTIAL PRESSURES AS A FUNCTION OF pH

The variation of the ammonia and nitric acid partial pressures as a function of pH can be evaluated using the expression for  $(\gamma_{\pm})_{\text{NH}_4\text{NO}_3}$  from Hamer and Wu (1972) and Equations (5), (10) and (13). The water activity of the  $\text{NH}_4\text{NO}_3\text{-HNO}_3$  solution,  $(a_w)_{\text{MIX}}$ , is given by

$$(a_w)_{\text{MIX}} = (a_w)_{\text{HNO}_3}^x (a_w)_{\text{NH}_4\text{NO}_3}^{1-x} \quad (14)$$

where  $(a_w)_{\text{HNO}_3}$  is obtained from Equation (10) and the Gibbs-Duhem relationship (Kusik and Meissner, 1978). The variation of  $p_{\text{NH}_3}$  and  $p_{\text{HNO}_3}$  with pH is shown in Fig. 4 for a relative humidity of 94.5%. Also shown are the results of Tang (1980a) and those calculated assuming an ideal solution. The solid lines labelled Tang (1980a) were taken directly from Tang (1980a), and the points labelled Tang (1980a) were calculated using his procedure to ensure an accurate duplication of that work. Figure 4 shows the approach of this work and that of Tang (1980a) differ in both the individual ammonia and nitric acid partial pressures, differences that become larger so the relative humidity decreases or ionic strength increases.

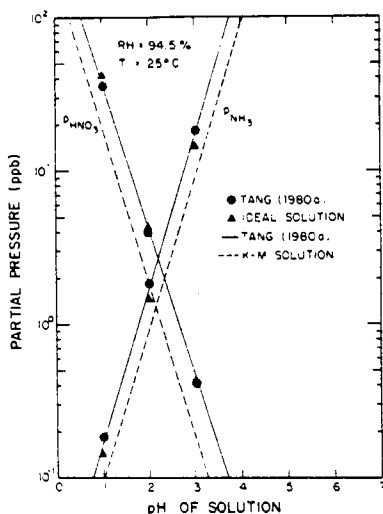


Fig. 4. Effect of pH on the ammonia and nitric acid partial pressures.

The product of the ammonia and nitric acid partial pressures calculated from Equations (5) and (13) as a function of relative humidity is compared to the equilibrium product calculated using ammonium nitrate activities in Fig. 2. By comparing the curves labelled K-M solution and non-ideal  $\text{NH}_4\text{NO}_3$  solution, the agreement is shown to be good. The major source of disagreement between the K-M solution and the non-ideal  $\text{NH}_4\text{NO}_3$  solution curves is the 9.2% difference between  $K_5 K_4 K_3 / K_6$  and  $K_2$ . The insensitivity of  $p_{\text{NH}_3} p_{\text{HNO}_3}$  to pH can be seen in the

range of relative humidity variation by multiplying Equations (5) and (13),

$$p_{\text{NH}_3} p_{\text{HNO}_3} = 2.46 (\gamma_{\pm})_{\text{HNO}_3}^x (\gamma_{\pm})_{\text{NH}_4\text{NO}_3}^{2-x} \times (1-x) m_{\text{NO}_3}^2 \text{ (ppb}^2\text{)}. \quad (15)$$

As the relative humidity decreases, the maximum  $x$ , which occurs at  $\text{pH} = 1$ , becomes smaller. Thus, the difference between an acidic ammonium nitrate solution ( $\text{pH} > 1$ ) and a pure ammonium nitrate solution partial pressure product decreases with relative humidity.

### EFFECT OF NEGLECTING UNDISSOCIATED NITRIC ACID AND ION-PAIRING

In developing quantitative expressions for the ammonia and nitric acid partial pressures, two assumptions were invoked. First, the effect of undissociated nitric acid on the  $(\gamma_{\pm})_{\text{HNO}_3}$  ionic strength functionality is small, below 7.0 M. Second, ion-pairing of  $\text{NH}_4^+$  and  $\text{NO}_3^-$  ions has a minimal effect on the ammonia partial pressures predicted. Equation (15) requires as  $x \rightarrow 0$ , the solute activity approaches  $(\gamma_{\pm})_{\text{NH}_4\text{NO}_3}^2 m_{\text{NH}_4\text{NO}_3}^2$ . Similarly, Equation (4) requires  $\gamma_{\text{H}} \gamma_{\text{NO}_3}$  to approach  $(\gamma_{\pm})_{\text{HNO}_3}^2$  as  $x \rightarrow 1$ . Inherent in Equations (4) and (15) are the correct limits but neither equation gives insight into the effect of these two assumptions. By an alternative expression for  $(\gamma_{\pm})_{\text{NH}_4\text{NO}_3}^2$ ,

$$(\gamma_{\pm})_{\text{NH}_4\text{NO}_3}^2 = \gamma_{\text{NH}_4} \gamma_{\text{NO}_3} = \frac{\gamma_{\text{NH}_4}}{\gamma_{\text{H}}} (\gamma_{\text{H}} \gamma_{\text{NO}_3}), \quad (16)$$

where  $\gamma_{\text{NH}_4} / \gamma_{\text{H}}$  and  $\gamma_{\text{H}} \gamma_{\text{NO}_3}$  are evaluated independently from  $\text{NH}_4\text{NO}_3$ , the relative error can be ascertained.

The  $\gamma_{\text{H}} \gamma_{\text{NO}_3}$  product will be given by  $(\gamma_{\pm})_{\text{HNO}_3}^2$ , which assumes the undissociated nitric acid contribution is small.

The ammonium to hydrogen ion activity coefficient ratio,  $\gamma_{\text{NH}_4} / \gamma_{\text{H}}$ , can be evaluated from mean molal activity coefficients of an ammoniated salt,  $\text{NH}_4\text{X}$ , and the acid with the same anion,  $\text{HX}$ , provided the acid completely dissociates. The ammonium to hydrogen ion activity coefficient ratio can be calculated noting that

$$\frac{\gamma_{\text{NH}_4}}{\gamma_{\text{H}}} = \left( \frac{(\gamma_{\pm})_{\text{NH}_4\text{X}}}{(\gamma_{\pm})_{\text{HX}}} \right)^2, \quad (17)$$

where  $(\gamma_{\pm})_{\text{NH}_4\text{X}}$  = the mean molal activity coefficient of salt  $\text{NH}_4\text{X}$  and  $(\gamma_{\pm})_{\text{HX}}$  = the mean molal activity coefficient of acid  $\text{HX}$ . This approach was tested with five different anions,  $\text{Cl}^-$ ,  $\text{NO}_3^-$ ,  $\text{I}^-$ ,  $\text{Br}^-$  and  $\text{ClO}_4^-$  (see Fig. 5). The assumption that  $\text{HCl}$ ,  $\text{HBr}$ ,  $\text{HI}$  and  $\text{HClO}_4$  totally dissociate in solutions below 7 M or saturation is appropriate since the dissociation constants are very large,  $> 10^7$  (McCoubrey, 1955; Bockris and Reddy, 1970). It is incorrect to assume that  $\text{HNO}_3$  completely dissociates, so the  $\text{NO}_3^-$  curve was calculated using  $(\gamma_{\pm})_{\text{HNO}_3}$  as previously derived.

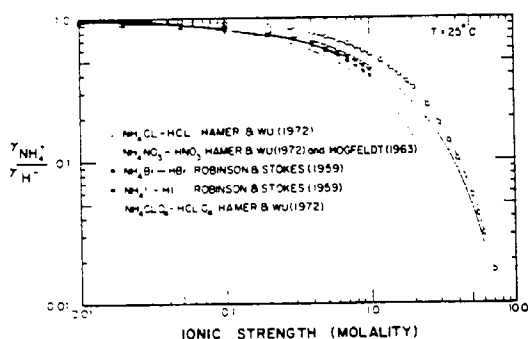


Fig. 5. Effect of ionic strength on calculated ammonium-hydrogen ion mean molal activity coefficient ratio.

Lee and Wilmschurst (1964) have shown that a 5 M  $\text{NH}_4\text{Cl}$  solution forms ion-pairs. The observed mean molal activity coefficient,  $(\gamma_{\pm})_{\text{NH}_4\text{X}}$ , must be corrected as follows (Bockris and Reddy, 1970),

$$(\gamma_{\pm})'_{\text{NH}_4\text{X}} = \frac{(\gamma_{\pm})_{\text{NH}_4\text{X}}}{1 - \theta} \quad (18)$$

where  $(\gamma_{\pm})'_{\text{NH}_4\text{X}}$  is the corrected mean molal activity coefficient for salt  $\text{NH}_4\text{X}$  and  $\theta$  = the fraction of  $\text{NH}_4$  and X ions forming ion-pairs. Equation (18) assumes the ion-pairs are symmetric (Robinson and Stokes, 1959). Also, the ionic strength would be corrected to  $(1 - \theta)m_{\text{NH}_4\text{X}}$ . The net effect of ion-pairing on the curves in Fig. 5 is not obvious since the  $\text{NH}_4\text{X}$  mean molal activity coefficient would increase and the ionic strength would decrease. Using density data of Pearce and Pumphlin (1937), a 5-M  $\text{NH}_4\text{Cl}$  solution in approximately 6.25 M. The  $\text{NH}_4\text{Cl}$ -HCl ammonium to hydrogen ion activity coefficient ratio is used to represent  $\gamma_{\text{NH}_4^+}/\gamma_{\text{H}^+}$  to 7.0 M. Thus, some  $\text{NH}_4\text{Cl}$  ion-pairing must be present above 6.25 M.

With (1), (10) (16) and (17) and replacing  $K_2$  by  $K_5K_4K_3, K_6$ , the effect of ion-pairing and the undissociated nitric acid can be ascertained. We refer the reader to the curve labelled non-ideal solution in Fig. 2. The water activity was calculated from (2). The agreement between the non-ideal, non-ideal  $\text{NH}_4\text{NO}_3$ , and K-M solution curves supports the assumptions of neglecting both the influence of undissociated nitric acid on the mean molal activity coefficient of dissociated nitric acid,  $(\gamma_{\pm})_{\text{HNO}_3}$ , and the presence of ion-pairing in calculating  $\gamma_{\text{NH}_4^+}/\gamma_{\text{H}^+}$ . By comparing the K-M and non-ideal solution curves, the maximum possible error in the individual partial pressures can be ascertained as about 30%.

Assuming  $\gamma_{\text{H}^+}\gamma_{\text{NO}_3^-} = (\gamma_{\pm})_{\text{HNO}_3}^2$  and (17) holds, the  $\gamma_{\text{H}^+}\gamma_{\text{HNO}_3}$  product and the  $\gamma_{\text{NH}_4^+}/\gamma_{\text{H}^+}$  ratio calculated cannot be used for calculating the individual partial pressures of ammonia and nitric acid because  $\gamma_{\text{H}^+}\gamma_{\text{NO}_3^-}$  goes to the wrong limit as  $x \rightarrow 0$  and  $\gamma_{\text{NH}_4^+}/\gamma_{\text{H}^+}$  goes to the wrong limit as  $x \rightarrow 1$ . Even though these expressions cannot be used for the individual partial pressures, they can be multiplied together to check the

ammonia-nitric acid partial pressure product calculated from (1) and (15) and the possible significance of ion-pairing and the undissociated nitric acid in calculating  $(\gamma_{\pm})_{\text{HNO}_3}$ .

## DISCUSSION

This approach gives theoretical justification for the results of Forrest *et al.* (1980) and Appel *et al.* (1980). As the relative humidity approaches 100%, the equilibrium vapor pressure product sharply decreases by several orders of magnitude. At 98% relative humidity and 25°C, the mass concentration of  $\text{NH}_3$  plus  $\text{HNO}_3$  (equimolar basis) in the gas in equilibrium with an aqueous ammonium nitrate solution is about  $1.9 \mu\text{g m}^{-3}$  vs  $17.9 \mu\text{g m}^{-3}$  needed if ammonium nitrate is present as a solid. Thus, the observation of Forrest *et al.* (1980) that greatest ammonium nitrate filter losses occurred at relative humidities below 60%, and no losses occurred at 100% relative humidity, and the observations of Appel *et al.* (1980) that nitrate aerosol is present even though the equilibrium product of ammonia and nitric acid is much less than the solid equilibrium product are consistent with this work.

The ammonia-nitric acid equilibrium product relative humidity functionality does not significantly change when the pH is varied between 1 and 7. The insensitivity of the ammonia-nitric acid equilibrium product with pH variation results from the ammonia-nitric acid equilibrium product being dominantly dependent on ionic strength. As the pH decreases below 1, the approach used in this work is not applicable since the role of undissociated nitric acid becomes significant and similarly for high pH undissociated dissolved ammonia would appear. From the electroneutrality balance and the average aerosol water data in Stelson and Seinfeld (1981), a range of possible mass distribution averaged pH's between 2 and 12 is calculable for several locations in the Los Angeles Basin. Since the atmospheric aerosol is often a mixture of acidic and basic particles, a distribution of aerosol pH would exist, the basic particles existing predominantly in the coarse mode ( $> 1 \mu\text{m}$ ) and the acidic particles in the fine mode ( $< 1 \mu\text{m}$ ). Thus, these results have limited applicability to the possible range of existing ambient aerosol acidity.

Qualitatively, the result of adding an unreactive solute on the vapor pressure product-relative humidity curve can be discussed. The unreactive solute would lower the water vapor pressure but would not affect the ammonia-nitric acid vapor pressure product. Thus, the resulting situation would be a measured vapor pressure product and relative humidity location lying below the  $\text{NH}_4\text{NO}_3$  non-ideal vapor pressure product-relative humidity curve in Fig. 2.

The presence of a saturated ammonium nitrate solution around a solid ammonium nitrate aerosol core can be examined. Since the saturated solution must be in equilibrium with solid ammonium nitrate, the vapor pressure product must be the same over the

saturated solution as for the solid ammonium nitrate. Thus, the presence of a saturated aqueous layer around a solid ammonium nitrate core at relative humidities below 62% would not affect the equilibrium vapor pressure product prediction.

An additional important thermodynamic concept is the Gibbs-Duhem relationship which shows that solute activities determine the water activity. Thus, the equilibrium product and the relative humidity cannot be varied independently and to be theoretically consistent the solute or water activity must be determined by the other activities. Equation (14) shows the water activity can be taken as the water activity of a pure ammonium nitrate solution since the solutions are > 90% ammonium nitrate and the correction to make this theoretically rigorous is small.

Finally, this work illustrates an important concept in devising methods for performing equilibrium analysis. The equilibrium approach must be consistent, and certain limits must be satisfied. Internal consistency was demonstrated by the agreement between  $K_2$  and  $K_5K_4K_3/K_6$  and by the ammonia-nitric acid vapor pressure products of solid ammonium nitrate and a saturated ammonium nitrate solution being equal.

### CONCLUSIONS

Some important conclusions are evident from this work:

(1) The ammonia-nitric acid equilibrium product is strongly and inversely dependent on the relative humidity.

(2) A consistent set of free energy data exists such that the ammonia-nitric acid equilibrium products for solid ammonium nitrate and for a saturated ammonium nitrate aqueous solution are equal; i.e. no discontinuity exists in the ammonia-nitric acid equilibrium product prediction at the relative humidity of deliquescence at 25°C.

(3) The ammonium to hydrogen ion molal activity coefficient ratio is not unity for concentrated ionic solutions. By assuming it is unity, significant error in the calculated ammonia partial pressure results.

(4) The predicted relative humidity dependence of the ammonia-nitric acid equilibrium product is consistent with filter study results of Forrest *et al.* (1980) and Appel *et al.* (1980).

*Acknowledgement*—This work was supported by Environmental Protection Agency Grant R806844 and State of California Air Resources Board Contract A7-169-30.

### REFERENCES

- Adams L. H. and Gibson R. E. (1932) Equilibrium in binary systems under pressure. III. The influence of pressure on the solubility of ammonium nitrate in water at 25°C. *J. Am. chem. Soc.* **54**, 4520-4537.
- Appel B. R., Wall S. M., Tokiwa Y. and Haik M. (1980) Simultaneous nitric acid, particulate nitrate and acidity measurements in ambient air. *Atmospheric Environment* **14**, 549-554.
- Bockris J. O'M. and Reddy A. K. N. (1970) *Modern Electrochemistry; An Introduction to an Interdisciplinary Area*. Vol. 1. Plenum Press, New York.
- Brandner J. D., Junk N. M., Lawrence J. W. and Robins J. (1962) Vapor pressure of ammonium nitrate. *J. chem. Engng Data* **7**, 227-228.
- Davis W. Jr. and De Bruin H. J. (1964) New activity coefficients of 0-100 per cent aqueous nitric acid. *J. inorg. nucl. Chem.* **26**, 1069-1083.
- Doyle G. J., Tuazon E. C., Graham R. S., Mischke T. M., Winer A. M. and Pitts J. N. Jr. (1979) Simultaneous concentrations of ammonia and nitric acid in a polluted atmosphere and their equilibrium relationship to particulate ammonium nitrate. *Envir. Sci. Technol.* **13**, 1416-1419.
- Forrest J., Tanner R. L., Spandau D., D'Ottavio T. and Newman L. (1980) Determination of total inorganic nitrate utilizing collection of nitric acid on NaCl-impregnated filters. *Atmospheric Environment* **14**, 137-144.
- Gordon R. J. and Bryan R. J. (1973) Ammonium nitrate in airborne particles in Los Angeles. *Envir. Sci. Technol.* **7**, 645-647.
- Granzhan V. A. and Laktionova S. K. (1975) The densities, viscosities and surface tensions of aqueous nitric acid solutions. *Russ. J. phys. Chem.* **49**, 1448.
- Hamer W. J. and Wu Y. C. (1972) Osmotic coefficients and mean activity coefficients of uni-univalent electrolytes in water at 25°C. *J. phys. Chem. Ref. Data* **1**, 1047-1099.
- Högfeldt E. (1963) The complex formation between water and strong acids. *Acta chem. scand.* **17**, 785-796.
- JANAF Thermochemical Tables. 2nd edition (1971). NSRDS-NBS 37.
- Krawetz A. A. (1955) A raman spectral study of equilibria in aqueous solutions of nitric acid. Thesis. University of Chicago.
- Kusik C. L. and Meissner H. P. (1978) Electrolyte activity coefficients in inorganic processing. *A.I.Ch. E. Symp. Ser.* **173**, 14-20.
- Lee H. and Wilmshurst J. K. (1964) Observation of ion-pairs in aqueous solutions by vibrational spectroscopy. *Aust. J. Chem.* **17**, 943-945.
- Lundgren D. A. (1970) Atmospheric aerosol composition and concentration as a function of particle size and of time. *J. Air Pollut. Control Ass.* **20**, 603-608.
- Mamane Y. and Puschel R. F. (1980) A method for the detection of individual nitrate particles. *Atmospheric Environment* **14**, 629-639.
- McCoubrey J. C. (1955) The acid strength of the hydrogen halides. *Trans. Faraday Soc.* **51**, 743-747.
- Parker V. B., Wagman D. D. and Garvin D. (1976) Selected thermochemical data compatible with the CODATA recommendations. NBSIR 75-968.
- Pearce J. N. and Pumplun G. G. (1937) The apparent and partial molal volumes of ammonium chloride and of cupric sulfate in aqueous solution at 25°C. *J. Am. chem. Soc.* **59**, 1221-1222.
- Redlich O., Duerst R. W. and Merbach A. (1968) Ionization of strong electrolytes. XI. The molecular states of nitric acid and perchloric acid. *J. chem. Phys.* **49**, 2986-2994.
- Robinson R. A. and Stokes R. H. (1959) *Electrolyte Solutions: The Measurement and Interpretation of Conductance. Chemical Potential and Diffusion in Solutions of Simple Electrolytes*. 2nd edition. Butterworths, London.
- Smith J. P., Grosjean D. and Pitts J. N. Jr. (1978) Observation of significant losses of particulate nitrate and ammonium from high volume glass fiber filter samples stored at room temperature. *J. Air Pollut. Control Ass.* **28**, 930-933.
- Spicer C. W. (1974) The fate of nitrogen oxides in the atmosphere. Batelle Columbus Rep. to Coordinating Res.

- Council and U.S. Environ. Protection Agency Rep. 600/3-76-030.
- Stelson A. W., Friedlander S. K. and Seinfeld J. H. (1979) A note on the equilibrium relationship between ammonia and nitric acid and particulate ammonium nitrate. *Atmospheric Environment* **13**, 369-371.
- Stelson A. W. and Seinfeld J. H. (1981) Chemical mass accounting of urban aerosol. *Envir. Sci. Technol.* **15**, 671-679.
- Stephens E. R. and Price M. A. (1972) Comparison of synthetic and smog aerosols. *J. Coll. Int. Sci.* **39**, 272-286.
- Tang I. N. (1980a) On the equilibrium partial pressures of nitric acid and ammonia in the atmosphere. *Atmospheric Environment* **14**, 819-828.
- Tang I. N. (1980b) Deliquescence properties and particle size change of hygroscopic aerosols. In *Generation of Aerosols*, (Edited by K. Willeke) Ch. 7. Ann Arbor Science Publisher, Ann Arbor, Michigan.
- Wagman D. D., Evans W. H., Parker V. B., Harlow I., Baily S. M. and Schumm R. H. (1968) Selected values of chemical thermodynamic properties; tables for the first thirty-four elements in the standard order of arrangement. NBS Technical Note 270-3.
- Weast R. C. (1973) *Handbook of Chemistry and Physics*, 54th edition. CRC Press, Cleveland.
- Young T. F., Maranville L. F. and Smith H. M. (1959) Raman spectral investigation of ionic equilibria in solutions of strong electrolytes. In *The Structure of Electrolytic Solutions*, (Edited by W. J. Hamer) Ch. 4, John Wiley, New York.

CHAPTER IV

MATHEMATICAL MODELING OF THE FORMATION AND TRANSPORT  
OF AMMONIUM NITRATE AEROSOL

Armistead G. Russell  
Gregory J. McRae  
Glen R. Cass

## MATHEMATICAL MODELING OF THE FORMATION AND TRANSPORT OF AMMONIUM NITRATE AEROSOL

ARMISTEAD G. RUSSELL,\* GREGORY J. McRAE† and GLEN R. CASS‡

\*Department of Mechanical Engineering, †Environmental Quality Laboratory, ‡Environmental Engineering Science Department, California Institute of Technology, Pasadena, CA 91125, U.S.A.

(First received 19 April 1982; and in revised form 11 August 1982)

**Abstract**—A mathematical model describing the transport and formation of aerosol  $\text{NH}_4\text{NO}_3$  is presented. Based on a vertically resolved Lagrangian trajectory formulation incorporating gas phase kinetics,  $\text{NH}_4\text{NO}_3$  concentrations are computed at thermodynamic equilibrium with precursor  $\text{HNO}_3$  vapor and  $\text{NH}_3$  concentrations. Sensitivity analysis shows that  $\text{NH}_4\text{NO}_3$  concentration predictions are strongly influenced by ambient temperature and  $\text{NH}_3$  levels. A brief description of the  $\text{NH}_3$  emissions inventory used in this study is included to indicate the important sources. The model was tested by comparison to ambient  $\text{NH}_3$ ,  $\text{NH}_4^+$  and  $\text{NO}_3^-$  concentrations measured at El Monte, California during June 1974. Model results compare favorably with the ambient measurements and are used to explain trends in those measurements. An early morning nitrate peak develops as  $\text{HNO}_3$  produced soon after sunrise reacts with  $\text{NH}_3$  accumulated overnight. A second peak in nitrate concentration is predicted and observed at El Monte later in the day. Potential applications of this model to control strategy decisions and to study the fate of  $\text{NO}_x$  are discussed.

### INTRODUCTION

Aerosol nitrates are important contributors to visibility reduction in cities with photochemical air pollution problems. White and Roberts (1977) estimate that during the ACHEX study, aerosol nitrates were responsible for about 40% of the light scattering observed at Riverside in the eastern Los Angeles Basin. Groblicki *et al.* (1981) report that 17% of the visibility problem in Denver is attributable to aerosol nitrates. Control strategies for urban visibility improvement in such cities will need to address aerosol nitrate abatement alternatives. Before this can be done, a reliable means is needed for predicting the relationship between pollutant emission sources and resulting nitrate concentrations.

Ammonium nitrate is a secondary pollutant formed from reactions between  $\text{NH}_3$  and  $\text{HNO}_3$  vapor. From thermodynamic considerations Stelson *et al.* (1979) and Stelson and Seinfeld (1982a, b) have shown that atmospheric  $\text{NH}_4\text{NO}_3$  should be in equilibrium with precursor  $\text{HNO}_3$  and  $\text{NH}_3$  concentrations. The validity of this assumption has been tested in field experiments by Doyle *et al.* (1979), where it was found that the  $\text{NH}_4\text{NO}_3$  equilibrium constant derived from published thermochemical data is consistent with atmospheric observations.

In this paper a mathematical model relating pollutant emissions to  $\text{NH}_4\text{NO}_3$  concentrations is proposed and tested. Based on a Lagrangian trajectory formulation, the model includes transport, gas phase kinetics and aerosol production. A sensitivity analysis is performed on the  $\text{NH}_4\text{NO}_3$  formation mechanism used in the trajectory model to indicate which parameters are most important to formation of atmospheric  $\text{NH}_4\text{NO}_3$ . A summary of the emissions inventory used in this modeling study details the import-

ant sources of  $\text{NH}_3$  and their spatial distribution (Cass *et al.*, 1982). Model results will be evaluated against  $\text{NH}_3$ ,  $\text{NH}_4^+$  and  $\text{NO}_3^-$  concentrations observed at El Monte, California on 28 June 1974. Potential use of this model for studying acid deposition and the fate of nitrogen containing pollutants is discussed.

### MODEL DESCRIPTION

Ammonium nitrate aerosol is classified as a secondary pollutant because it is formed in the atmosphere from reactions involving gas phase precursors. To predict  $\text{NH}_4\text{NO}_3$  formation, this paper utilizes a photochemical trajectory model coupled with an equilibrium treatment of aerosol production. Concentrations of the gas phase precursors of  $\text{NH}_4\text{NO}_3$  as well as other pollutant concentrations are calculated using a vertically resolved, Lagrangian trajectory form of the atmospheric diffusion equation presented in McRae *et al.* (1982a). The equation governing the concentration of species  $i$ ,  $c_i(z, t)$ , is

$$\frac{\partial c_i}{\partial t} = \frac{\partial}{\partial z} \left( K_{zz} \frac{\partial c_i}{\partial z} \right) + R_i(c_1, c_2, \dots, c_n, T) - \frac{\partial v_z c_i}{\partial z}; \quad i = 1, 2, \dots, n \quad (1)$$

with initial conditions

$$c_i(z, 0) = c_i^0(z) \quad t = 0 \quad (2)$$

and boundary conditions

$$\left( K_{zz} \frac{\partial c_i}{\partial z} \right) = 0 \quad z = H \quad (3a)$$

$$\left[ v_z^i c_i - K_{zz} \frac{\partial c_i}{\partial z} \right] = E_i \quad z = 0, \quad (3b)$$

where  $K_{zz}(z)$  is the vertical turbulent eddy diffusivity,  $R_i(c_1, \dots, c_n, T)$  is the rate of chemical production of species  $i$  at temperature  $T$ ,  $H$  is the height of the air column and  $v_s$  is the settling velocity. As used in (1),  $v_s$  is used to describe gravitational settling, but its effect on (1) is negligible for aerosol particles smaller than about  $1 \mu\text{m}$ . Aerosol  $\text{NH}_4\text{NO}_3$  is generally associated with  $\mu\text{m}$ -sized particles, so gravitational settling can be neglected in the following calculations. Parameters associated with the boundary conditions are  $v_g^i$ , the deposition velocity, and  $E_i$ , the species mass flux per unit area. Treatment of surface deposition and the relationship of  $K_{zz}$  to atmospheric stability is described in McRae *et al.* (1982a) and will not be repeated here. Vertical transport of both gases and aerosols is dominated by turbulent eddies. It is important to note that models described by (1) are based on the assumptions that horizontal diffusion and vertical advection are small, and that the effects of wind shear are negligible. The effects of these simplifications are discussed in Liu and Seinfeld (1975).

Ground level ( $z = 0$ ) boundary conditions are a statement of mass continuity, accounting for surface deposition, diffusive transport and emissions. Since the top of the region ( $z = H$ ) is well above the mixing depth, turbulent transport through the top of the air column is negligible. Deposition velocities are used to describe the interaction and reaction of gases and aerosols with surfaces. In general,  $v_g^i$  is dependent on meteorological conditions and on the reactivity of species  $i$  with the underlying surface. Limits on the aerosol deposition rates can be found using the same modeling techniques as those for gaseous pollutants. The vertically resolved trajectory model and computational cells are shown schematically in Fig. 1.

The chemical kinetics associated with the term  $R_i(c_1, \dots, c_n, T)$  in (1) are described with the photochemical reaction mechanism of Falls and Seinfeld (1978), Falls *et al.* (1979), McRae *et al.* (1982a) and McRae and Seinfeld (1983). Only those homogeneous gas phase pathways producing  $\text{HNO}_3$  and their corresponding rate constants, at 25 C, will be given here. These pathways are:

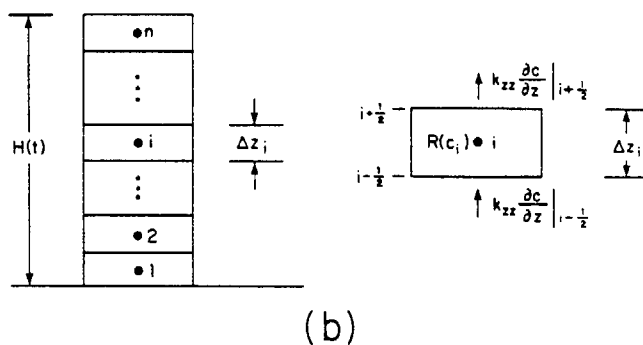
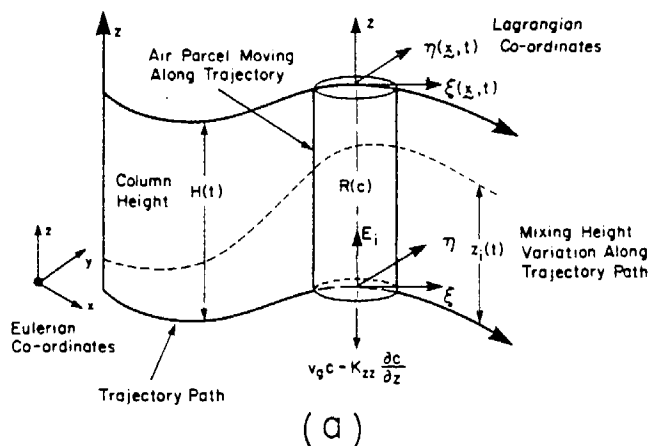
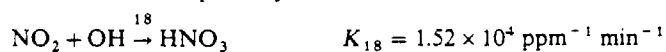


Fig. 1. Schematic representation of (a) vertically resolved Lagrangian trajectory model and (b) the computational grid cell convention.

Other than direct emissions, the only source of  $\text{HNO}_3$  is assumed to be the photochemical production through the above reactions. Reaction 18 is the dominant route producing  $\text{HNO}_3$  for typical daytime atmospheric conditions. Photolytic loss of  $\text{HNO}_3$  is ignored since it is small.

Equilibrium concentrations of gaseous  $\text{NH}_3$  and  $\text{HNO}_3$ , and the resulting concentration of solid or aqueous  $\text{NH}_4\text{NO}_3$  can be calculated from fundamental thermodynamic principles using the method presented by Stelson and Seinfeld (1982a). The procedure is composed of several steps, requiring as input the ambient temperature and relative humidity (r.h.). First, the equilibrium state of  $\text{NH}_4\text{NO}_3$  is defined. If the ambient relative humidity is less than the relative humidity of deliquescence, (r.h.d.), given by

$$\ln(\text{r.h.d.}) = 723.7/T + 1.7037. \quad (4)$$

then the equilibrium state of  $\text{NH}_4\text{NO}_3$  is modeled as a solid. Supersaturated solutions also are possible. Formation of solid  $\text{NH}_4\text{NO}_3$ , from the gas phase precursors, is described by the equilibrium system

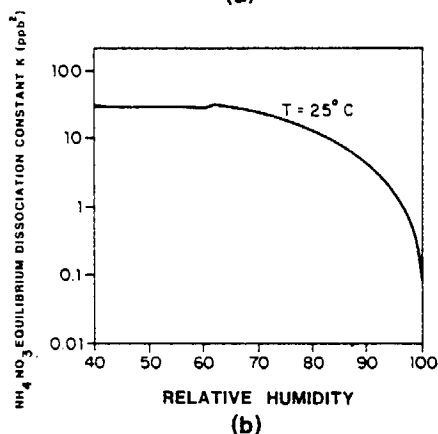
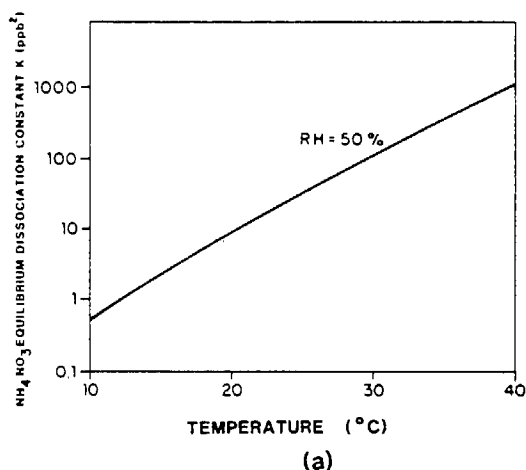
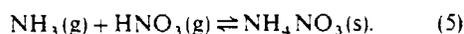


Fig. 2. (a)  $\text{NH}_4\text{NO}_3$  equilibrium dissociation constant as a function of temperature (r.h. 50%). (b)  $\text{NH}_4\text{NO}_3$  equilibrium dissociation constant as a function of r.h. (temperature, 25°C).

The dissociation constant is given by  $K = P_{\text{NH}_3}P_{\text{HNO}_3}$ , where  $P_{\text{NH}_3}$  and  $P_{\text{HNO}_3}$  are the partial pressures of  $\text{NH}_3$  and  $\text{HNO}_3$ , respectively.  $K$  can be estimated by integrating the van't Hoff equation. The resulting equation for  $K$ , in units of  $\text{ppb}^2$  (assuming 1 atm of total pressure) is

$$\ln K = 84.6 - 24220/T - 6.1 \ln(T/298). \quad (6)$$

At relative humidities above that of deliquescence,  $\text{NH}_4\text{NO}_3$  will be found in the aqueous state. A dissociation constant for the comparable reaction involving aqueous  $\text{NH}_4\text{NO}_3$  can be found and is a function of both temperature and relative humidity. Temperature dependent equilibrium relative humidities above ionic solutions (r.h.t.) can be calculated from

$$\text{r.h.t.} = 100 \exp\left(\frac{-vmM\phi_T}{1000}\right), \quad (7)$$

where  $v$  is the number of moles of ions formed by ionization of one mole of solute,  $M$  the molecular weight of water,  $m$  the molality of the solution and  $\phi_T$  is the osmotic coefficient given by

$$\phi_T = 1 + \frac{1}{m} \int_0^m m d(\ln \gamma^\pm)_T, \quad (8)$$

where  $\gamma^\pm$  is the mean molal activity of  $\text{NH}_4\text{NO}_3$  in the solution at temperature  $T$ . The activity coefficient depends on temperature and molality. An iterative scheme is used to match the relative humidity calculated from (7) to the ambient relative humidity. This calculation gives the equilibrium solution molality and activity that are needed to evaluate  $K$ , the equilibrium dissociation constant, from the expression

$$\ln(K; (\gamma^\pm m)^2) = 54.18 - 15860/T + 11.206 \ln(T/298). \quad (9)$$

If the ambient relative humidity is between that of deliquescence and the value given by (7) for a saturated solution at  $m = 25.954$ , linear interpolation is used between the corresponding dissociation constants.

Figures 2(a) and (b) depict the dependence of  $K$  on  $T$  and r.h. For typical atmospheric conditions, the mechanism predicts an equilibrium dissociation constant between  $0.04 (\text{ppb})^2$  at 5°C and 90% r.h. and  $1400 (\text{ppb})^2$  at 40°C and a r.h. of 30%. Figure 2(b) indicates that extrapolation of the calculation scheme used for aqueous solutions to that for supersaturated solutions would give results slightly different than those found using (6) for solid  $\text{NH}_4\text{NO}_3$ . In the case of a saturated solution surrounding solid  $\text{NH}_4\text{NO}_3$ , equating the chemical potentials across interfaces shows that the appropriate dissociation constant is the same as that for the solid. This model assumes that the time required for the gaseous precursors, and water, to come to equilibrium is short compared to the characteristic time for the production of  $\text{HNO}_3$ . This may not be true if the concentrations of the precursors differ by orders of magnitude, though this is seldom the case in

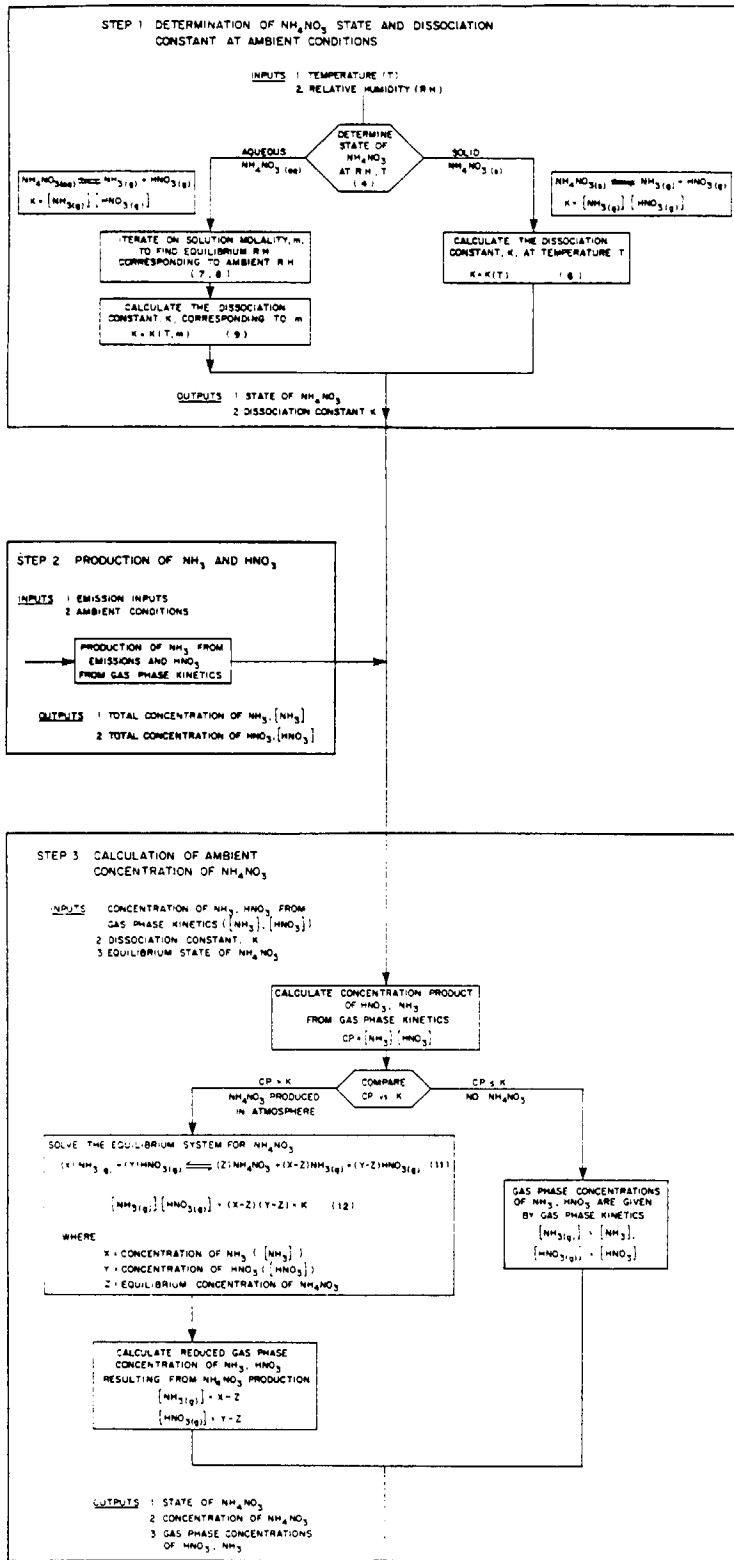


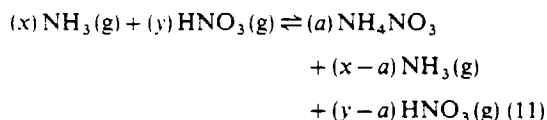
Figure 3

urban basins. Nitric acid and  $\text{NH}_3$  losses to other aerosol species are neglected at this point, and thus mixed aerosols are not considered. These effects can be incorporated once sufficient, appropriate field data become available to verify a more complex model.

Gas phase concentrations of  $\text{NH}_3$  and  $\text{HNO}_3$  and the concentration of  $\text{NH}_4\text{NO}_3$  are then calculated from precursor concentrations and the equilibrium system



Concentrations of the different species can be determined mathematically by solving the following system of equations.



and

$$[\text{NH}_3(\text{g})][\text{HNO}_3(\text{g})] = (x-a)(y-a) = K. \quad (12)$$

where  $x$  is the total concentration of  $\text{NH}_3$  plus  $\text{NH}_4^+$ ,  $y$  is the total concentration of  $\text{HNO}_3$  plus nitrate,  $a$  is the resulting concentration of  $\text{NH}_4\text{NO}_3$  aerosol, and  $(x-a)$ ,  $(y-a)$  are the equilibrium gas phase concentrations of  $\text{NH}_3$  and  $\text{HNO}_3$ , respectively.

If the product of the concentrations of  $\text{NH}_3$  and  $\text{HNO}_3$  is smaller than the dissociation constant,

$$[\text{NH}_3(\text{g})][\text{HNO}_3(\text{g})] = (x)(y) < K \quad (13)$$

no  $\text{NH}_4\text{NO}_3$  should be present. In this case the gas phase concentrations are as given by the gas phase kinetics. The steps involved in predicting the nitrate concentrations are shown schematically in Fig. 3.

#### SENSITIVITY STUDY

A Fourier amplitude sensitivity test (FAST) (Koda *et al.*, 1979; McRae *et al.*, 1982b) was performed on the  $\text{NH}_4\text{NO}_3$  calculation scheme to assess which parameters contribute most to the formation of  $\text{NH}_4\text{NO}_3$  in the atmosphere. The ranges of species concentrations used in the analysis are representative of those observed by Tuazon *et al.* (1981) for Claremont, California and were measured by Fourier transform infrared (FTIR) spectroscopy. In these experiments the FTIR sampling cell temperature was often considerably higher than ambient, which could volatilize some of the  $\text{NH}_4\text{NO}_3$ , so the measurements may give  $\text{NH}_3(\text{g})$  and  $\text{HNO}_3(\text{g})$  levels higher than ambient. The results of the FAST analysis are shown in Table 1, where it can be seen that  $\text{NH}_4\text{NO}_3$  formation is most sensitive to variations in temperature. The reason for this is the strong dependence of the dissociation constant on  $T$ . Two insights can be gained from FAST analysis, the first being that it is critically important to specify the temperature field accurately. Secondly, since nitrate formation is sensitive to  $\text{NH}_3$  over the range encountered, control of upwind  $\text{NH}_3$  emissions

Table 1. Sensitivity of ammonium nitrate formation model to input parameters

Parameter	Range	Sensitivity* (%)
Temperature	10–40°C	41
Ammonia	4–23 ppb <sup>†</sup>	39
Nitric acid	6–49 ppb <sup>†</sup>	17
Relative humidity	20–90%	3

\* Partial variance, normalized to 100%, indicates the relative importance of variation of model inputs on  $\text{NH}_4\text{NO}_3$  formation.

<sup>†</sup> Values representative of those found in Tuazon *et al.* (1981) for Claremont, California.

should prove to be beneficial in limiting  $\text{NH}_4\text{NO}_3$  concentrations at Claremont and that an accurate description of the  $\text{NH}_3$  emissions is required for modeling purposes.

To show how the concentrations of  $\text{NH}_4\text{NO}_3$  change with ambient meteorological conditions, representative levels of total  $\text{NH}_3$  (i.e.  $\text{NH}_3(\text{g}) + \text{NH}_4^+$ ) and total  $\text{HNO}_3$  (i.e.  $\text{HNO}_3(\text{g}) + \text{NO}_3^-$ ) were used to calculate  $\text{NH}_4\text{NO}_3$  concentrations over a range of atmospheric conditions. Predicted concentrations of  $\text{NH}_4\text{NO}_3$  ranged from 0 to  $67.6 \mu\text{g m}^{-3}$ , with typical values of about  $10 \mu\text{g m}^{-3}$  corresponding to 25°C, 65% r.h., 8 ppb of total  $\text{NH}_3$  and 16 ppb of total  $\text{HNO}_3$ . Concentration plots in Fig. 4 again show that  $\text{NH}_4\text{NO}_3$  formation is sensitive to temperature, decreasing rapidly as temperature increases. An interesting aspect of the temperature dependence is the flat area indicating that no  $\text{NH}_4\text{NO}_3$  is present. Above 35°C little  $\text{NH}_4\text{NO}_3$  would be present except at high ambient levels of the gas phase precursors, while at 15°C some  $\text{NH}_4\text{NO}_3$  would be present at most precursor concentrations. Figure 4 also shows that there is little change in  $\text{NH}_4\text{NO}_3$  formation as the r.h. changes, although the effect is to create slightly more  $\text{NH}_4\text{NO}_3$  as r.h. increases.

#### EMISSIONS DATA REQUIRED FOR MODEL EVALUATION

Once the model has been formulated the next step is to evaluate its ability to predict ambient levels of  $\text{NH}_4\text{NO}_3$ . The data required for such tests include; pollutant emissions, observed air quality and the prevailing meteorology. In the Los Angeles Basin accurate emission inventories exist only for the period between 26 and 28 June 1974, limiting model evaluation to those three days. Descriptions of the emission inventories for  $\text{NO}_x$  and reactive hydrocarbons together with the local meteorological conditions for this period are available in McRae and Seinfeld (1983). As indicated by the sensitivity analysis, there is a need for an accurate description of the  $\text{NH}_3$  emissions. Cass *et al.* (1982) have recently completed such a study for the year 1974, and the principal results are summarized here. A grid system composed of  $5 \times 5$  km cells was

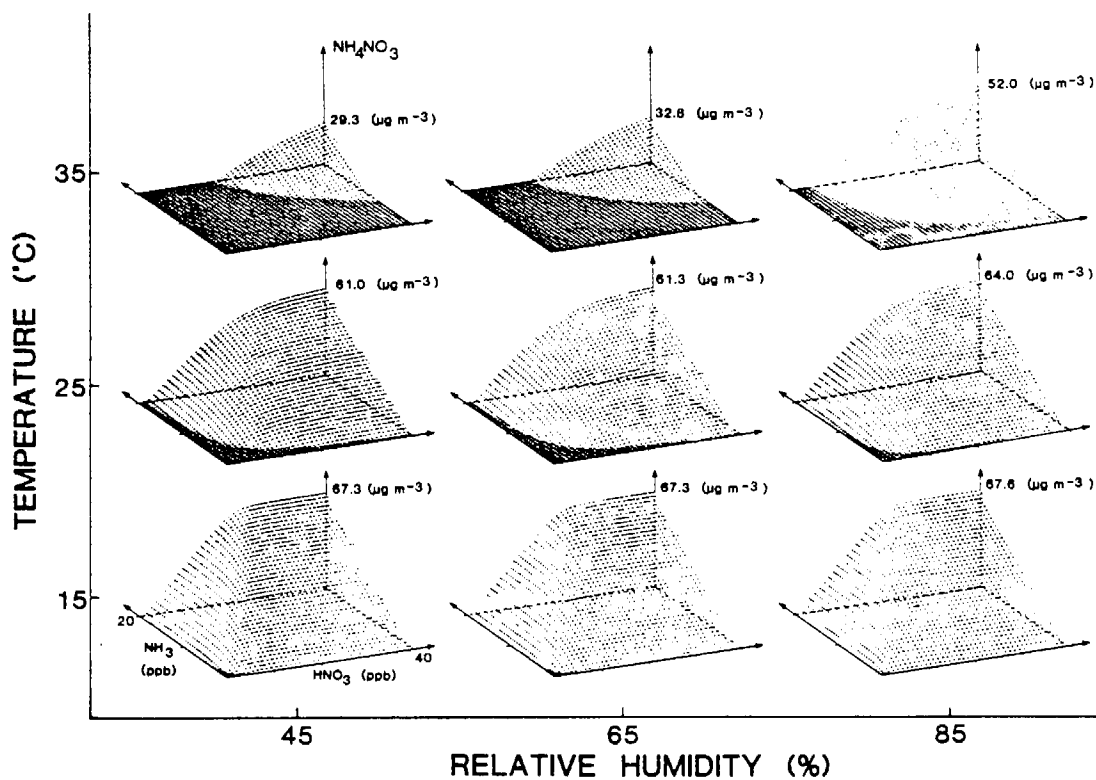


Fig. 4. Predicted  $\text{NH}_4\text{NO}_3$  concentration surfaces at 15, 25 and 35 C and 45, 65 and 85% r.h. for total  $\text{NH}_3$  and total  $\text{HNO}_3$  concentrations up to 20 and 40 ppb, respectively.

superimposed on the South Coast Air Basin map (Fig. 5). Ammonia emissions were estimated within each grid cell for the 53 classes of mobile and stationary source types listed in Table 2.

Source tests show that trace amounts of  $\text{NH}_3$  are present in the exhaust of both mobile and stationary

combustion sources (Cadle and Mulawa, 1980; Gentel *et al.*, 1973; Harkins and Nicksic, 1967; Heinein, 1975; Hovey *et al.*, 1966; Hunter, 1971; Muzio and Arand, 1976; Wohlers and Bell, 1956). Emission factors for  $\text{NH}_3$  release obtained from these and other references were combined with fuel use data reported by Cass

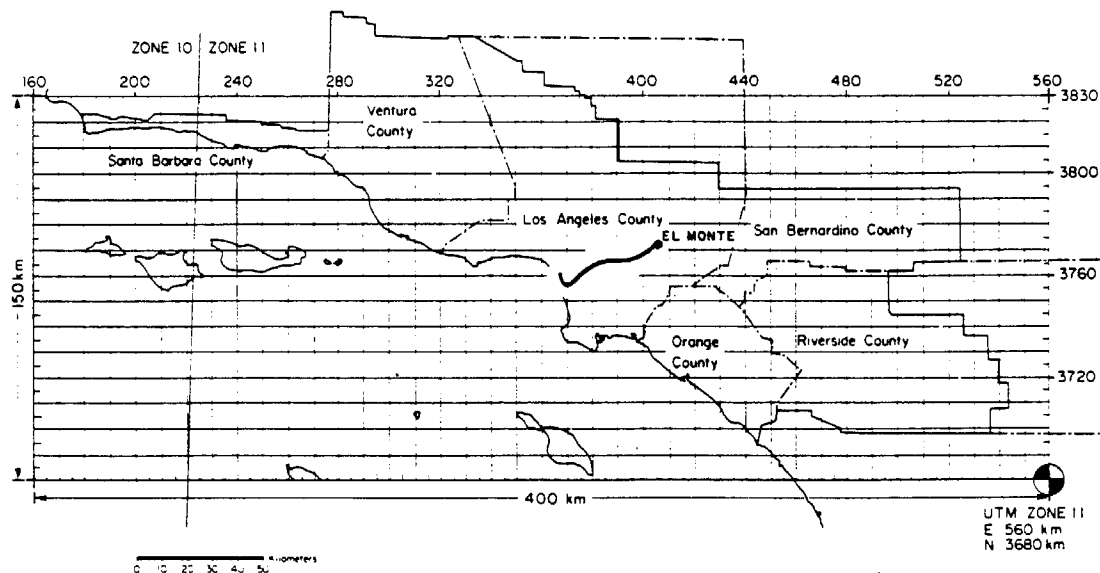


Fig. 5. Gridded map of the South Coast Air Basin used for constructing  $\text{NH}_3$  emissions inventory. Superimposed on the map is the trajectory path that reaches El Monte at 3 p.m. (PDT) on 28 June 1974.

Table 2. Summary of ammonia emissions by source category in the South Coast Air Basin 1974

Source category	Total emissions (kg day <sup>-1</sup> )
<b>Stationary fuel combustion</b>	
Electric utility	
Natural gas	590.0
Residual oil	2000.0
Digester gas	0.5
Refinery fuel burning	
Natural gas	160.0
Residual oil	99.0
Refinery gas	420.0
Industrial fuel burning	
Natural gas	610.0
Liquified petroleum gas (LPG)	4.0
Residual oil	150.0
Distillate oil	140.0
Digester gas	9.0
Coke oven gas	15.0
Residential commercial fuel burning	
Natural gas	270.0
Liquified petroleum gas (LPG)	4.0
Residual oil	62.0
Distillate oil	73.0
Coal	20.0
Sub totals	4626.5 (3.09%)
<b>Mobile source fuel combustion</b>	
Automotive	
Non-catalyst autos and light trucks	3309.0
Medium and heavy duty trucks	449.9
Diesel vehicles	370.0
LPG for carburetion	10.0
Civilian aircraft	
Jet	150.0
Piston	2.9
Shipping	
Residual oil boilers	70.0
Diesel ships	50.0
Railroad-diesel oil	90.0
Military	
Gasoline	10.0
Diesel	60.0
Jet fuel	50.0
Residual oil	0.8
Off highway vehicles	120.0
Sub totals	4742.6 (3.17%)
Industrial point sources	2070.0 (1.38%)
Soil surface	23790.0 (15.9%)
Fertilizer	
Farm crop	2870.0
Orchards	2390.0
Handling	380.0
Non-farm	7420.0
Sub totals	13060.0 (8.72%)
Livestock	
Cattle	
Dairy	24390.0
Feedlot	6880.0
Range	12160.0
Horses	16220.0
Sheep	990.0
Hogs	250.0
Chickens	18200.0
Turkeys	1120.0
Sub totals	80210.0 (53.6%)

Table 2. (contd).

Source category	Total emissions (kg day <sup>-1</sup> )
Domestic	
Dogs	10350.0
Cats	3230.0
Human respiration	46.0
Human perspiration	7000.0
Household ammonia use	600.0
Sub totals	21226.0 (14.2%)
Total	149725.1 (100.0)%

(1978) to give total NH<sub>3</sub> emissions from autos, trucks, railroads, shipping, plus industrial, residential and commercial fuel use. Within each fuel use category, the NH<sub>3</sub> emissions shown in Table 2 were distributed spatially in the same manner as NO<sub>x</sub> emissions. A number of industrial processes are known to emit NH<sub>3</sub> (National Research Council, 1979; Miner, 1969), including refinery operations, NH<sub>3</sub>-based fertilizer manufacturing, NH<sub>3</sub> storage facilities, refrigeration plants, chemical plants and steel mill coke ovens. Estimates of NH<sub>3</sub> emissions from industrial facilities were derived from source test information and questionnaires sent to individual companies.

Biological decay processes also produce NH<sub>3</sub> and the release rates from a variety of soil surface types are available (Porter *et al.*, 1975; Elliot *et al.*, 1971; Denmead *et al.*, 1978; Denmead *et al.*, 1976; Miner, 1976). Using aerial photographs and maps available from the U.S. Geological Survey (1976) the land use within each grid square was summarized by type. Emissions from exposed land surfaces were estimated within each square by matching emission rate data to soil surface types.

Chemical fertilizers used in the air basin include NH<sub>3</sub>, urea, NH<sub>4</sub>NO<sub>3</sub> and (NH<sub>4</sub>)<sub>2</sub>SO<sub>4</sub>. Depending on fertilizer type and method of application, anywhere from a few percent to several tenths of the nitrogen content may be lost to the atmosphere as NH<sub>3</sub> (Baker *et al.*, 1959; Ernst and Massey, 1960; Gasser, 1964; McDowell and Smith, 1958; Stanley and Smith, 1955; Trickey and Smith, 1955; Wahhab *et al.*, 1957; Walkup and Nevins, 1966). The NH<sub>3</sub> loss characteristics of fertilizers were estimated by consultation with a local agricultural expert (Meyer, personal communication). Fertilizer use statistics were obtained from the California Department of Food and Agriculture (1974) and from the U.S. Bureau of the Census (1977). Chemical fertilizer consumption, subdivided into cropland, orchard and non-farm use, was combined with the NH<sub>3</sub> loss data to compute total NH<sub>3</sub> emissions.

Decomposition of livestock wastes is a major source of NH<sub>3</sub> emissions. Animal inventories by county were obtained from the U.S. Bureau of the Census (1977) and from state and county agricultural agents. Waste production rates, nitrogen content and NH<sub>3</sub> volatiliz-

ation rates were estimated for each major commercial animal type from previous studies (Adriano *et al.*, 1974; Fogg, 1971; Giddens and Rao, 1975; Lauer *et al.*, 1976; Luebs *et al.*, 1973a,b; Stewart, 1970; Taiganides and Hazen, 1966; Viets, 1971). Emissions from range animals were distributed spatially in proportion to pasture and herbaceous range land areas. U.S. Geological Survey (1976) maps were used to locate emissions from animals raised in confinement (e.g. dairy cattle, feedlot cattle). Ammonia losses from domestic animals (cats and dogs only) plus human respiration, perspiration and household cleaning chemicals were distributed in proportion to residential land use.

The overall spatial distribution of NH<sub>3</sub>, NO<sub>x</sub>, reactive hydrocarbon and CO emissions in the South Coast Air Basin is shown in Fig. 6. The largest spike in the NH<sub>3</sub> diagram is centered over the town of Chino on the prevailing upwind side of the city of Riverside, and results from the intensity of livestock operations in that area.

#### AIR QUALITY DATA FOR MODEL EVALUATION

Within the three day time period for which emission data are available, aerosol nitrate measurements were sought that were taken over short sampling intervals (1-2 h) using methods that would minimize the possible interferences. Simultaneous concentration measurements of related aerosol species such as sulfate and ammonium were desired, as well as the concentration of relevant gas phase species, such as NH<sub>3</sub>, HNO<sub>3</sub>, NO<sub>x</sub> and O<sub>3</sub>. The data set most nearly fulfilling the requirements was found for El Monte, California. The measurements were taken on 28 June 1974, and consist of 2-h averaged concentrations of aerosol nitrate and NH<sub>4</sub><sup>+</sup>, and gas phase NH<sub>3</sub> (Reynolds *et al.*, 1975). Aerosol nitrate and ammonium concentrations were obtained by using a low volume sampler with Gelman A glass fiber filters for collection followed by wet chemical analysis. Gaseous NH<sub>3</sub> concentrations were found using oxalic acid impregnated backup filters.

Ammonium nitrate data for other time periods in the Los Angeles area are available and are consistent with the results presented in Reynolds *et al.* (1975). These studies have found measured ambient nitrate

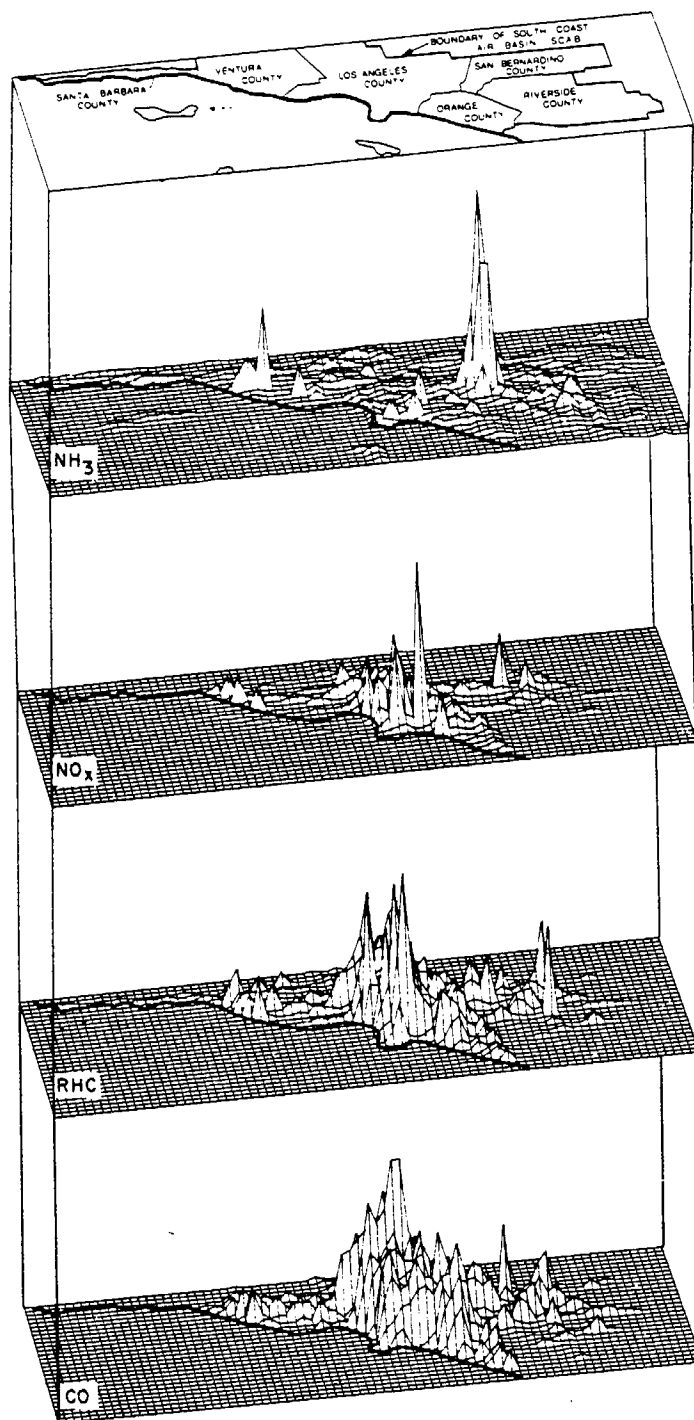


Fig. 6. Spatial representation of daily emissions of  $\text{NH}_3$ ,  $\text{NO}_x$ , reactive hydrocarbons (RHC) and CO in the South Coast Air Basin. (Inventory period June 1974.)

concentrations ranging up to  $149 \mu\text{g m}^{-3}$ , though values are generally lower (Lundgren, 1970; Hidy *et al.*, 1980; Appel *et al.*, 1978; Spicer, 1974; Appel *et al.*, 1981; Tuazon *et al.*, 1981). In Claremont, California, ambient levels of gaseous  $\text{HNO}_3$  and  $\text{NH}_3$  have been observed up to 49 and 23 ppb, respectively (Tuazon *et al.*, 1981). Concentrations of up to  $86.4 \mu\text{g m}^{-3}$  of particulate

nitrate were also found at Claremont (Appel *et al.*, 1980). Nitrate levels were found to vary diurnally, peaking in the midmorning. Ozone and  $\text{HNO}_3$  peaked later in the afternoon. Partial pressure products of  $\text{NH}_3$  (g) and  $\text{HNO}_3$  (g) from data taken at Claremont were compared against relative humidity and temperature. The product decreased with relative humidity and

increased with temperature, the same trend predicted from thermodynamic considerations.

When interpreting ambient measurements, it is important to be aware of the potential for artifact nitrate formation on filter substrates (Pierson *et al.*, 1980; Spicer and Schumacher, 1979; Appel *et al.*, 1979; Witz and McPhee, 1977). The physical nature of the nitrate artifact problem is that the gaseous  $\text{HNO}_3$  may react with the filter substrate forming nitrate on the filter. This results in a positive error as more nitrate is measured on the filter than was deposited as an aerosol. A negative error can result from revolatilization of the  $\text{NH}_4\text{NO}_3$  prior to sample analysis, or by reaction with other gaseous or particulate acids displacing the  $\text{HNO}_3$  (Appel *et al.*, 1980). The observed revolatilization is in agreement with the equilibrium hypothesis employed in this paper. If the filter, after being loaded and before being analyzed, is exposed to a change in environment it would set up a new equilibrium between the aerosol and its environment, possibly altering the aerosol's measured composition. The new equilibrium could be due either to a change in temperature or to a change in the gaseous environment during or after sampling. To prevent this problem the  $\text{NH}_4\text{NO}_3$  would have to be collected, stored and analyzed in a manner that prevents volatilization of the aerosol from the filter.

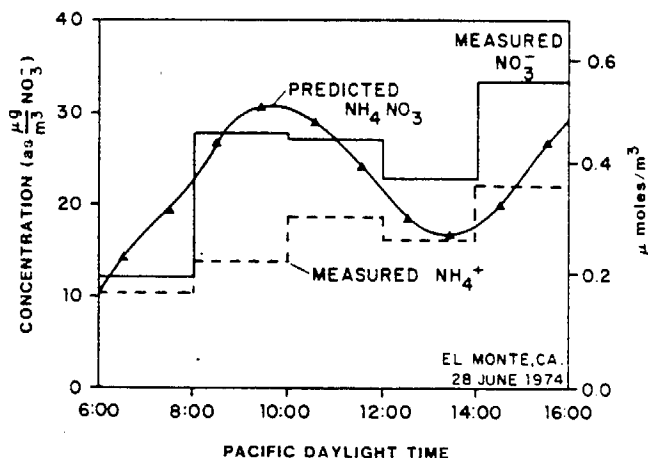
Steps have been taken to correct the filter artifact problem, the most direct being the use of a substrate that does not react with gaseous  $\text{HNO}_3$  to form nitrate. Substrates that have been tested and show little reactivity with  $\text{HNO}_3$  include polycarbonate, Teflon and quartz fiber (Spicer and Shumacher, 1979). Most glass fiber and nylon filters prove to be quite susceptible to artifact nitrate formation, although Gelman A filters are not as susceptible as many others (Appel *et al.*, 1979). Another method involves stripping the  $\text{HNO}_3$  (g) from the sampling stream prior to filtration by passing the gas through a denuder, then measuring total nitrate downstream (Appel *et al.*, 1981).

#### MODEL EVALUATION AGAINST AMBIENT MEASUREMENTS

Usually ambient measurements are made at a fixed location. A Lagrangian model, however, predicts concentrations along a trajectory in a single air mass as it flows through the air basin. The path of a sample trajectory, the one starting at 1 a.m. and reaching E1 Monte at 3 p.m. Pacific Daylight Time (PDT) on 28 June 1974, is shown on a map of the Los Angeles basin (Fig. 5). Use of a trajectory model to predict concentrations at different times for a fixed geographical location then requires finding the path that each air mass takes to reach that location at the appropriate time. This is done for trajectories reaching E1 Monte throughout the day of 28 June 1974 using the method prescribed in Goodin *et al.* (1979).

By taking a series of trajectories reaching E1 Monte during the day, a time history of species concentrations can be constructed (Fig. 7). Each concentration prediction shown represents a weighted average of three trajectories arriving at E1 Monte at 1 h intervals, and are plotted on the half hour. In Fig. 7(a), the predicted ground level  $\text{NH}_4\text{NO}_3$  concentration is plotted along with the measured nitrate and  $\text{NH}_4^+$  concentration. Concentrations are given in  $\mu\text{mol m}^{-3}$  for all species and  $\text{NO}_3^-$  concentrations are restated in  $\mu\text{g m}^{-3}$ . Gas phase concentrations are also shown in ppm or ppb. Use of a system based on molar concentrations is more convenient in the presence of chemical reactions, and clarifies the relationship between aerosols and their gas phase precursors. Considering the difficulty in obtaining ambient nitrate measurements, comparison between observed and predicted nitrate concentrations is quite good.

From Fig. 7(a), it can be seen that the measured molar concentrations of aerosol nitrate exceed that of  $\text{NH}_4^+$ . The difference could arise if species other than  $\text{NH}_4\text{NO}_3$  were present in the aerosol (e.g.  $\text{NaNO}_3$ ), or as a result of the filter artifact problem. Filter artifact problems can lead to either a positive error due to



(a)

Fig. 7(a).

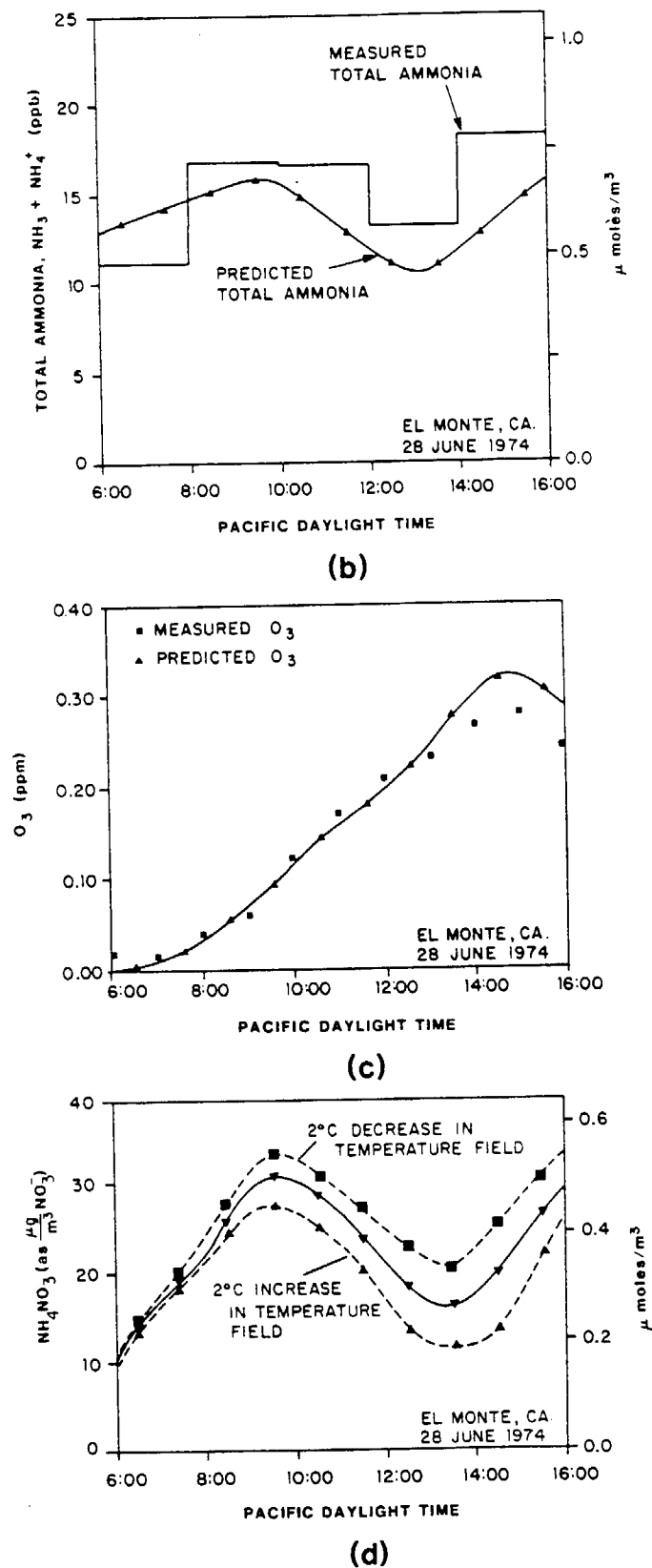


Fig. 7. Concentration profiles at El Monte on 28 June 1974. (a) Predicted  $\text{NH}_4\text{NO}_3$ , measured  $\text{NH}_4^+$  and measured  $\text{NO}_3^-$ . (b) Predicted total ammonia ( $\text{NH}_3 + \text{NH}_4^+$ ) and measured total ammonia. (c) Predicted and measured  $\text{O}_3$  concentrations. (d) Sensitivity of  $\text{NH}_4\text{NO}_3$  formation to a  $\pm 2^\circ\text{C}$  change in the temperature field.

$\text{HNO}_3$  reacting with the filter or a negative error from the volatilization of either ammonium or nitrate containing species. Twenty four hour averaged measurements for the day modeled showed only  $5.1 \mu\text{g m}^{-3}$  of sulfate. Previous studies (e.g. Appel *et al.*, 1978) showed that most of the sulfate aerosol appears in the late afternoon. Thus, the interference from sulfate should be small for the period modeled. It is impossible to say how the predicted nitrate should compare to the measured nitrate concentrations without knowing the magnitude of the two types of possible sampling error.

Relatively little  $\text{NH}_4\text{NO}_3$  is measured or predicted in the early morning. The concentration rises until about 10 a.m. (PDT) at which time it starts to decrease as the temperature increases. The same trend is found by other investigators (Appel *et al.*, 1980). Both the measurements and predictions for 28 June 1974, show an afternoon rise that is uncharacteristic of the usual decrease in  $\text{NH}_4\text{NO}_3$  as the temperature increases. Figure 7(b), the plot of the predicted and measured total (gas plus aerosol phase)  $\text{NH}_3$  concentrations, shows that the reason for the unexpected afternoon peak is that the air mass contains more  $\text{NH}_3$ . Figure 7(b) also serves as a check on the  $\text{NH}_3$  emissions inventory. Even in the presence of possible transfer of revolatilized  $\text{NH}_3$  to the oxalic acid impregnated backup filter used to measure  $\text{NH}_3$ , the sum of measured  $\text{NH}_3$  and  $\text{NH}_4^+$  should give total  $\text{NH}_3$ . Predicted total  $\text{NH}_3$  is about 10–20% low through most of the day, except in the early morning. Predictions follow the same diurnal trends as the measurements, indicating the spatial accuracy of the inventory over which the trajectory passed.

In view of the possible effects occurring from nitrate artifact formation, it is interesting to note that the predicted nitrate levels are high in the morning when the potential to form artifact nitrate is small. In the afternoon the increasing  $\text{HNO}_3$  concentration raises the potential formation of artifact nitrate, and it is seen that the predicted nitrate concentrations begin to fall below the measured levels.

As an additional check on model performance, predicted  $\text{O}_3$  concentrations at El Monte are compared to measurements in Fig. 7(c), and the two profiles compare well. Ozone measurements were not taken at El Monte, so the measured values being used are interpolated from surrounding monitoring sites.

A good measure of the sensitivity of nitrate formation to temperature variations is obtained from Fig. 7(d). Increase in the separation between the curves is due almost totally to the change in  $K$  from the temperature change, not from a change in the amount of total inorganic nitrate produced. This figure also illustrates the potential problems arising from either upsetting the equilibrium, or from errors in the temperature field specification.

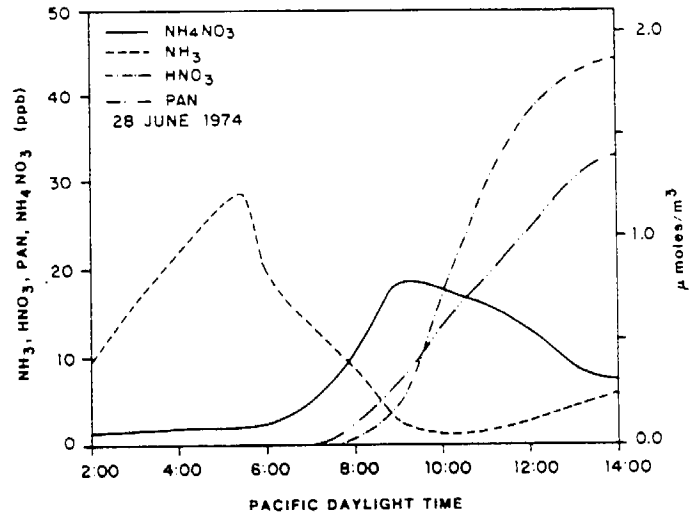
For model evaluation purposes it was necessary to compare predictions and observations at a fixed point; however, it is more illuminating to investigate dynamics of the nitrate aerosol production along a single

trajectory. In this manner the effects of the physical processes are more easily isolated. In the series of plots shown in Fig. 8, the evolution of pollutant concentrations is shown as the air mass traverses the basin. Early morning  $\text{NH}_3$  emissions into the air parcel increase the  $\text{NH}_3$  concentrations but have only a small effect on the aerosol levels because little  $\text{HNO}_3$  has been produced by photochemical reactions (Fig. 8a). After sunrise, photochemical reactions start forming inorganic nitrate from the oxidation of  $\text{NO}_x$  emissions. Initially most of the nitrate formed is tied up in the aerosol phase increasing the  $\text{NH}_4\text{NO}_3$  concentration and decreasing that of  $\text{NH}_3$ . Nitric acid continues to be the limiting species for aerosol formation until 8 a.m. when the  $\text{HNO}_3$  concentration begins to rise rapidly. Both  $\text{NH}_4\text{NO}_3$  and  $\text{HNO}_3$  levels continue to increase, and  $\text{NH}_3$  to drop, until about 9 a.m. when a midmorning  $\text{NH}_4\text{NO}_3$  peak occurs. After this time the  $\text{NH}_4\text{NO}_3$  concentration decreases due to two effects, aerosol volatilization by the increasing temperature and dilution by the growing mixed layer. The profile for PAN, an organic nitrate, is shown in Fig. 8(a). PAN follows the same diurnal trend as  $\text{HNO}_3$ , peaking at 33 ppb compared to 44 ppb for  $\text{HNO}_3$ . The peak  $\text{HNO}_3$  concentration was 13% that of  $\text{O}_3$ . Tuazon *et al.* (1981) found a similar PAN to  $\text{HNO}_3$  ratio and approximately the same maximum values. For example, the peak  $\text{HNO}_3$  levels were 11% of the observed  $\text{O}_3$  concentrations at Claremont, California in 1978.

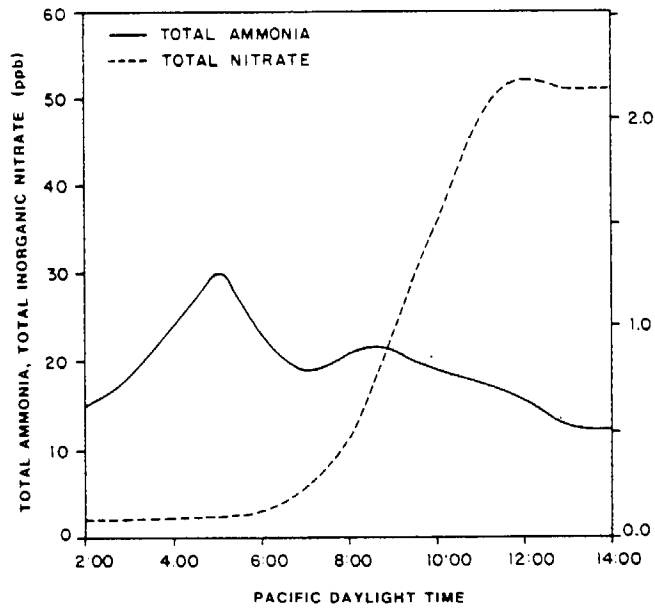
Figure 8(b) graphically illustrates the initial rise in  $\text{NH}_3$  from emissions. Photochemical reaction of  $\text{NO}_x$  causes a rapid increase in the concentration of total inorganic nitrate shortly after sunrise at 5:45 a.m. Total nitrate increases until about noon when dilution and deposition of  $\text{HNO}_3$  and  $\text{NH}_4\text{NO}_3$  cause the total nitrate concentrations to stabilize. Profiles of three pollutants related to  $\text{HNO}_3$  formation,  $\text{O}_3$ ,  $\text{NO}$  and  $\text{NO}_2$ , are shown in Fig. 8(c) for comparison.

Vertically-resolved profiles of  $\text{NH}_4\text{NO}_3$  and its precursors are plotted in Fig. 9 at three different times during the day. Early in the morning, the most marked profile is that of  $\text{NH}_3$  showing that the emissions are being trapped within the mixed layer. Four hours later, at 8 a.m., the mixing depth has increased and so has the  $\text{NH}_4\text{NO}_3$ , but the availability of  $\text{HNO}_3$  is still limiting the formation. By noon,  $\text{HNO}_3$  is the most abundant species below the temperature inversion and  $\text{NH}_3$  availability now limits aerosol formation. Directly above the inversion base the change in the  $\text{NH}_3$  profile is created by the decrease in  $\text{HNO}_3$  allowing a higher equilibrium  $\text{NH}_3$  concentration.

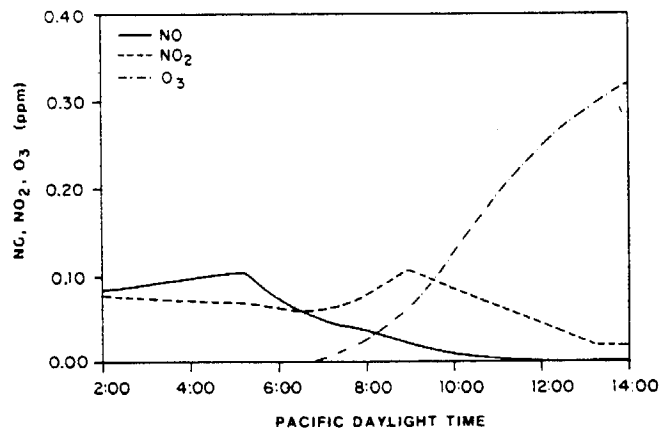
In this study, the currently available collection of simultaneous observations on emissions and air quality has been pursued as far as it can be taken, and it is apparent that additional model applications should be supported by a data set explicitly designed for nitrate air quality model verification. Such a data set should include simultaneous measurements on all species of interest including  $\text{NH}_3$  and  $\text{HNO}_3$  vapor, plus  $\text{NH}_4^+$  and  $\text{NO}_3^-$  concentrations. Measurement



(a)

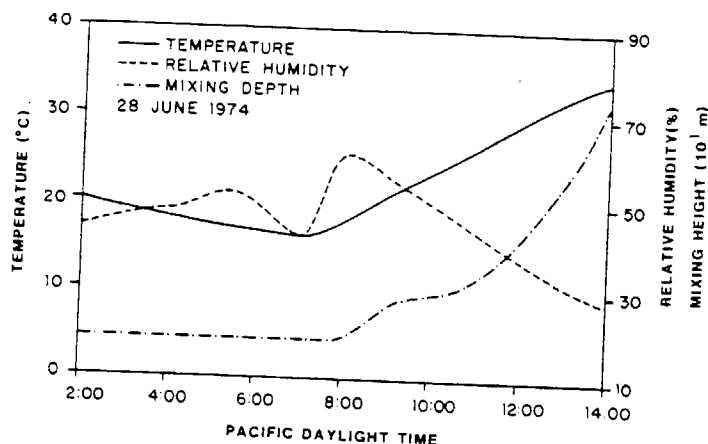


(b)



(c)

Figs 8(a)-(c).



(d)

Fig. 8. Predicted concentrations and observed meteorological variables for the air parcel reaching El Monte at 2 p.m. (PDT) 28 June 1974. (a)  $\text{NH}_4\text{NO}_3$ ,  $\text{NH}_3$ ,  $\text{HNO}_3$  and PAN profiles. (b) Total ammonia and total nitrate profiles (c)  $\text{NO}$ ,  $\text{NO}_2$  and  $\text{O}_3$  profiles. (d) Meteorological parameters: mixing depth, temperature and relative humidity.

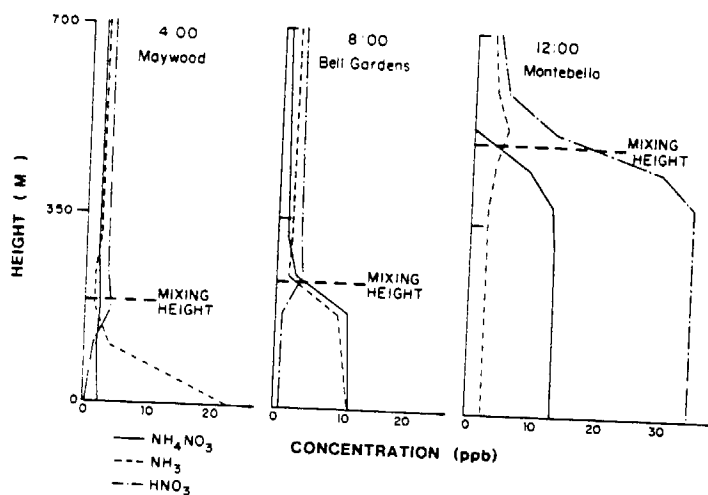


Fig. 9. Evolution of vertical concentration profiles of  $\text{NH}_3$  (---),  $\text{HNO}_3$  (- - -) and  $\text{NH}_4\text{NO}_3$  (—) in the air parcel that reaches El Monte at 2 p.m. (PDT) 28 June 1974. Results shown are for 4 a.m., 8 a.m. and 12 noon and the location is given for the air parcel at those times.

methods should be selected that will minimize sampling artifact problems. The sensitivity analysis presented in this paper points to the need for highly accurate temperature data. Model structure dictates that temperature measurements must be available along the trajectory considered, not just at the end point of the trajectory.

#### FUTURE MODEL APPLICATIONS

Potential uses of this model include control strategy determination for visibility improvement and the

study of aerosol processes, acid deposition and the fate of nitrogen containing species. Results from this model as well as field measurements (Tuazon *et al.*, 1981) indicate that along most of the trajectories in the western portion of the Los Angeles Basin there is more  $\text{HNO}_3$  than  $\text{NH}_3$ , and that the main factors limiting the formation of aerosol are warm temperatures and lack of  $\text{NH}_3$ . This result was also indicated by the sensitivity analysis performed on the formation mechanism alone. In the eastern part of the basin, downwind of the dairies, the situation may well be reversed, resulting in a  $\text{HNO}_3$  deficiency.

- development of air contaminant emission tables for non-process emissions. *J. Air Pollut. Control Ass.* **16**, 362-366.
- Hunter J. E., Jr. (1971) Effect of catalytic converters on automotive ammonia emissions. General Motors Research Laboratories. Research Publication GMR-1061, Warren, MI.
- Koda M., McRae G. J. and Seinfeld J. H. (1979) Automatic sensitivity analysis of kinetic mechanisms. *Int. J. chem. Kinetics* **11**, 427-444.
- Lauer D. A., Bouldin D. R. and Klausner S. D. (1976) Ammonia volatilization from dairy manure spread on the soil surface. *J. envir. Quality* **5**, 134-141.
- Liu M.-K. and Seinfeld J. H. (1975) On the validity of grid and trajectory models of urban air pollution. *Atmospheric Environment* **9**, 555-574.
- Luebs R. E., Davis K. R. and Laag A. E. (1973a) Enrichment of the atmosphere with nitrogen compounds volatilized from a large dairy area. *J. envir. Quality* **2**, 137-141.
- Luebs R. E., Laag A. E. and Davis K. R. (1973b) Ammonia and related gases emanating from a large dairy area. *Calif. Agric.* February pp. 10-12.
- Lundgren D. A. (1970) Atmospheric aerosol composition and concentration as a function of particle size and of time. *J. Air Pollut Control Ass.* **20**, 603-608.
- McDowell L. L. and Smith G. E. (1958) The retention and reactions of anhydrous ammonia on different soil types. *Soil Sci. Soc. Am. Proc.* **22**, 38-42.
- McRae G. J. and Seinfeld J. H. (1983) Development of a second generation mathematical model for urban air pollution. II. Performance evaluation. *Atmospheric Environment* **17**, 501-523.
- McRae G. J., Goodin W. R. and Seinfeld J. H. (1982a) Development of a second generation mathematical model for urban air pollution. I. Model formulation. *Atmospheric Environment* **16**, 679-696.
- McRae G. J., Tilden J. W. and Seinfeld J. H. (1982b) Global sensitivity analysis—A computational implementation of the fourier amplitude sensitivity test (FAST). *Computers chem. Engng* **6**, 15-25.
- Miner J. R. (1976) Production and Transport of Gaseous NH<sub>3</sub> and H<sub>2</sub>S Associated With Livestock Production. U.S. Environmental Protection Agency Document EPA-600-2-76-239. Ada, OK.
- Miner S. (1969) Air pollution aspects of ammonia. Litton Systems Inc., National Air Pollution Control Administration Document APTD 69-25. Bethesda, MD.
- Muzio L. J. and Arand J. K. (1976) Homogeneous gas phase decomposition of oxides of nitrogen. KVB Incorporated, Electric Power Research Institute Report FP-253, Project 461-1, Tustin, CA.
- National Research Council (1979) Ammonia. A report by the Subcommittee on Ammonia. Committee on Medical and Biologic Effects of Environmental Pollutants. National Research Council, University Park Press, Baltimore, MD.
- Pierson W. R., Brachaczek W. W., Korniski T. J., Truex T. J. and Butler J. W. (1980) Artifact formation of sulfate, nitrate and hydrogen ion on backup filters: Allegheny Mountain experiment. *J. Air Pollut. Control Ass.* **30**, 30-34.
- Porter L. K., Viets F. G., Jr., McCalla T. M. *et al.* (1975) Pollution Abatement from Cattle Feedlots in Northeastern Colorado and Nebraska. U.S. Environmental Protection Agency Report No. EPA-660-2-75-015. Corvallis, OR.
- Reynolds R., Tsou G. and Holmes J. (1975) The influence of gas phase ammonia on formation of aerosol. California Air Resources Board report, El Monte, CA.
- Spicer C. W. (1974) The fate of nitrogen oxides in the atmosphere. In *Advances in Environmental Science and Technology*, Vol. 7 (Edited by Pitts J. N. and Metcalf R. L.). Wiley, New York, pp. 163-261.
- Spicer C. W. and Schumacher P. M. (1979) Particulate nitrate: laboratory and field studies of major sampling interferences. *Atmospheric Environment* **13**, 543-552.
- Stanley F. A. and Smith G. E. (1955) Proper application improves value of NH<sub>3</sub>. *Agricultural Ammonia News*, April-June.
- Stelson A. W., Friedlander S. K. and Seinfeld J. H. (1979) A note on the equilibrium relationship between ammonia and nitric acid and particulate ammonium nitrate. *Atmospheric Environment* **13**, 369-371.
- Stelson A. W. and Seinfeld J. H. (1982a) Relative humidity and temperature dependence of the ammonium nitrate dissociation constant. *Atmospheric Environment* **16**, 983-992.
- Stelson A. W. and Seinfeld J. H. (1982b) Relative humidity and pH dependence of the vapor pressure of ammonium nitrate-nitric acid solutions at 25°C. *Atmospheric Environment* **16**, 993-1000.
- Stewart B. A. (1970) Volatilization and nitrification of nitrogen from urine under simulated cattle feedlot conditions. *Envir. Sci. Technol.* **4**, 579-582.
- Taiganides E. P. and Hazen T. E. (1966) Properties of farm animal excreta. *Trans. Am. Soc. agric. Engrs* **9**, 374-376.
- Trickey N. G. and Smith G. E. (1955) Losses of nitrogen from solution materials. *Soil Sci. Soc. Am. Proc.* **19**, 222-224.
- Tuazon E. C., Winer A. M. and Pitts J. N. (1981) Trace pollutant concentrations in a multiday smog episode in the California South Coast Air Basin by long pathlength FT-IR spectroscopy. *Envir. Sci. Technol.* **15**, 1232-1237.
- U.S. Bureau of the Census (1977) 1974 Census of Agriculture, Vol. 1, Part 5, California State and County Data, U.S. Department of Commerce, Washington, DC.
- U.S. Geological Survey (1976) Land Use and Land Cover 1972-1975, Santa Ana, CA (1971-1974, San Bernardino, CA; 1971-1974, Santa Maria, CA; 1972-1975, Long Beach, CA; 1973-1975, Los Angeles, CA) U.S. Department of the Interior, Geological Survey, Open File Maps No. 76-114-1 (76-115-1; 76-117-1; 76-118-1; 76-119-1), Land Use Series.
- Viets F. G., Jr. (1971) Cattle feedlot pollution. Animal Waste Management. *Proc. Nat. Symp. Animal Waste Management*, Washington, DC, Council of State Governments, pp. 97-106. Also published in *Agric. Sci. Rev.* **9**, 1-8.
- Wahhab A., Randhawa M. S. and Alam S. Q. (1957) Loss of ammonia from ammonium sulphate under different conditions when applied to soils. *Soil Sci.* **84**, 249-255.
- Walkup H. G. and Nevins J. L. (1966) The cost of doing business in agricultural ammonia for direct application. *Agric. Ammonia News* **16**, 96-100.
- White W. H. and Roberts P. T. (1977) On the nature and origins of visibility reducing species in the Los Angeles Basin. *Atmospheric Environment* **11**, 803-812.
- Witz S. and McPhee R. D. (1977) Effect of different types of glass filters on total suspended particulates and their chemical composition. *J. Air Pollut. Control Ass.* **27**, 239-241.
- Wohlert H. C. and Bell G. B. (1956) Literature Review of Metropolitan Air Pollutant Concentrations—Preparation, Sampling, and Assay of Synthetic Atmospheres. Stanford Research Institute, final report on Project No. SU1816, Menlo Park, CA.

APPENDIX A

THE ORIGIN OF AMMONIA EMISSIONS TO THE  
ATMOSPHERE IN AN URBAN AREA

G.R. Cass, S. Gharib, M. Peterson  
and J.W. Tilden

An accurate description of ammonia emissions to the atmosphere of the South Coast Air Basin is needed to support air quality models for  $\text{NH}_4\text{NO}_3$  formation. Such a study has been completed for the year 1974, and the principal results are summarized here. A grid system composed of 5 km x 5 km cells was superimposed on the South Coast Air Basin map shown in Figure 1. Ammonia emissions were estimated within each grid cell for the 53 classes of mobile and stationary source types listed in Table 1.

Source tests show that trace amounts of ammonia are present in the exhaust of both mobile and stationary combustion sources (Cadle and Mulawa, 1980; Gentel et al., 1973; Harkins and Nicksic, 1967; Henein, 1975; Hovey et al., 1966; Hunter, 1971; Muzio and Arand, 1976; Wohlers and Bell, 1956). Emission factors for ammonia release obtained from these and other references were combined with fuel use data reported by Cass (1978) to give total  $\text{NH}_3$  emissions from autos, trucks, railroads, shipping, plus industrial, residential and commercial fuel use. Within each fuel use category, the  $\text{NH}_3$  emissions shown in Table 1 were distributed spatially in the same manner as  $\text{NO}_x$  emissions. A number of industrial processes are known to emit ammonia (National Research Council, 1979; Miner, 1969), including refinery operations, ammonia-based fertilizer manufacturing, ammonia storage facilities, refrigeration plants, chemical plants and steel mill coke ovens. Estimates of  $\text{NH}_3$  emissions from industrial facilities were derived from source test information and questionnaires sent to individual companies.

Biological decay processes also produce ammonia and the release rates from a variety of soil surface types are available (Porter et al., 1975; Elliot et al., 1971; Denmead et al., 1978; Denmead et al., 1976; Miner, 1976). Using aerial photographs and maps available from the U.S. Geological Survey (1976) the land use within each grid square was summarized by type. Emissions from exposed land surfaces were estimated within each square by matching emission rate data to soil surface types.

Chemical fertilizers used in the air basin include ammonia, urea, ammonium nitrate and ammonium sulfate. Depending on fertilizer type and method of application, anywhere from a few percent to several tenths of the nitrogen content may be lost to the atmosphere as ammonia (Allison, 1966; Baker et al., 1959; Ernst and Massey, 1960; Gasser, 1964; McDowell and Smith, 1958; Stanley and Smith, 1955; Trickey and Smith, 1955; Wahhab et al., 1957; Walkup and Nevins, 1966). The ammonia loss characteristics of fertilizers were estimated by consultation with a local agricultural expert (Meyer, 1981). Fertilizer use statistics were obtained from the California Department of Food and Agriculture (1974) and from the U.S. Bureau of the Census (1977). Chemical fertilizer consumption, subdivided into cropland, orchard and non-farm use, was combined with the ammonia loss data to compute total  $\text{NH}_3$  emissions.

Decomposition of livestock wastes is a major source of  $\text{NH}_3$  emissions. Animal inventories by county were obtained from the U.S. Bureau of the Census (1977) and from state and county agricultural

agents. Waste production rates, nitrogen content and ammonia volatilization rates were estimated for each major commercial animal type from previous studies (Adriano, et al., 1971; Adriano et al., 1974; Fogg, 1971; Giddens and Rao, 1975; Lauer et al., 1976; Luebs et al., 1973ab; Stewart, 1970; Taiganides and Hazen, 1966; Viets, 1971). Emissions from range animals were distributed spatially in proportion to pasture and herbaceous range land areas. U.S. Geological Survey (1976) maps were used to locate emissions from animals raised in confinement (e.g. dairy cattle, feedlot cattle).  $\text{NH}_3$  losses from domestic animals (cats and dogs only) plus human respiration, perspiration and household cleaning chemicals were distributed in proportion to residential land use.

The overall spatial distribution of  $\text{NH}_3$  emissions in the South Coast Air Basin is shown in Figure 2. The largest spike in the  $\text{NH}_3$  diagram is centered over the town of Chino on the prevailing upwind side of the city of Riverside, and results from the intensity of livestock operations in that area. Details of the ammonia emission inventory calculations are presented in the Appendix to this report.

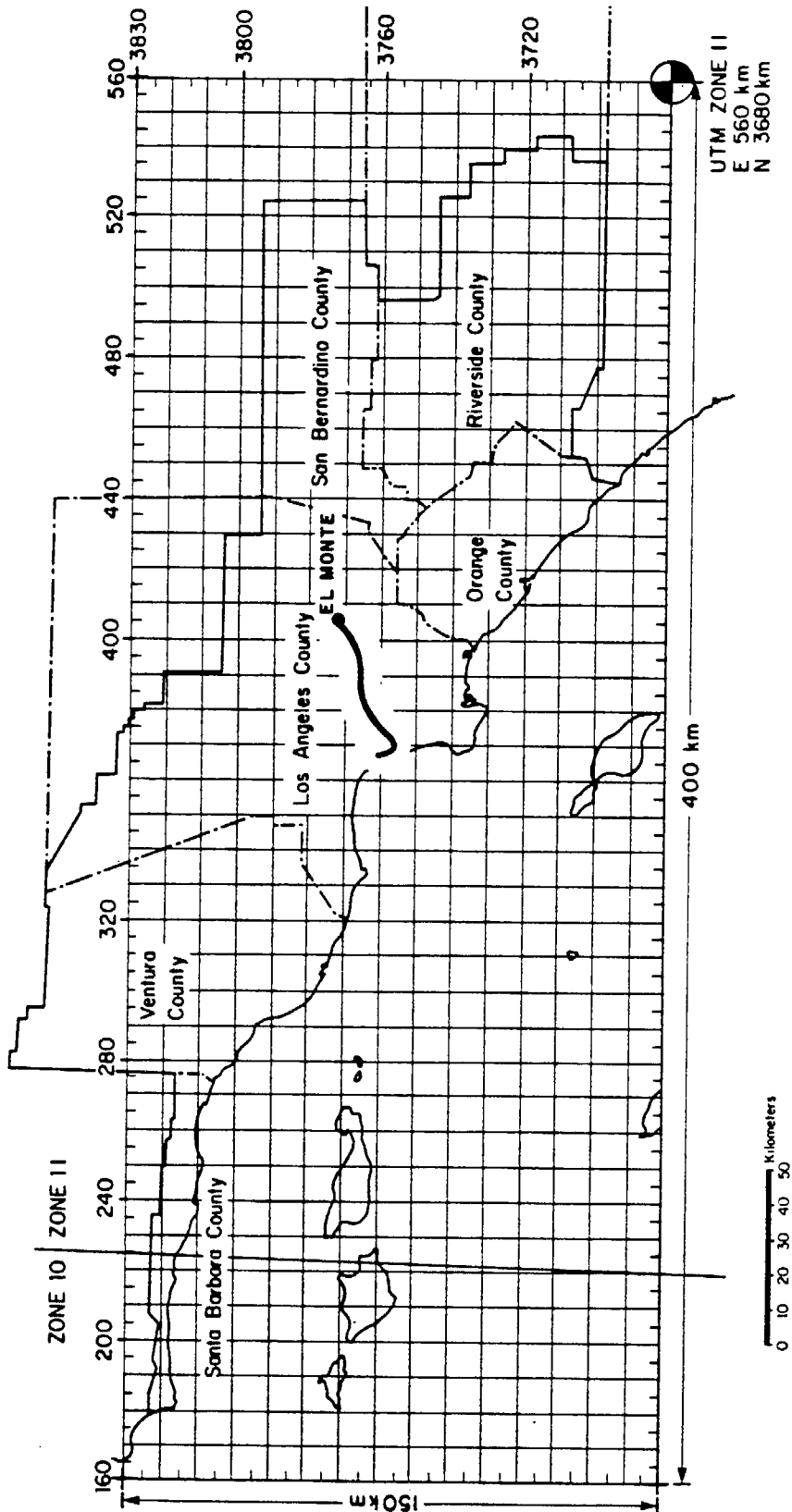


FIGURE 1  
The South Coast Air Basin Showing the Grid System Used

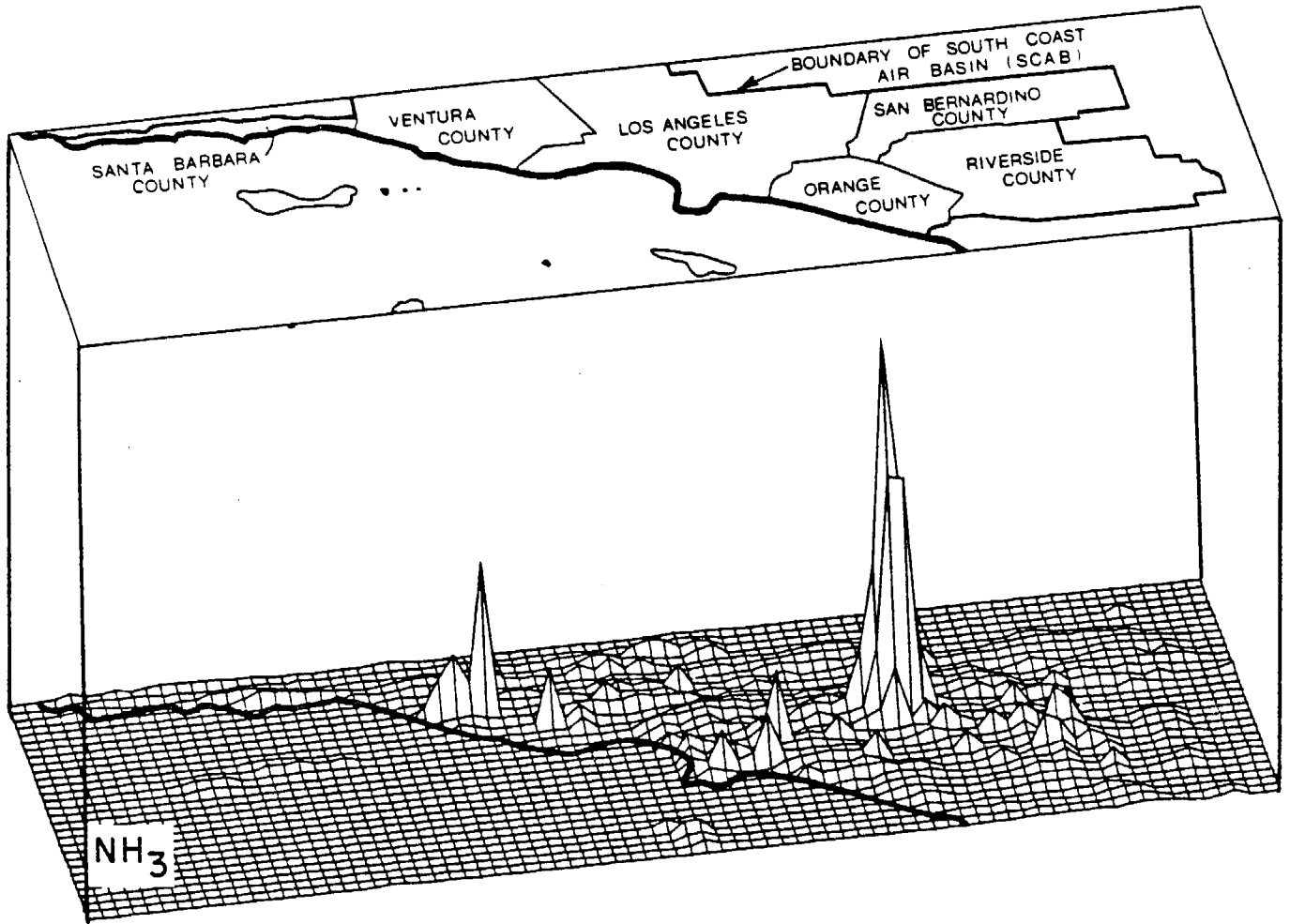


FIGURE 2

The Spatial Distribution of Ammonia Emissions  
in the South Coast Air Basin - 1974

51  
TABLE 1

Summary of Ammonia Emissions By Source Category  
in the South Coast Air Basin  
1974

SOURCE CATEGORY	TOTAL EMISSIONS (kg/day)	
<b>Stationary Fuel Combustion</b>		
Electric Utility		
Natural Gas	590.0	
Residual Oil	2000.0	
Digester Gas	0.5	
Refinery Fuel Burning		
Natural Gas	160.0	
Residual Oil	99.0	
Refinery Gas	420.0	
Industrial Fuel Burning		
Natural Gas	610.0	
Liquified Petroleum Gas (LPG)	4.0	
Residual Oil	150.0	s
Distillate Oil	140.0	
Digester Gas	9.0	
Coke Oven Gas	15.0	
Residential/Commercial Fuel Burning		
Natural Gas	270.0	
Liquid Propane Gas (LPG)	4.0	anic
Residual Oil	62.0	
Distillate Oil	73.0	
Coal	20.0	
*** Sub totals ***	4626.5	(3.09%)
<b>Mobile Source Fuel Combustion</b>		
Automotive		anced
Non-catalyst Autos and Light Trucks	3309.0	
Medium and Heavy Duty Trucks	449.9	
Diesel Vehicles	370.0	
LPG for Carburetion	10.0	
Civilian Aircraft		
Jet	150.0	
Piston	2.9	
Shipping		
Residual Oil Boilers	70.0	er
Diesel Ships	50.0	nty
Railroad-Diesel Oil	90.0	
Military		
Gasoline	10.0	
Diesel	60.0	
Jet Fuel	50.0	
Residual Oil	0.8	
Off Highway Vehicles	120.0	
*** Sub totals ***	4742.6	(3.17%)
Industrial Point Sources	2070.0	(1.38%)
Soil Surface	23790.0	(15.9%)
Fertilizer		rces port
Farm Crop	2870.0	
Orchards	2390.0	
Handling	380.0	
Non-farm	7420.0	
*** Sub totals ***	13060.0	(8.72%)
Livestock		c
Cattle		
Dairy	24390.0	
Feedlot	6880.0	
Range	12160.0	
Horses	16220.0	
Sheep	990.0	
Hogs	250.0	
Chickens	18200.0	
Turkeys	1120.0	
*** Sub totals ***	80210.0	(53.6%)
Domestic		of
Dogs	10350.0	
Cats	3230.0	
Human Respiration	46.0	
Human Perspiration	7000.0	
Household Ammonia Use	600.0	
*** Sub totals ***	21226.0	(14.2%)
*** Total ***	149725.1	(100.0%)

## References

- Addis, D. (1981) Personal Communication, Cooperative Extension Service, University of California at Riverside, April 15, 1981.
- Adriano, D.C., Chang, A.C. and Sharpless, R. (1974) "Nitrogen Loss from Manure as Influenced by Moisture and Temperature," J. Environmental Quality, 3, 258-261.
- Adriano, D.C., Pratt, P.F. and Bishop, S.E. (1971) "Fate of Inorganic Forms of N and Salt from Land-disposed Manures from Dairies," Livestock Waste Management and Pollution Abatement-Proceedings -International Symposium of Livestock Wastes St. Joseph, MI, American Society of Agricultural Engineers, pp. 243-246.
- Allison, F.E. (1966) "The Fate of Nitrogen Applied to Soils," Advanced Agronomy, 18, 219-258.
- Altman, P.L. and Dittmer, D.S. (1968) Metabolism, Bethesda, MD, Federation of American Societies for Experimental Biology.
- Anderson, E.E. (1979) Personal Communication by letter of September 19, 1979. Forwarded 1971 inventory of horse population by county from vaccination records.
- Baker, J.H., Peech, M. and Musgrove, R.B. (1959) "Determination of Application Losses of Anhydrous Ammonia," Agronomy Journal, 51, 361-362.
- Bartz, D.R., Arledge, K.W., Gabrielson, J.E. Hays, L.G., and Hunter, S.C. (1974) Control of Oxides of Nitrogen from Stationary Sources in the South Coast Air Basin, Tustin, California, KVB, Inc., Report No. 5800-179.
- Bishop, S. (1981) Personal Communication, Cooperative Extension Service, University of California at Riverside, April 9, 1981.
- Cadle, S.H. and Mulawa, P.A. (1980) "Low Molecular Weight Aliphatic Amines in Exhaust from Catalyst-Equipped Cars," Environmental Science and Technology, 14, 718-723.
- California Department of Food and Agriculture (1974) Fertilizing Materials - Tonnage Report, Oct-Nov-Dec 1974, Sacramento, CA, California Department of Food and Agriculture.
- Cass, G.R. (1978) "Methods for Sulfate Air Quality Management with Applications to Los Angeles," Ph.D. Thesis, California Institute of Technology, Pasadena, CA.

- Cass, G.R., McMurry, P.S., Houseworth, J.E. (1980) Methods for Sulfate Air Quality Management, Pasadena, CA, California Institute of Technology Environmental Quality Laboratory Report 16, 3 vols.
- Chambers, L.A. (1959) "Transportation Sources of Air Pollution (1) - Comparison with Other Sources in Los Angeles," Proceedings - National Conference on Air Pollution, Washington, D. C., U.S. Public Health Service Publication No. 654.
- Dale, A.C. (1971) "Status of Dairy Cattle Waste Treatment and Management Research," Animal Waste Management-Proceedings of National Symposium on Animal Waste Management, Washington, D.C., Council of State Governments, pp. 85-95.
- Denmead, O.T., Nulsen, R. and Thurtell, G.W. (1978) "Ammonia Exchange over a Corn Crop," Soil Science Soc. Amer. J., 42, 840-842.
- Denmead, O.T., Freney, J.R., and Simpson, J.R. (1976) "A Closed Ammonia Cycle Within a Plant Canopy," Soil Biol. Biochem., 8, 161-164.
- Elliot, L.F., Schuman, G.E., and Viets, F.G. Jr. (1971) "Volatilization of Nitrogen-Containing Compounds from Beef Cattle Areas," Soil Sci. Soc. Amer. Proc., 35, 752-755.
- Ernst, J.W. and Massey, H.F. (1960) "The Effects of Several Factors on Volatilization of Ammonia Formed from Urea in the Soil," Soil Sci. Soc. Am. Proc., 24, 87-90.
- Fogg, C.E. (1971) "Livestock Waste Management and the Conservation Plan," Livestock Waste Management and Pollution Abatement - Proceedings International Symposium on Livestock Wastes, St. Joseph, MI, American Society of Agricultural Engineers, pp. 34-35.
- Fretz, R. (1980) Jet Propulsion Laboratory, California Institute of Technology, Pasadena, California, Provided photographs.
- Gasser, J.K.R. (1964) "Some Factors Affecting Losses of Ammonia from Urea and Ammonium Sulphate Applied to Soils," J. Soil Sci., 15, 258-272.
- Gentel, J.E., Manary, O.J., Valenta, J.C. (1973) Characterization of Particulates and Other Non-Regulated Emissions from Mobile Sources and the Effects of Exhaust Emissions Control Devices on These Emissions, Midland, MI, Dow Chemical Company, U.S. Environmental Protection Agency Document APTD-1567.
- Giddens, J. and Rao, A.M. (1975) "Effect of Incubation and Contact with Soil on Microbial and Nitrogen Changes in Poultry Manure," J. Environmental Quality, 4, 275-278.

- Greek, B.F. (1975) "Ammonia Squeeze Loosens, Outlook Stays Good," Chemical & Engineering News, April 28, 10-13.
- Harkins, J.H. and Nicksic, S.W. (1967) "Ammonia in Auto Exhaust," Environmental Science and Technology, 1, 751-752.
- Healy, T.V., McKay, H.A.C., Plibeam, A. and Scargill, D. (1970) "Ammonia and Ammonium Sulfate in the Troposphere over the United Kingdom," J. Geophysical Research, 75, 2317-2321.
- Henein, N. (1975) "The Diesel as an Alternative Automobile Engine," Wayne State University, SAE Paper 750931.
- Hovey, H.H., Risman, A., Cunnann, J.F. (1966) "The Development of Air Contaminant Emission Tables for Nonprocess Emissions, J. Air Pollution Control Association, 16, 362-366.
- Hudson, R. (1981) Personal Communication by telephone, April 7, 1981, Orange County Animal Control.
- Hunter, J.E. Jr. (1971) Effect of Catalytic Converters on Automotive Ammonia Emissions, Warren, MI, General Motors Research Laboratories, Research Publication GMR-1061.
- Kirk-Othmer Encyclopedia (1963) Kirk-Othmer Encyclopedia of Chemical Technology, 2nd Ed., Vol. 2, New York, John Wiley & Sons.
- Kupprat, I., Johnson, R.E., and Hertig, B.A. (1976) "Ammonia: A Normal Constituent of Expired Air During Rest and Exercise," Federation of American Societies for Experimental Biology, 60th Annual Meeting, Anaheim, CA, April 11-16, 1976 (abstract), Federation Proceedings, 35, 1499.
- Lauer, D.A., Bouldin, D.R. and Klausner, S.D. (1976) "Ammonia Volatilization from Dairy Manure Spread on the Soil Surface," J. Environmental Quality, 5, 134-141.
- Luebs, R.E., Lagg, A.E., and Davis, K.R. (1973a) "Ammonia and Related Gases Emanating from a Large Dairy Area," California Agriculture, February 1973 edition, pp. 10-12.
- Luebs, R.E., Davis, K.R. and Lagg, A.E. (1973b) "Enrichment of the Atmosphere with Nitrogen Compounds Volatilized from a Large Dairy Area, J. Environmental Quality, 2, 137-141.
- Magill, P.L. and Benoliel, R.W. (1952) "Air Pollution in Los Angeles County," Industrial and Engineering Chemistry, 44, 1347-1351.
- McDowell, L.L. and Smith, G.E. (1958) "The Retention and Reactions of Anhydrous Ammonia on Different Soil Types," Soil Sci. Soc. Am. Proc., 22, 38-42.

- Meyer, J.L. (1981) personal communication, Cooperative Extension Service, University of California at Riverside, provided data on fertilization practices in the Los Angeles area and estimates of the fractional loss of  $\text{NH}_3$  from fertilizers as used locally.
- Miner, J. R. (1976) "Production and Transport of Gaseous  $\text{NH}_3$  and  $\text{H}_2\text{S}$  Associated With Livestock Production," Ada, OK, U.S. Environmental Protection Agency document EPA-600/2-76-239.
- Miner, S. (1969) Air Pollution Aspects of Ammonia, Bethesda, MD, Litton Systems Inc., National Air Pollution Control Administration document APTD 69-25.
- Muehling, A.J. (1971) "Swine Waste Management," Animal Waste Management-Proceedings of National Symposium on Animal Waste Management, Washington, D. C., Council of State Governments, pp. 111-120.
- Muzio, L.J. and Arand, J.K. (1976) Homogeneous Gas Phase Decomposition of Oxides of Nitrogen, Tustin, CA, KVB Incorporated, Electric Power Research Institute report FP-253, Project 461-1.
- National Research Council (1979) Ammonia, Baltimore, MD, University Park Press, a report by the Subcommittee on Ammonia, Committee on Medical and Biologic Effects of Environmental Pollutants, National Research Council.
- Peters, J.A. and Blackwood, T.R. (1977) Source Assessment: Beef Cattle Feedlots, Washington, D.C., U.S. Environmental Protection Agency document EPA-600/2-77-107.
- Porter, L.K. et al. (1975) Pollution Abatement from Cattle Feedlots in Northeastern Colorado and Nebraska, Corvallis, OR, U.S. Environmental Protection Agency document EPA-660/2-75-015.
- Richards, B. (1981) Personal Communication by telephone, April 7, 1981, Los Angeles County Animal Control.
- San Bernardino (1981) Personal Communication by telephone, April 7, 1981, San Bernardino Animal Licenses Office.
- Scholz, H.G. (1971) "Systems for the Dehydration of Livestock Wastes - A Technical and Economical Review, Livestock Waste Management and Pollution Abatement - Proceedings - International Symposium on Livestock Wastes, St. Joseph, MI, American Society of Agricultural Engineers, pp. 27-29.
- Sonderlund, R. (1977) " $\text{NO}_x$  Pollutants and Ammonia Emissions - A Mass Balance for the Atmosphere over NW Europe," Ambio, 6, 118-122.

- Southern California Association of Governments (1977) "Regional Population, Housing, Employment and Land Use Forecasts: Baseline and Range," Los Angeles, CA, Southern California Association of Governments, Report 208-5.
- Stanley, F.A. and Smith, G.E. (1955) "Proper Application Improves Value of  $\text{NH}_3$ ," Agricultural Ammonia News, April-June, 1955.
- Stewart, B.A. (1970) "Volatilization and Nitrification of Nitrogen from Urine under Simulated Cattle Feedlot Conditions," Environmental Science and Technology, 4, 579-582.
- Taigonides, E.P. and Hazen, T.E. (1966) "Properties of Farm Animal Excreta," Trans. Am. Soc. Agri. Engrs., 9, 374-376.
- Trickey, N.G. and Smith, G.E. (1955) "Losses of Nitrogen from Solution Materials," Soil Sci. Soc. Am. Proc., 19, 222-224.
- U.S. Bureau of the Census (1980) Statistical Abstract of the United States, 1980, Washington, D.C., U.S. Department of Commerce.
- U.S. Bureau of the Census (1977) 1974 Census of Agriculture, Volume 1, Part 5, California State and County Data, Washington, D. C., U.S. Department of Commerce.
- U.S. Bureau of the Census (1972) 1970 Census of Population and Housing - Santa Barbara, California, Washington, D.C., U.S. Department of Commerce.
- U.S. Geological Survey (1976) Land Use and Land Cover 1972-1975, Santa Ana, CA (1971-1974, San Bernardino, CA; 1971-1974, Santa Maria, CA; 1972-1975, Long Beach, CA; 1973-1975, Los Angeles, CA) U.S. Department of the Interior, Geological Survey, Open File Maps No. 76-114-1 (76-115-1; 76-117-1; 76-118-1; 76-119-1) Land Use Series.
- Viets, F.G. Jr. (1971) "Cattle Feedlot Pollution," Animal Waste Management-Proceedings of National Symposium on Animal Waste Management, Washington, D. C., Council of State Governments, pp. 97-106. Also published in Agricultural Science Review, 9, 1-8.
- Wahhab, A., Randhawa, M.S. and Alam, S.Q. (1957) "Loss of Ammonia from Ammonium Sulphate Under Different Conditions When Applied to Soils," Soil Sci., 84, 249-255.
- Walkup, H.G. and Nevins, J.L. (1966) "The Cost of Doing Business in Agricultural Ammonia for Direct Application," Agricultural Ammonia News, 16, 96-100.

Wohlers, H.C. and Bell, G.B. (1956) Literature Review of Metropolitan Air Pollutant Concentrations - Preparation, Sampling, and Assay of Synthetic Atmospheres, Menlo Park, CA, Stanford Research Institute, final report on Project No. S-1816.

APPENDIX

Tabulation of Emission Factors, Activity Levels,  
and Ammonia Emission Rates

STATIONARY SOURCES

REFERENCE	EMISSION FACTOR (Kg NH <sub>3</sub> /10 <sup>9</sup> Btu)	VALUE ADOPTED FOR EMISSION INVENTORY USE (Kg NH <sub>3</sub> /10 <sup>9</sup> Btu)
<b>Fuel Combustion</b>		
<b>Natural Gas</b>		
Average of Los Angeles Source Tests		
New York Emission Inventory Emission Factor		
Literature Survey (1969)		
Literature Review (1956)		
Recent Source Test: 200,000 Btu/hr combustor		
(a)	0.119	0.4 mg/m <sup>3</sup> NH <sub>3</sub> in exhaust
(b)	0.214	0.5 lb NH <sub>3</sub> /10 <sup>6</sup> ft <sup>3</sup> gas burned
(c)	0.128-0.240	0.3 to 0.56 lb NH <sub>3</sub> /10 <sup>6</sup> ft <sup>3</sup> gas
(d)	8.56	0.010 tons NH <sub>3</sub> /10 <sup>6</sup> ft <sup>3</sup> gas
(e)	3.25	14.44 ppm NH <sub>3</sub> in exhaust
(e)	1.351	6.00 ppm NH <sub>3</sub> in exhaust
(e)	0.225	1.00 ppm NH <sub>3</sub> in exhaust
<b>Residual Fuel Oil</b>		
Average of Los Angeles Source Tests		
New York Emission Inventory Emission Factor		
Literature Survey (1956)		
Recent Source Test: 200,000 Btu/hr combustor at 2% excess air; avg of 2 tests		
(a)	0.125	0.4 mg/m <sup>3</sup> NH <sub>3</sub> in exhaust
(f)	3.03	1 lb/1000 gal oil
(g)	23.1	0.001 tons NH <sub>3</sub> /ton oil
(h)	2.8	11.3 ppm in exhaust
(i)	3.29	1 lb/1000 gal oil
<b>Distillate Oil</b>		
New York Emission Inventory Emission Factor		
<b>Coal</b>		
Literature Review (1956)		
Mass Balance over N.W. Europe		
Recent Source Test: 200,000 Btu/hr combustor at 4% excess air, 1 test		
(j)	37.8	2 lb NH <sub>3</sub> /ton coal
(k)	50	1.21 g NH <sub>3</sub> /920 g coal
(l)	~20	85 ppm NH <sub>3</sub> in exhaust
<b>Wood</b>		
Literature Review (1956)		
(m)		2.4 lb NH <sub>3</sub> /ton wood

## Notes:

- (a) Magill and Benoliel (1952)
- (b) Hovey, Risman and Cunnan (1966), Range reported 0.3 to 20 lb  $\text{NH}_3/10^6 \text{ ft}^3$  natural gas
- (c) Miner (1969); literature survey
- (d) Wohlers and Bell (1956)
- (e) Muzio and Arand (1976)
- (f) Hovey, Risman and Cunnan (1966); Range reported 0.06 lb/1000 gal to 8 lb/1000 gal; converted at 0.011 scf prod/btu;  $6.11 \times 10^6$  btu/bbl
- (g) Wohlers and Bell (1956); value appears high but note that data may be rounded up to 0.001 tons  $\text{NH}_3/\text{ton oil}$
- (h) Muzio and Arand (1976); 2 tests range 20 ppm - 2.54 ppm
- (i) Hovey, Risman and Cunnan (1966); converted at 0.011 scf prod/btu;  $5.8 \times 10^6$  btu/bbl
- (j) Wohlers and Bell (1956)
- (k) Soderlund (1977)
- (l) Muzio and Arand (1976); combustion product data unavailable, converted from ppm to  $\text{Kg}/10^9$  btu in proportion to oil and natural gas data
- (m) Wohlers and Bell (1956)

TABLE A.2

## Emission Factors for Ammonia from Highway Vehicles

VALUE REPORTED	REFERENCE	EMISSION FACTOR (Kg NH <sub>3</sub> /10 <sup>9</sup> Btu)	VALUE ADOPTED FOR EMISSIONS INVENTORY USE (Kg NH <sub>3</sub> /10 <sup>9</sup> Btu)
<b>HIGHWAY VEHICLES</b>			
<b>Autos and Lt. Trucks (gasoline)</b>			
<b>Non-Catalyst Equipped Pre-1975</b>			
1. Typical auto (1952 data)	(a)	7.27 (1)	2.11 (m)
2. Fleet average (1959 data)	(b)	7.27 (1)	
3. 1956 Oldsmobile engine on driving cycle	(c)	0.44 (1)	
4. 1972 Hew driving cycle	(d)	0.87 (1)	
5. 1972 Pontiac, unleaded fuel, 30 mph	(e)	1.2 (1)	
6. 1972 Pontiac, unleaded fuel, 60 mph	(f)	2.65 (1)	
7. 1972 Pontiac, unleaded fuel, driving cycle	(g)	2.43 (1)	
8. 1972 Pontiac, leaded fuel, driving cycle	(h)	2.62 (1)	
9. 1972 Pontiac, leaded fuel, 30 mph	(i)	1.56 (1)	
10. Aged auto, unleaded fuel, driving cycle	(j)	4.21 (1)	
11. Aged auto, unleaded fuel, 60 mph	(k)	3.52 (1)	
<b>Catalyst Equipped Engines</b>			
1. California emission controls, 1975 FTP cycle	(n)	0.69 (r)	1.6 (t)
2. Aged auto, unleaded fuel, driving cycle	(o)	2.07 (r)	
3. 1972 Pontiac, unleaded fuel, beaded base metal catalyst, driving cycle	(p)	2.01 (r)	
<b>Medium and Heavy Duty Gasoline Trucks</b>			
<b>Diesel Vehicles</b>			
Peugot, diesel fuel, driving cycle	(q)	3.11 (s)	2.11 (u)
<b>LPG for Carburetion</b>			
			2.11 (u)

NOTES:

- (a) Magill and Benoliel (1952)
- (b) Chambers (1959)
- (c) Harkins and Nicksic (1967)
- (d) Hunter (1971)
- (e) Gentel et al. (1973); Average of 3 tests
- (f) Gentel et al. (1973)
- (g) Gentel et al. (1973)
- (h) Gebtel et al. (1973)
- (i) Gentel et al. (1973); 1 test (a second test under lean combustion conditions showed 31 ppm NH<sub>3</sub> in exhaust)
- (j) Hensein (1975)
- (k) Hensein (1975)
- (l) Emissions calculated assuming: Non-catalyst fleet fuel economy = 13.6 miles/gallon, 5248 x 10<sup>3</sup> Btu/bbl of gasoline; air/fuel ratio = 15; gasoline density = 6.19 lb/gal
- (m) average of driving cycle tests (lines 3,4,7,8,10 within this category)
- (n) Cadle and Mulawa (1980), Table V, average of 5 tests (runs 9 through 13), range 0.6 mg NH<sub>3</sub>/mile to 14.8 mg NH<sub>3</sub>/mile
- (o) Hensein (1975), average of 3 tests, range: 25.31 to 2.52 ppm, air; fuel ratio assumed to be 15
- (p) Gentel et al. (1973), Table 27 air/fuel ratio assumed to be 15
- (q) Hensein (1975) air/fuel ratio assumed to be 22
- (r) Calculated assuming catalyst fleet fuel economy of 17.8 miles/gallon; 5248 x 10<sup>3</sup> Btu/bbl gasoline, gasoline density 6.19 lb/gal.
- (s) Calculated assuming 5812 x 10<sup>3</sup> Btu/bbl of diesel fuel; composition of diesel fuel assumed to be CH<sub>1.5</sub>.
- (t) Average of lines 1,2,3 within this category
- (u) Assumed similar to non-catalyst gasoline automobiles

TABLE A.3  
Ammonia Emission Estimates for Stationary Combustion Sources

	ESTIMATED 1974 FUEL USE (10 <sup>9</sup> Btu/day)	EMISSION FACTOR (Kg NH <sub>3</sub> /10 <sup>9</sup> Btu)	NH <sub>3</sub> EMISSIONS (metric tons/day)
<b>STATIONARY SOURCES</b>			
<b>Fuel Combustion</b>			
<b>Electric Utilities</b>			
Natural Gas	398.31 (a)	1.47 (d)	0.59
Residual Oil	715.01 (a)	2.8 (e)	2
Digester Gas	0.37 (a)	1.47 (f)	0.0005
<b>Refinery Fuel</b>			
Natural Gas	134.06 (b)	1.17 (g)	0.16
Residual Oil	35.47 (b)	2.8 (h)	0.099
Refinery Gas	357.53 (b)	1.17 (i)	0.42
<b>Non-Refinery Industrial Fuel</b>			
Natural Gas	421.64 (c)	1.45 (j)	0.61
LPG	2.74 (c)	1.45 (k)	0.004
Residual Oil	53.42 (c)	2.8 (l)	0.15
Distillate Oil	42.74 (c)	~3.3 (m)	0.14
Digester Gas	6.30 (c)	1.45 (k)	0.009
Coke Oven Gas	37.53 (c)	0.40 (n)	0.015
<b>Residential/Commercial</b>			
Natural Gas	1181.92 (c)	0.225 (o)	0.27
LPG	18.08 (c)	0.225 (p)	0.004
Residual Oil	22.19 (c)	~2.8 (q)	0.062
Distillate Oil	22.19 (c)	~3.3 (q)	0.073
Coal	0.55 (c)	38 (q)	0.02
<b>TOTAL</b>			<b>4.63</b>

NOTES:

- (a) June 1974 average daily use, from Cass, McMurry and Houseworth (1980), Table A2.3
- (b) June 1974 average daily use, from Cass, McMurry and Houseworth (1980), Table A2.5
- (c) 1973 annual average daily use, from Cass, McMurry and Houseworth (1980), Table A3.6
- (d) Weighted average: 33% emission factor at 2% O<sub>2</sub> in stack, 22% factor at 4% O<sub>2</sub>, 45% factor at 6% O<sub>2</sub> based on frequency of occurrence of O<sub>2</sub> levels given by Bartz et al. (1974; tests 279-289; 298-301) From Table A.1
- (e) From Table A.1
- (f) Assumed similar to utility boiler burning natural gas
- (g) Weighted average: 19% emission factor at 2% O<sub>2</sub> in stack, 33% factor at 4% O<sub>2</sub>, 48% factor at 6% O<sub>2</sub> based on frequency of occurrence of O<sub>2</sub> levels given by Bartz et al. (1974; tests 12-73; 95-103) From Table A.1
- (h) From Table A.1
- (i) Assumed similar to refinery equipment burning natural gas
- (j) Weighted average: 35% emission factor at 2% O<sub>2</sub> in stack, 15% factor at 4% O<sub>2</sub>, 50% factor at 6% O<sub>2</sub> based on frequency of occurrence of O<sub>2</sub> levels for industrial fuel burning equipment given by Bartz et al. (1974). From Table A.1
- (k) Assumed similar to industrial equipment burning natural gas
- (l) From Table A.1
- (m) From Table A.1
- (n) Weighted average: 2% emission factor at 2% O<sub>2</sub> in stack, 10% factor at 4% O<sub>2</sub>, 88% factor at 6% O<sub>2</sub> based on frequency of occurrence of O<sub>2</sub> levels for steel mill equipment given by Bartz et al. (1974; tests 104-157)
- (o) Source tests by Bartz et al. (1974) show that home heaters have high levels of excess O<sub>2</sub> in their exhaust
- (p) Assumed similar to home heaters burning natural gas
- (q) From Table A.1

TABLE A.4

## Ammonia Emission Estimates for Mobile Combustion Sources

	ESTIMATED 1974 FUEL USE (a) (10 <sup>9</sup> Btu/day)	EMISSION FACTOR (Kg NH <sub>3</sub> /10 <sup>9</sup> Btu)	NH <sub>3</sub> EMISSIONS (metric tons/day)
<b>MOBILE SOURCES</b>			
Highway Vehicles			
Non-catalyst Autos & Lt. Trucks	1566.58	2.11	3.31
Medium & Heavy Gasoline Vehicles	213.64	2.11	0.45
Diesel Vehicles	117.53	3.11	0.37
LPG for Carburetion	5.20	2.11	0.01
Civil Aviation			
Jet Aircraft	47.40	3.11	0.15
Aviation Gasoline	1.37	2.11	0.0029
Commercial Shipping			
Residual Oil-Fired Ship's Boilers	24.66	2.8	0.07
Diesel Ships	17.26	3.11	0.05
Railroad			
Diesel Oil	29.32	3.11	0.09
Military			
Gasoline	6.03	2.11	0.01
Diesel Oil	17.81	3.11	0.06
Jet Fuel	16.71	3.11	0.05
Residual Oil (Bunker Fuel)	0.27	2.8	0.0008
Miscellaneous			
Off-Highway Vehicles	39.73	3.11	0.12
<b>TOTAL</b>			<b>4.74</b>

Note:  
(a) 1973 annual average fuel use from Cass, McMurry and Houseworth (1980).

TABLE A.5  
Emissions from Industrial Process Sources

	NH <sub>3</sub> EMISSIONS (metric tons/day)
Ammonia Storage	0.06
Refinery FCC Units	0.67
Refinery Waste Water Treatment	0.35
Steel Industry	0.23
Chemical Plants	0.76

TABLE A.6

## Emission Factors for Ammonia Release from Soil Surface

LAND SURFACE TYPE	VALUE REPORTED	REFERENCE	EMISSION FACTOR ADOPTED (kg NH <sub>3</sub> /km <sup>2</sup> -day)
Cropland	11 kg N/ha-yr	(a)	3.65
Lawn Surface (campus sidewalk)	0.5 to 1.5 mg NH <sub>3</sub> /m <sup>2</sup> -day	(b)	1
Bare Soil	1 to 2 mg NH <sub>3</sub> /m <sup>2</sup> -day	(c)	1 (f)
Ungrazed Grass-Clover Pasture	2 g N/ha-hr	(d)	5.81
Forest Land (estimate)		(e)	(1)
Pasture (near animals - no manure)	1 to 2 mg NH <sub>3</sub> /m <sup>2</sup> -day	(b)	1.5
Pasture Grass (>30 m from manure source)	2 to 3 mg NH <sub>3</sub> /m <sup>2</sup> -day	(b)	2.5
Grassland Near Swine Barn with no manure			
Pasture (with manure)	2 to 5 mg NH <sub>3</sub> /m <sup>2</sup> -day	(b)	(g)
Pasture with dried manure	5 to 20 mg NH <sub>3</sub> /m <sup>2</sup> -day	(b)	(g)
Pasture with recent liquid dairy manure	15 kg N/ha-yr	(a)	(g)
Grazed Pasture	13 g N/ha-hr	(d)	(g)

## NOTES

- (a) Porter et al. (1975) and Elliot et al. (1971). Note that Denmead et al. (1978) give much higher values over short periods of time.  
 (b) Miner (1976)  
 (c) Miner (1976); bare soil located more than 30 m from university dairy farm  
 (d) Denmead et al. (1976)  
 (e) Release from decomposition of organic matter in forests estimated as being low  
 (f) Taken at low end of range given in order not to exceed estimate for lawns  
 (g) Not used; emissions of NH<sub>3</sub> due to presence of animal wastes will be estimated separately

TABLE A.7

## Ammonia Estimates for Release from Soil Surfaces

	LAND AREA DEVOTED TO THIS USE (km <sup>2</sup> ) (a)	FRACTION OF LAND NOT MASKED BY BUILDINGS AND PAVEMENT	EMISSION FACTOR (Kg NH <sub>3</sub> /Km <sup>2</sup> -day)	NH <sub>3</sub> EMISSIONS METRIC TONS PER DAY
<b>SOIL SURFACE RELEASE</b> (Excluding Chemical Fertilizers & Manures)				
Urban or Built-up Land				
11 Residential (single and multiple)	2884.41	44% (b)	1 (e)	1.27
12 Commercial and Services	826.21	34% (b)	1 (e)	0.28
13 Industrial	429.16	47% (b)	1 (e)	0.2
14 Transportation, Communication & Utilities	218.91	55% (b)	1 (e)	0.12
15 Industrial and Commercial Complexes	20.83	40% (c)	1 (e)	0.01
16 Mixed Urban or Built-Up Land	43.95	43% (d)	1 (e)	0.02
17 Other Urban or Built-Up Land	348.23	43% (d)	1 (e)	0.15
Agricultural Land				
21 Cropland and Pasture	1770.72		3.4 (f)	6.02
22 Orchards, Groves, Vineyards, Nurseries, and Ornamental	857.65		(3.6)(g)	3.09
23 Confined Animal Feeding Operations	47.26		estimated separately (h)	
24 Other Agricultural Land	25.32		(3.4)(i)	0.09
Rangeland				
31 Herbaceous Rangeland	686.48		(1) (j)	0.69
32 Shrub and Brush Rangeland	8053.08		(1) (j)	8.05
33 Mixed Rangeland	1165.01		(1) (j)	1.17
Forest Land				
41 Deciduous Forest Land	12.53		(1) (k)	<0.01
42 Evergreen Forest Land	2291.58		(1) (k)	<2.29
43 Mixed Forest Land	40.08		(1) (k)	<0.04
Wetland				
61 Forested Wetland	33.10			neglected
62 Non-Forested Wetland	53.89			neglected
Barren Land				
72 Beaches	16.21		< (1) (l)	<0.02
73 Sandy Areas (other than beaches)	107.35		< (1) (l)	<0.11
76 Transitional Areas	149.76		1 (m)	0.15
77 Mixed Barren Land	10.62		1 (m)	0.01
				<23.79

88

## NOTES

- (a) Obtained by counting areas in each category as shown on land use maps prepared by U.S. Geological Survey (1976a-e)
- (b) Obtained by examination of aerial photographs (Fretz, 1980). Twenty-four zone photos distributed widely over Los Angeles County were overlaid with land use categories and examined to estimate the fraction of land in each category which had been paved or build-upon. Values shown are averages of the 24 photographs examined.
- (c) Estimated by average of commercial and industrial categories shown above.
- (d) Estimated by weighted average of land use categories 11 through 14
- (e) Emission factor for lawn and bare soil from Table A.6
- (f) Average of cropland, ungrazed clover, and two types of grass land without animals present on land
- (g) Assumed same as cropland from Table A.6
- (h) Emissions from livestock operations estimated separately based on animal head count and wastes produced
- (i) Assumed similar to crop and pasture combination
- (j) Assumed similar to bare soil/grass combination
- (k) Estimate
- (l) Less than or equal to bare soil data from Table A.6
- (m) Bare soil data from Table A.6

TABLE A.8  
 Dry and Liquid Fertilizers for Farm Plus Non-Farm Use  
 (California Department of Agriculture, 1974)

COUNTY	FERTILIZER TOTAL NITROGEN (metric tons/yr)	PARTITION	
		DRY <sup>(a)</sup>	LIQUID <sup>(a)</sup>
Los Angeles	7124	0.781	0.219
Orange	4619	0.751	0.249
Riverside	17614	0.445	0.555
San Bernardino	1984	0.919	0.081
Santa Barbara	7495	0.56	0.44
Ventura	7885	0.629	0.371

(a) Fraction of total N applied in liquid and dry form estimated by summing N content of those liquid and dry fertilizers for which nitrogen content data were given.

TABLE A.9

Percentage of N Applied, Apportioned Between Farm and Non-Farm Use  
(California Department of Agriculture, 1974)

COUNTY	FARM		NON-FARM	
	DRY <sup>(a)</sup>	LIQUID	DRY	LIQUID
Los Angeles	36	10	42	12
Orange	48	16	27	9
Riverside	42	52	3	3
San Bernardino	69	6	23	2
Santa Barbara	52	40	4	4
Ventura	60	36	3	1

(a) Example: Fraction (farm N/total N) x fraction dry from Table A.8

TABLE A.10  
Fertilizer Nitrogen Applied  
(Tons N/Yr)

COUNTY	DRY		LIQUID	
	FARM	NON-FARM	FARM	NON-FARM
Los Angeles	2565	2992	712	855
Orange	2217	1247	739	416
Riverside	7398	528	9159	528
San Bernardino	1369	456	119	40
Santa Barbara	3897	300	2998	300
Ventura	4731	237	2839	79

Estimated by combining data of Tables A.8 and A.9

TABLE A.11  
 Partition of Farm Fertilizer Use Between Crops and Orchards<sup>(a)</sup>  
 (From U.S. Department of Commerce, 1977)

COUNTY	DRY (METRIC TONS/YR)		LIQUID (METRIC TONS/YR)		% OF FARM FERTILIZER APPLIED ON CROPS	
	CROP	ORCHARD	CROP	ORCHARD	% DRY	% LIQUID
Los Angeles	3503	2039	1353	357	63	80
Orange	3603	2672	1067	2032	57	34
Riverside	17041	9842	13210	2428	63	84
San Bernardino	1545	3473	156	218	31	42
Santa Barbara	12099	3214	6927	400	79	95
Ventura	13521	8870	2405	3815	60	39

(a) The Census of Agriculture (U.S. Department of Commerce, 1977) shows lower total fertilizer applied than does the California Department of Food and Agriculture (1974).

TABLE A.12  
 Nitrogen Applied on Crops, Orchards, and Non-Farm Areas  
 (County Totals in Metric Tons/Year)

COUNTY	CROP <sup>(a)</sup>	DRY		LIQUID		
		ORCHARDS AND ORNAMENTALS	NON-FARM	CROP <sup>(a)</sup>	ORCHARDS AND ORNAMENTALS	NON-FARM
Los Angeles	1616	949	2992	570	142	855
Orange	1264	953	1247	251	488	416
Riverside	4661	2737	528	7694	1465	528
San Bernardino	424	945	456	50	69	40
Santa Barbara	3079	818	300	2848	150	300
Ventura	2839	1892	237	1107	1732	79

(a) Farm use split between crops vs. orchards and ornamentals using crop percentages of Table A.11 applied to total farm use given in Table A.10.

TABLE A.13  
 Percentage of Land Use in Each County Located Within the Gridded  
 Inventory Map Area and Within the South Coast Air Basin

COUNTY	CROPLAND	ORCHARDS	NON-FARM FERTILIZED LAND <sup>(a)</sup>
Los Angeles	34	84	99
Orange	100	100	100
Riverside	53	43	74
San Bernardino	69	100	85
Santa Barbara	7	100	78
Ventura	95	100	100

(a) Estimated from percentage of county population living within the air basin in 1975.

TABLE A.14  
 Fertilizer Nitrogen Applied Inside the South Coast Air Basin  
 (Metric Tons/Year) (a)

COUNTY	CROP	DRY		CROP	LIQUID	
		ORCHARDS AND ORNAMENTALS	NON FARM		ORCHARDS AND ORNAMENTALS	NON FARM
Los Angeles	549	797	2962	194	120	846
Orange	1264	953	1247	251	488	416
Riverside	2470	1177	391	4078	630	391
San Bernardino	293	945	388	35	69	34
Santa Barbara	216	818	234	199	150	234
Ventura	2697	1892	237	1052	1732	79
TOTAL	7489	6582	5459	5809	3189	2000

(a) Data of Tables A.12 and A.13 combined

TABLE A.15

Ammonia Loss Due to Fertilizer Application by County - 1974  
(handling loss given separately)

COUNTY	LIQUID												TOTAL NH <sub>3</sub> LOSS KG/DAY
	DRY						NON-FARM						
	CROPLAND		ORCHARDS AND ORNAMENTALS		NON-FARM		CROPLAND		ORCHARDS AND ORNAMENTALS		NON-FARM		
FERTILIZER N APPLIED MT/YR	NH <sub>3</sub> LOSS KG/DAY(a)	FERTILIZER N APPLIED MT/YR	NH <sub>3</sub> LOSS KG/DAY(a)	FERTILIZER N APPLIED MT/YR	NH <sub>3</sub> LOSS KG/DAY(a)	FERTILIZER N APPLIED MT/YR	NH <sub>3</sub> LOSS KG/DAY(b)	FERTILIZER N APPLIED MT/YR	NH <sub>3</sub> LOSS KG/DAY(c)	FERTILIZER N APPLIED MT/YR	NH <sub>3</sub> LOSS KG/DAY(c)	FERTILIZER N APPLIED MT/YR	NH <sub>3</sub> LOSS KG/DAY(b)
Los Angeles	549	182	797	264	2962	2946	13	194	120	8	846	841	4254
Orange	1264	419	953	316	1247	1240	17	251	488	32	416	414	2438
Riverside	2470	819	1177	390	391	389	270	4078	630	42	391	389	2299
San Bernardino	293	97	945	313	388	386	2	35	69	5	34	34	837
Santa Barbara	216	72	818	271	234	233	13	199	150	10	234	233	832
Ventura	2697	894	1892	627	237	236	70	1052	1732	115	79	79	2021
TOTAL	7489	2483	6582	2181	5459	5430	385	5809	3189	212	2000	1990	12681

Total NH<sub>3</sub> Loss = 12681 kg/day

= 12.68 metric tons/day

(a) Assuming 10% of N applied is lost to atmosphere as NH<sub>3</sub> (Meyer, 1981)

(b) Assuming 30% of N applied is lost to atmosphere as NH<sub>3</sub> (Meyer, 1981)

(c) Assuming 2% of N applied is lost to atmosphere as NH<sub>3</sub> (Meyer, 1981)

TABLE A.16  
Loss of Anhydrous Ammonia Due to Handling and Field Application

COUNTY	ANHYDROUS AMMONIA (metric tons N/yr) (County Total) (a)	% OF LIQUID FERTILIZER APPLIED ON CROPS	% OF CROPLAND IN BASIN	% OF ORCHARDS IN BASIN	ANHYDROUS AMMONIA IN BASIN (b) (metric tons N/yr)	1% LOSS DUE TO HANDLING (c) APPLICATION (tons N/yr)	3% LOSS DURING APPLICATION ON FIELD (c) (tons N/yr)
Los Angeles	918	80	34	84	404	4	12
Orange	2.73	34	100	100	2.73	0.03	0.08
Riverside	4151	84	53	43	2134	21	64
San Bernardino	102	42	69	100	89	0.9	3
Santa Barbara	524	95	7	100	61	0.6	2
Ventura	208	39	95	100	204	2	6
TOTAL	5906				2895	29	87

Total Loss = 116 tons N/yr

= 0.38 metric tons NH<sub>3</sub>/day

- (a) From liquid fertilizer sales classed as 82-00-00 by the California Department of Agriculture (1974)  
 (b) County total multiplied by [% of liquid fertilizer applied to crops (Table A.11) x % cropland in basin (Table A.13) + % of liquid fertilizer applied to orchards x % orchard land in basin]  
 (c) Walkup and Nevins (1966)

TABLE A.17  
 Summary of NH<sub>3</sub> Emissions from Fertilizer Application and Handling

COUNTY	LOSS FROM FARM APPLICATION OF FERTILIZER (metric tons/day)		LOSS FROM NON-FARM APPLICATION (metric tons/day)	LOSS DUE TO HANDLING (metric tons/day)
	CROPS	ORCHARDS		
Los Angeles	0.195	0.272	3.79	0.05
Orange	0.436	0.348	1.65	4x10 <sup>-5</sup>
Riverside	1.09	0.432	0.778	0.28
San Bernardino	0.099	0.318	0.48	0.013
Santa Barbara	0.085	0.281	0.466	0.009
Ventura	0.964	0.742	0.315	0.027

TABLE A.18  
Summary of Animal Waste Data

ANIMAL	SOURCE	ANIMAL WEIGHT (kg)	MANURE (TOTAL WASTE) kg/head-day	TOTAL NITROGEN EXCRETED kg/head-day
Dairy Cattle	Dale (1971)	680	49	
	Fogg (1971)	600	45	0.17
	Luebs et al. (1973b)			0.18
	Adriano et al. (1974)			0.19
Value Used		640	47	0.18
Beef Cattle	Fogg (1971)	400	34	0.24
	Peters & Blackwood (1977)	500	27	
	Taiganides & Hazen (1966)	450	29	0.17
	Scholz (1971)	500	45	
Value Used		450	32	0.21
Horses	Fogg (1971)	450	25	0.22*
Hogs	Fogg (1971)	70	3.9	0.03
	Muehling (1971)	70	5.5	0.038
	Scholz (1971)	70	3.6	
	Taiganides & Hazen (1966)	45	3.2	0.023
Value Used		70	3.9	0.03
Sheep	Fogg (1971)	45	1.8	0.018
Chickens	Fogg (1971)	2	0.11	0.0014
	Scholz (1971)		0.185	
	Taiganides & Hazen (1966)	2	0.11	0.0019
Value Used		2	0.14	0.0016
Turkey	taken in proportion to chickens on body weight basis	5.5	0.39	0.0044

TABLE A.19a  
1974 Livestock Inventory - Cattle

COUNTY	COUNTY TOTALS (a)			LOCATED IN SOUTH COAST AIR BASIN (b)		
	DAIRY	FEEDLOT	RANGE	DAIRY	FEEDLOT	RANGE
Los Angeles	20,160	18,488	15,007	18,144	11,093	15,007
Orange	3,592	49	11,287	3,592	49	11,287
Riverside	86,592	90,418	35,553	86,592	18,084	35,553
San Bernardino	148,882	15,123	22,936	144,415	15,123	22,936
Santa Barbara	10,187	54,564	52,105	---	---	8,337
Ventura	10,734	19,393	2,593	10,734	19,393	2,593
				<u>263,477</u>	<u>63,742</u>	<u>95,713</u>

(a) U.S. Bureau of the Census (1977)

(b) See Table A.20

TABLE A.19b  
1974 Livestock Inventory - Continued

COUNTY	HORSES		SHEEP		HOGS	
	COUNTY TOTAL(c)	IN SOUTH COAST AIR BASIN(b)	COUNTY TOTAL(a)	IN SOUTH COAST AIR BASIN(b)	COUNTY TOTAL(a)	IN SOUTH COAST AIR BASIN(b)
Los Angeles	54,700	53,606	29,902	2,990	3,864	386
Orange	10,500	10,500	2,407	2,407	142	142
Riverside	30,300	29,694	43,289	21,645	5,780	5,202
San Bernardino	19,900	19,502	25,757	25,757	7,165	6,449
Santa Barbara	8,300	1,328	16,674	2,668	1,737	278
Ventura	7,200	7,200	35,465	35,465	892	892
		121,830		90,932		13,349

(a) U.S. Bureau of the Census (1977)

(b) See Table A.20

(c) Anderson (1979)

TABLE A.19c  
1974 Livestock Inventory - Continued

COUNTY	CHICKENS			TURKEYS	
	COUNTY TOTAL(a)	IN SOUTH COAST AIR BASIN (b)	COUNTY TOTAL (a)	IN SOUTH COAST AIR BASIN (b)	
Los Angeles	739,473	739,473	140,700	140,700	
Orange	925,477	925,477	10	10	
Riverside	7,378,963	7,378,963	100,869	100,869	
San Bernardino	5,504,799	5,504,799	160,062	160,062	
Santa Barbara	797,009	127,521	---	---	
Ventura	4,130,477	4,130,477	18,705	18,705	
		<u>18,806,710</u>		<u>420,346</u>	

(a) U.S. Bureau of the Census (1977)

(b) See Table A.20

TABLE A.20

## Fraction of Animals Located Inside South Coast Air Basin Portion of Each County

ANIMAL TYPE	LOS ANGELES	ORANGE	RIVERSIDE	PERCENTAGES				SANTA BARBARA	VENTURA
				SAN BERNARDINO	SAN BERNARDINO	SANTA BARBARA	VENTURA		
Dairy Cattle	90 <sup>(b)</sup>	100 <sup>(a)</sup>	100 <sup>(a)</sup>	97 <sup>(b)</sup>	0 <sup>(d)</sup>	100			
Feedlot Cattle	60 <sup>(c)</sup>	100	20	100	0 <sup>(d)</sup>	100			
Range Cattle	100	100	100	100	16 <sup>(e)</sup>	100			
Horses	98	100	98	98	16 <sup>(e)</sup>	100			
Sheep	10	100	50	100	16 <sup>(e)</sup>	100			
Hogs	10	100	90	90	16 <sup>(e)</sup>	100			
Chickens	100	100	100	100	16 <sup>(e)</sup>	100			
Turkeys	100	100	100	100	---	100			

84

Estimates are by Addis (1981) unless noted otherwise:

- (a) Bishop (1981)
- (b) 2000 dairy cows in desert area of Los Angeles County and 3835 dairy cows located in desert portion of San Bernardino County (Bishop, 1981).
- (c) Most Los Angeles County feedlot cattle are located within the South Coast Air Basin; Addis (1981) estimates more than 10,000 within the air basin (i.e. 54% or greater are in the air basin). We will estimate that 60% of the total are in the air basin.
- (d) U.S. Geological Survey (1976) maps show negligible land area devoted to confined animal feeding in the South Coast Air Basin portion of Santa Barbara County.
- (e) Estimated in rough proportion to the fraction of the county land area within the air basin boundary.

TABLE A.21

Total NH<sub>3</sub> Emissions From Livestock in the  
Modeling Region of the South Coast Air Basin - 1974

ANIMAL	INVENTORY IN SOUTH COAST AIR BASIN (HEAD)	TOTAL ANIMAL WASTE kg/head-day	NITROGEN EXCRETED kg/head-day	NH <sub>3</sub> EMISSIONS AT 50% RATE OF NITROGEN EXCRETED IN TOTAL WASTE (a) metric tons/day
Dairy Cattle	263,477	47	0.18	24.39 (b)
Feedlot Cattle	63,742	32	0.21	6.88 (b)
Range Cattle	95,713		0.21	12.16
Horses	121,830	25	0.22	16.22
Sheep	90,932	1.8	0.018	0.99
Hogs	13,349	3.9	0.03	0.25
Chickens	18,806,710	0.14	0.0016	18.2
Turkeys	420,346	0.39	0.0044	1.12
				80.21

(a) Adriano et al. (1971); Adriano et al. (1974); Giddens and Rao (1975); Leubs et al. (1973b); Viets (1971).

(b) Since only 85% of manure from these animals is spread on soil, totals have been multiplied by 0.85 (see Adriano et al., 1974).

TABLE A.22  
Emission Factors for Ammonia Loss Due to Non-Farm Animals

NON-FARM ANIMALS	ANIMAL WEIGHT (kg) (a)	TOTAL N EXCRETED IN URINE (a) (mg/kg body wt-day)	NITROGEN EXCRETED IN URINE DAILY (b) (kg/head-day)	EMISSION FACTOR (c) (kg NH <sub>3</sub> /head-day)
Cats	2.5	500 - 1100	$2 \times 10^{-3}$	$2.2 \times 10^{-3}$
Dogs	12	250 - 800	$6.3 \times 10^{-3}$	$6.9 \times 10^{-3}$
Goats	50	120 - 400	$1.3 \times 10^{-2}$	$1.4 \times 10^{-2}$
Monkey	12	140 - 400	$3.2 \times 10^{-3}$	$3.5 \times 10^{-3}$
Rabbits	2	120 - 300	$4.2 \times 10^{-4}$	$4.6 \times 10^{-4}$
Rats	0.33	200 - 1000	$2.0 \times 10^{-4}$	$2.2 \times 10^{-4}$

(a) From Altman and Dittmer (1968) p. 528.

(b) Based on body weight and mid-point of range of nitrogen excretion rates given in adjacent columns.

(c) Cattle data show that about half of the nitrogen excreted in manure is in urine and half is in feces, and that when manure is applied to dry alkaline soil half of the total nitrogen is lost to the atmosphere as NH<sub>3</sub> (i.e. total N lost as NH<sub>3</sub> is approximately equal to nitrogen content of urine). We will estimate that loss rate is similar for other animals and that in the absence of data on total animal waste a value equal to 90% of urine N will reasonably estimate loss of N from total animal wastes.

TABLE A.23

NH<sub>3</sub> Emissions from Human and Domestic Animal Populations

COUNTY	COUNTY POPULATION (1975) (a)	RATIO: PEOPLE TO DOGS	RATIO: PEOPLE TO CATS	SOUTH COAST AIR BASIN POPULATION (a)	SOUTH COAST AIR BASIN ANIMAL WASTE		EMISSIONS HUMANS	
					DOGS	(tons NH <sub>3</sub> /day) (1)	CATS	(tons NH <sub>3</sub> /day) RESPIR. (j) PERSPIR. (k)
Los Angeles	7,020,772	7.8(b)	7.0(g)	6,936,982	6.1	2.18	0.03	4.7
Orange	1,722,094	5.8(c)	(7.0)(h)	1,722,094	2.0	0.54	0.008	1.2
Riverside	531,679	(4.5)(d)	(7.0)(h)	393,972	0.6	0.12	0.002	0.27
San Bernardino	696,061	4.5(e)	(7.0)(h)	592,522	0.9	0.19	0.003	0.40
Santa Barbara	264,324	(5.8)(f)	(7.0)(h)	≤ 206,291	0.25	0.06	0.001	0.14
Ventura	432,407	(5.8)(f)	(7.0)(h)	432,199	0.5	0.14	0.002	0.29
					10.35	3.23	0.046	7.00

87

(a) County population figures from Southern California Association of Governments (1977) except for Santa Barbara County, which is 1970 data from U.S. Bureau of the Census (1972) South Coast Air Basin population of Santa Barbara County estimated from county total less the cities of Lompoc and Santa Maria

(b) Richards, B. (1981)

(c) Hudson, R. (1981)

(d) Estimated from San Bernardino data

(e) San Bernardino (1981)

(f) Estimated from Orange County data

(g) Richards, B. (1981)

(h) Estimated from Los Angeles County response

(i) Computed using emission factors from Table A.22: (dogs,  $6.9 \times 10^{-3}$  kg NH<sub>3</sub>/head day; cats  $2.2 \times 10^{-3}$  kg/head-day

(j) Respiration loss estimated at 4 μl NH<sub>3</sub> per min per person (Kupprat et al., 1976) This implies  $4.4 \times 10^{-6}$  kg NH<sub>3</sub> respired/person-day

(k) 24.5 g urea produced in human body/day (Altman and Dittmer, 1968); 5% released in perspiration (Healy et al., 1970; all of that assumed lost as NH<sub>3</sub>. This implies 0.68 g NH<sub>3</sub>/person-day.

TABLE A.24  
Ammonia Emission Estimates for Refrigerants and Household Cleaning Chemicals

COUNTY	SOUTH COAST AIR BASIN POPULATION (a)	NH <sub>3</sub> EMISSIONS (d) metric tons/day	
		CLEANING AGENTS (b)	REFRIGERATION (c)
Los Angeles	6,936,982	0.4	0.27
Orange	1,722,094	0.1	0.07
Riverside	393,972	0.02	0.02
San Bernardino	592,522	0.03	0.02
Santa Barbara	≤ 206,291	0.01	0.01
Ventura	432,199	0.03	0.02

(a) See Table A.23  
 (b) U.S. Ammonia Production for 1974:  $16.5 \times 10^6$  short tons/yr from Chem. & Eng. News (April, 1975); 0.03% of total synthetic ammonia is used in the manufacture of household ammonia from Kirk-Othmer Encyclopedia (1963)  
 (c) 0.02% of total synthetic ammonia is used for refrigeration (Kirk-Othmer Encyclopedia, 1963)  
 (d) Emissions were calculated based on ratio of air basin population to U.S. population in 1974. 100% NH<sub>3</sub> loss to the atmosphere was assumed. The population of the United States in 1974 was  $211.389 \times 10^6$  persons from U.S. Bureau of the Census (1980).

TABLE A.25

Summary of Ammonia Emissions By Source Category  
in the South Coast Air Basin  
1974

SOURCE CATEGORY	TOTAL EMISSIONS (kg/day)
<b>Stationary Fuel Combustion</b>	
Electric Utility	
Natural Gas	590.0
Residual Oil	2000.0
Digester Gas	0.5
Refinery Fuel Burning	
Natural Gas	160.0
Residual Oil	99.0
Refinery Gas	420.0
Industrial Fuel Burning	
Natural Gas	610.0
Liquified Petroleum Gas (LPG)	4.0
Residual Oil	150.0
Distillate Oil	140.0
Digester Gas	9.0
Coke Oven Gas	15.0
Residential/Commercial Fuel Burning	
Natural Gas	270.0
Liquid Propane Gas (LPG)	4.0
Residual Oil	62.0
Distillate Oil	73.0
Coal	20.0
*** Sub totals ***	4626.5 (3.09%)
<b>Mobile Source Fuel Combustion</b>	
Automotive	
Non-catalyst Autos and Light Trucks	3309.0
Medium and Heavy Duty Trucks	449.9
Diesel Vehicles	370.0
LPG for Carburetion	10.0
Civilian Aircraft	
Jet	150.0
Piston	2.9
Shipping	
Residual Oil Boilers	70.0
Diesel Ships	50.0
Railroad-Diesel Oil	90.0
Military	
Gasoline	10.0
Diesel	60.0
Jet Fuel	50.0
Residual Oil	0.8
Off Highway Vehicles	120.0
*** Sub totals ***	4742.6 (3.17%)
Industrial Point Sources	2070.0 (1.38%)
Soil Surface	23790.0 (15.9%)
Fertilizer	
Farm Crop	2870.0
Orchards	2390.0
Handling	380.0
Non-farm	7420.0
*** Sub totals ***	13060.0 (8.72%)
Livestock	
Cattle	
Dairy	24390.0
Feedlot	6880.0
Range	12160.0
Horses	16220.0
Sheep	990.0
Hogs	250.0
Chickens	18200.0
Turkeys	1120.0
*** Sub totals ***	80210.0 (53.6%)
Domestic	
Dogs	10350.0
Cats	3230.0
Human Respiration	46.0
Human Perspiration	7000.0
Household Ammonia Use	600.0
*** Sub totals ***	21226.0 (14.2%)
*** Total ***	149725.1 (100.0%)

APPENDIX B  
CHEMICAL MASS ACCOUNTING OF URBAN AEROSOL

A. W. Stelson and J. H. Seinfeld

Reprinted from ENVIRONMENTAL SCIENCE & TECHNOLOGY, Vol. 15, Page 671, June 1981  
 Copyright © 1981 by the American Chemical Society and reprinted by permission of the copyright owner

## Chemical Mass Accounting of Urban Aerosol

Arthur W. Stelson and John H. Seinfeld\*

Department of Chemical Engineering, California Institute of Technology, Pasadena, California 91125

■ A chemical mass accounting technique emphasizing the importance of chemical speciation is developed for analyzing atmospheric-aerosol data. The technique demonstrates that total aerosol mass can generally be characterized from measurements of SO<sub>4</sub>, Cl, Br, NO<sub>3</sub>, NH<sub>4</sub>, Na, K, Ca, Fe, Mg, Al, Si, Pb, carbonaceous material, and aerosol water, the predominant species being SO<sub>4</sub>, NO<sub>3</sub>, NH<sub>4</sub>, Si, carbonaceous material, and aerosol water. Since water is the major species distributed between the gas and aerosol phases, the interrelation between water and electrolyte mass is explored. It is shown that aerosol water is significantly correlated with electrolyte mass. Calculated aerosol ionic strengths lie in the region where the relative humidity/ionic strength relation is most sensitive, thereby suggesting the importance of relative-humidity monitoring during aerosol sampling.

### Introduction

The urban aerosol consists in general of a complex mixture of ionic salts, metal oxides, glasses, carbonaceous material, and water. Partitioning the aerosol into groups of materials with similar physical and thermodynamic properties can simplify the interpretation of experimental data and facilitate theoretical analysis. The main objective of this paper is to develop methods for obtaining an accurate overall aerosol mass balance from the least number of measured quantities.

The urban aerosol usually exhibits a bimodal volume distribution (see Figure 1). The fine-particle mode generally results from gas-to-particle conversion, whereas the coarse-particle mode arises from mechanically generated particles. The coarse mode is usually basic since the particles are formed from basic materials such as soil, cement, and fly ash. The fine mode can be neutral or acidic depending on the relative degree of neutralization of acidic material. In the eastern United States, the fine-particle mode in the urban aerosol generally dominates the total mass, so that the net aerosol pH is likely to be acidic, whereas Western aerosol has a greater tendency to be basic (1, 3, 4). Because the nature of the atmospheric aerosol depends strongly on its chemical speciation, it is important to be able to estimate its chemical composition based on measurements of elemental composition.

The atmospheric aerosol can be considered to consist of five major classes of constituents: ionic solids, electrolytes (dissolved ionic species), carbonaceous material, metal oxides and glasses, and water. An equation expressing this relation is

$$\text{TSP} = \sum_i \sum_j [\text{M}_i\text{O}_j] + \sum_i [\text{E}_i] + \sum_i [\text{CM}_i] + \sum_i [\text{I}_i] + [\text{H}_2\text{O}] \quad (1)$$

where TSP = total suspended particulate matter ( $\mu\text{g m}^{-3}$ ),  $[\text{M}_i\text{O}_j]$  = mass concentration of metal oxide or glass ( $\mu\text{g m}^{-3}$ ),  $[\text{E}_i]$  = mass concentration of electrolyte *i* ( $\mu\text{g m}^{-3}$ ),  $[\text{CM}_i]$  = mass concentration of carbonaceous material *i* ( $\mu\text{g m}^{-3}$ ),  $[\text{I}_i]$  = mass concentration of ionic solid *i* ( $\mu\text{g m}^{-3}$ ), and  $[\text{H}_2\text{O}]$  = aerosol water concentration ( $\mu\text{g m}^{-3}$ ). Electrolytes are dissociating ionic substances dissolved in water, whereas ionic solids are undissolved electrolytic material. Carbonaceous material refers to carbon-containing species, present as elemental carbon or organic or inorganic compounds. Metal oxides and glasses refer to oxidized elemental species, such as those present in soil and cement dust and fly ash. The water content refers to "free" water unassociated with hydrated salts.

The object of this paper is to show that, by making assumptions about each term on the right-hand side of eq 1, one can calculate the total suspended particulate mass concentration on the basis of conventional aerosol measurements.

From an accurate aerosol mass accounting, several important issues can be explored: (1) the possibility of biased total-mass measurements through alteration of the aerosol between sampling and analysis, (2) the relation between measured electrolyte mass-to-water ratios and solubilities of atmospherically significant electrolytes, (3) the aerosol ionic strength and possible dependence of aerosol water content on the prevailing relative humidity, (4) the net aerosol pH, and (5) the relative importance of different aerosol fractions—electrolytic, metal oxide and glass, carbonaceous, and aqueous—to the total aerosol mass and the possible interrelation between different fractions. Each of these issues will be evaluated and discussed with particular reference to the Los Angeles aerosol.

One of the most detailed urban aerosol studies involving chemical analysis was the California Aerosol Characterization Experiment (ACHEX) (5). Ambient atmospheric aerosol was deposited on high-volume filters (Whatman 41) and analyzed for many chemical species. In addition,  $\beta$ -gauge, waterometer, and total-filter (47-mm Gelman GA-1 and Gelman A) measurements were performed. During some sampling periods, the aerosol carbonaceous material was analyzed (6). From the ACHEX data, 6 days are chosen for individual mass-balance analyses. More sampling periods would have been desirable, but these days were the only ones in which the aerosol was chemically analyzed for the major inorganic species, water, and carbonaceous material, in addition to continuous total-mass measurements. Even for these 6 days, the aerosol water content was not measured throughout the high-volume-filter sampling period. In Table I the sampling times and locations are summarized. Only at West Covina, CA (TC), did the aerosol water concentration and high-volume-filter sampling times totally overlap. Since the waterometer measurements overlapped the majority of the high-volume sampling period, it will be assumed that the time-averaged aerosol water concentration over its sampling time typifies the time-averaged aerosol water concentration over the total high-volume-filter sampling period.

The ACHEX ambient atmospheric aerosol high-volume-filter samples were analyzed for many chemical species. When only the major species,  $\text{SO}_4$ , Cl, Br,  $\text{NO}_3$ ,  $\text{NH}_4$ , Na, K, Ca, Mg, Al, Si, and Pb, were considered, greater than 90% of the measured moles, excluding water and carbonaceous material, were accounted for. Therefore, the major species will only be considered in this study. Equation 1 will be modified as

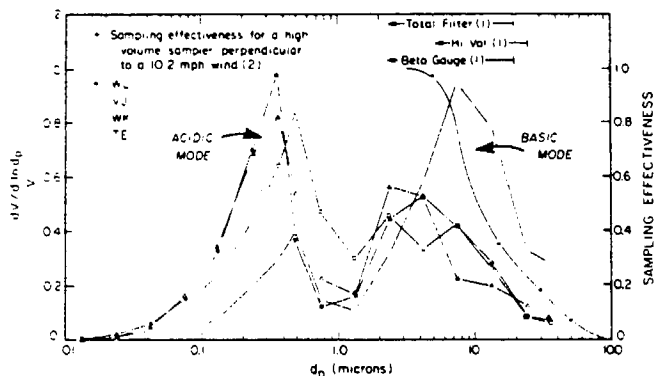


Figure 1. Time-averaged normalized aerosol volume distributions and sampler upper effective size limit (1, 2, 5). (See Table I for aerosol volume distribution sample code definition.)

Table I. ACHEX Sampling Time and Location Summary (5)\*

site	sample code	date	high-volume (HVM) sampling period	total-filter (TF, TV) sampling period	$\beta$ -gauge ( $\beta$ ) sampling period	waterometer ( $\text{H}_2\text{O}$ ) sampling period
Dominguez Hills, CA	WK	10/4-10/5/73	2100-2105	2100-2100	2100-2100	2115-1515
Dominguez Hills, CA	WL	10/10-10/11/73	2100-2100	2100-2100	2100-2100	0000-1800
Rubidoux, CA	VJ	9/24-9/25/73	2300-1802	2300-1801	2300-1900	0400-1900
West Covina, CA	TC	7/24-7/25/73	2320-1605	2300-1600	2300-1600	2300-1600
West Covina, CA	TD	7/25-7/26/73	0500-1826	0500-1800	0500-1600	0445-1545
West Covina, CA	TE	8/8-8/9/73	2100-2100	2100-2100	2100-1800	2200-1400

\* HVM = total mass from Whatman 41  $\times$  10 in. high-volume filter ( $\mu\text{g m}^{-3}$ ).  $\overline{\text{TF}}$  = time-averaged total mass from Gelman GA-1, 47-mm filters ( $\mu\text{g m}^{-3}$ ).  $\overline{\text{TV}}$  = time-averaged total mass from Gelman A, 47-mm filters ( $\mu\text{g m}^{-3}$ ).  $\overline{\beta}$  = time-averaged total mass from  $\beta$  gauge ( $\mu\text{g m}^{-3}$ ).  $\overline{\text{H}_2\text{O}}$  = time-averaged total water concentration from waterometer ( $\mu\text{g m}^{-3}$ ).

$$\text{TSP} = \sum_i \sum_j [\text{M}_i\text{O}_j] + \sum_i [\text{E}_i] + \sum_i [\text{CM}_i] + \sum_i [\text{I}_i] + [\text{H}_2\text{O}] + \sum_i [\text{N}_i] \quad (2)$$

where  $[\text{N}_i]$  is the concentration of minor specie  $i$  ( $\mu\text{g m}^{-3}$ ). In Table II the sum of the minor species for the ACHEX data is listed. We see that this term is less than 1% of the total for the 6 days.

A basic object of this paper is to attempt to reconcile TSP measurements with eq 2 by studying the means of estimating the contributions of each of the terms on the right-hand side of eq 2. Although we focus on the ACHEX data, the techniques to be discussed will have general applicability. To evaluate the terms on the right-hand side of eq 2 other than  $\sum[\text{N}_i]$ , one must make assumptions about the chemical form of the different species. Each term and the assumptions needed in evaluating each will now be discussed. Then, the right-hand side of eq 2 will be evaluated theoretically and compared with the total suspended particulate measurements from ACHEX.

### Aerosol Components

**Ionic Solids.** Measurements of ionic-solid concentrations present difficult problems. In the measurement of the ion concentration in an aerosol, the filter is washed with a solvent and the ion concentration in the solvent is measured. Using this procedure, it is impossible to tell whether the ion was present in an ionic solid or an aqueous solution. Indirectly, the presence of ionic solids can be inferred. If the ambient relative humidity is less than the deliquescent humidity of the ionic solid, then it can be assumed that the salt is present as a solid. An additional check can be invoked if the solid is volatile, for example,  $\text{NH}_4\text{NO}_3$  (7). The gas-phase concentrations of the precursors can be measured along with the temperature, and, if the calculated equilibrium coefficient matches the theoretical equilibrium coefficient for the ionic solid, it is assumed that the ionic solid is present. Both indirect methods fail if solid or supersaturated solutions are present.

For our analysis, it will be assumed that the ionic-solid concentration is zero. If the calculated ionic strength of the electrolytic aerosol solution is unreasonably high, then a correction must be made for the presence of ionic solids. For the mass accounting, it is immaterial whether the ionic-solid material is treated as an ionic solid or an electrolyte.

**Metal Oxides and Glasses.** The major elements possibly occurring in the form of oxides and glasses are Al, Ca, Fe, Si, Mg, Pb, K, and Na. When one follows the approach of Macias et al. (8), the chemical form of these elements can be assigned (see Table III). The majority of the oxides listed in Table III are known to be formed in combustion processes (9, 10). Additionally, Biggins et al. (11) have identified  $\text{Fe}_2\text{O}_3$ ,  $\text{Al}_2\text{O}_3$ , and

Table II. Summary of Measured and Calculated Los Angeles Aerosol Concentrations (5)<sup>a</sup>

metal oxide and glass concn. $\mu\text{g m}^{-3}$								
sample	[Al <sub>2</sub> O <sub>3</sub> ]	[Fe <sub>2</sub> O <sub>3</sub> ]	[SiO <sub>2</sub> ]	[PbO]	[CaO]	[MgO]	[K <sub>2</sub> O]	[Na <sub>2</sub> O]
WK	4.9	2.2	14.3	1.2	1.8	2.6	0.7	5.5
WL	3.8	2.8	13.4	4.0	2.4	1.8	0.7	3.0
VJ	8.6	5.9	28.5	0.8	4.1	1.9	1.7	1.5
TC	8.2	5.2	27.4	4.0	3.4	3.0	1.4	5.3
TD	6.4	3.7	19.8	3.2	2.8	1.8	1.0	3.9
TE	4.7	2.6	16.5	2.2	1.9	1.9	0.9	3.4

electrolyte concn. $\mu\text{g m}^{-3}$													
sample	[Cl]	[NO <sub>3</sub> ]	[Br]	[NH <sub>4</sub> ]	[Na]	[SO <sub>4</sub> ]	[Pb]	[Ca]	[K]	[Mg]	[H]	[H']	[OH']
WK	0.3	0.9	0.2	6.7	4.1	31.4	1.1	1.3	0.6	1.6	0.3		1.3
WL	1.2	7.3	1.2	3.1	2.2	4.2	3.8	1.7	0.6	1.1	0.1		3.8
VJ	0.7	11.8	0.1	4.7	1.1	2.0	0.7	2.9	1.5	1.1	0.2		2.3
TC	0.6	9.9	0.7	9.5	3.9	26.3	3.8	2.4	1.2	1.8	0.5	0.1	
TD	0.9	12.0	0.5	8.1	2.9	16.6	2.9	2.0	0.8	1.1	0.4	0.1	
]TE	0.7	7.2	0.4	3.2	2.5	6.5	2.1	1.4	0.7	1.2	0.2		1.5

summations, $\mu\text{g m}^{-3}$								
sample	$\Sigma_i \Sigma_j [M_i O_j]$	$\Sigma_i \Sigma_j [M_i O_j]'$	$\Sigma_i [M_i]$	$\Sigma_i [E_i]$	$\Sigma_i [E_i]'$	$\Sigma_i [N_i]$	$\Sigma_i [CM_i]$	[H <sub>2</sub> O]
WK	33.2	21.4	11.4	39.8	49.5	0.7	18.7	54.2
WL	31.9	20.0	10.8	17.1	30.2	0.9	16.4	24.9
VJ	52.9	43.0	23.5	19.5	28.9	0.7	8.0	34.5
TC	55.9	40.8	22.0	47.5	60.2	1.4	29.8	75.2
TD	42.6	29.9	16.1	38.5	47.9	1.1	11.7	74.4
TE	34.1	23.8	12.7	18.2	27.4	0.8	10.8	29.7

<sup>a</sup> [A] = mass concentration of specie A. [H] = hydrogen concentration calculated from electroneutrality when  $x_{\text{Pb}} = 0$ ,  $x_{\text{Ca}} = 0$ ,  $x_{\text{Na}} = 0$ ,  $x_{\text{K}} = 0$ , and  $x_{\text{Mg}} = 1$ . [H'] or [OH'] = hydrogen or hydroxyl ion concentration when  $x_{\text{Pb}} = 1$ ,  $x_{\text{Ca}} = 1$ ,  $x_{\text{Na}} = 1$ ,  $x_{\text{K}} = 1$ , and  $x_{\text{Mg}} = 1$ .  $\Sigma_i \Sigma_j [M_i O_j]$  = sum of metal oxide and glass concentrations when  $x_{\text{Pb}} = 0$ ,  $x_{\text{Ca}} = 0$ ,  $x_{\text{Na}} = 0$ ,  $x_{\text{K}} = 0$ , and  $x_{\text{Mg}} = 0$ .  $\Sigma_i \Sigma_j [M_i O_j]'$  = sum of metal oxide and glass concentrations when  $x_{\text{Pb}} = 1$ ,  $x_{\text{Ca}} = 1$ ,  $x_{\text{Na}} = 1$ ,  $x_{\text{K}} = 1$ , and  $x_{\text{Mg}} = 1$ .  $\Sigma_i [M_i]$  = sum of metal oxide and glass forming elements assuming no oxygen is present and  $x_{\text{Pb}} = 1$ ,  $x_{\text{Ca}} = 1$ ,  $x_{\text{Na}} = 1$ ,  $x_{\text{K}} = 1$ , and  $x_{\text{Mg}} = 1$ .  $\Sigma_i [E_i]$  = sum of electrolyte concentrations when  $x_{\text{Pb}} = 0$ ,  $x_{\text{Ca}} = 0$ ,  $x_{\text{Na}} = 0$ ,  $x_{\text{K}} = 0$ , and  $x_{\text{Mg}} = 0$ .  $\Sigma_i [E_i]'$  = sum of electrolyte concentrations when  $x_{\text{Pb}} = 1$ ,  $x_{\text{Ca}} = 1$ ,  $x_{\text{Na}} = 1$ ,  $x_{\text{K}} = 1$ , and  $x_{\text{Mg}} = 1$ .  $\Sigma_i [N_i]$  = sum of minor species concentrations.  $\Sigma_i [CM_i]$  = sum of carbonaceous material.

Table III. Aerosol Metal Oxides

element	oxide form	element	oxide form
Al	Al <sub>2</sub> O <sub>3</sub>	Mg	MgO <sup>a</sup>
Ca	CaO <sup>a</sup>	Pb	PbO
Fe	Fe <sub>2</sub> O <sub>3</sub>	Na	Na <sub>2</sub> O <sup>a</sup>
Si	SiO <sub>2</sub>	K	K <sub>2</sub> O <sup>a</sup>

<sup>a</sup> Assumed.

SiO<sub>2</sub> in roadside aerosol. The presence of CaO, MgO, and PbO can be examined from considerations of chemical equilibrium. Equilibrium constants for the reactions of CaO, MgO, and PbO with water are given in Table IV. The equilibrium analysis indicates that CaO and MgO should readily react to form Ca(OH)<sub>2</sub> and Mg(OH)<sub>2</sub>, whereas the PbO should not. Na<sub>2</sub>O should readily react with water to form NaOH, and K<sub>2</sub>O should react similarly to CaO and MgO to form KOH. Biggins et al. (11) have measured Pb<sub>3</sub>O<sub>4</sub> in roadside dust in addition to elemental lead, lead sulfates, lead carbonates, and lead hydroxides. The assumed form of lead, e.g., Pb<sub>3</sub>O<sub>4</sub>, PbO, or Pb, will not substantially affect the mass balance because of the high molecular weight of lead. We will assume lead to exist as PbO. Reiter et al. (13) have measured insoluble CaO, in disagreement with the pure thermochemical analysis. Ca(OH)<sub>2</sub> has a solubility similar to that of CaO, as shown in Table V. Thus, the insoluble CaO reported by Reiter et al. (13) could be Ca(OH)<sub>2</sub>. MgO, Na<sub>2</sub>O, and K<sub>2</sub>O have not apparently been identified in tropospheric aerosol.

Table IV. Equilibrium Analysis of Hydroxide Formation

free energy of formation data (12)			
species	$\Delta G^\circ_{298}$ , kcal/(g-mol)	species	$\Delta G^\circ_{298}$ , kcal/(g-mol)
CaO(s)	-144.4	PbO(s)	-45.25, <sup>a</sup> -45.05 <sup>b</sup>
Ca(OH) <sub>2</sub> (s)	-214.33	Pb(OH) <sub>2</sub> (s)	-100.6
MgO(s)	-136.13	H <sub>2</sub> O(g)	-54.64
Mg(OH) <sub>2</sub> (s)	-199.27		

oxide reactions with water		
reaction	$\Delta G^\circ_{298}$ , kcal/(g-mol)	$P_{\text{H}_2\text{O}}$ , atm
CaO(s) + H <sub>2</sub> O(g) $\rightleftharpoons$ Ca(OH) <sub>2</sub> (s)	-15.29	$6.0 \times 10^{-12}$
MgO(s) + H <sub>2</sub> O(g) $\rightleftharpoons$ Mg(OH) <sub>2</sub> (s)	-8.5	$6.0 \times 10^{-7}$
PbO(s) + H <sub>2</sub> O(g) $\rightleftharpoons$ Pb(OH) <sub>2</sub> (s)	-0.71, <sup>a</sup> -0.91 <sup>b</sup>	0.3, <sup>a</sup> 0.2 <sup>b</sup>

<sup>a</sup> Red form. <sup>b</sup> Yellow form.

MgO, Na<sub>2</sub>O, K<sub>2</sub>O, and CaO could exist in the atmospheric aerosol in solid solutions with SiO<sub>2</sub>, Al<sub>2</sub>O<sub>3</sub>, and Fe<sub>2</sub>O<sub>3</sub> in soil dust or rock flour. The ability to remove these elements by forming hydroxides depends on particle size, rock structure, and the acidic nature of the leaching agent. Goldich (14) measured the weathering loss in sedimentary rocks and obtained the following ordering: Na<sub>2</sub>O, CaO, MgO, K<sub>2</sub>O, SiO<sub>2</sub>, Al<sub>2</sub>O<sub>3</sub>, and iron, where Na<sub>2</sub>O is the easiest to remove and iron is the hardest. This ordering supports the preceding thermodynamic and qualitative discussion. An additional calculation supporting the weathering ordering is obtained by using

Table V. Solubility of Inorganic Salts

metal oxides and glasses	solubility, <sup>a</sup> g/100 g of H <sub>2</sub> O	ref	metal oxides and glasses	solubility, <sup>a</sup> g/100 g of H <sub>2</sub> O	ref
SiO <sub>2</sub>	insoluble in H <sub>2</sub> O	12	Na <sub>2</sub> O	decomposes	12
Al <sub>2</sub> O <sub>3</sub>	insoluble in H <sub>2</sub> O	12	MgO	0.0086 <sup>30</sup>	12
Fe <sub>2</sub> O <sub>3</sub>	insoluble in H <sub>2</sub> O	12	PbO	0.0023 <sup>22</sup>	12
CaO	0.131 <sup>10</sup> , decomposes	12	K <sub>2</sub> O	very soluble	12
electrolytes	solubility, <sup>a</sup> g/100 g of H <sub>2</sub> O	ref	electrolytes	solubility, <sup>a</sup> g/100 g of H <sub>2</sub> O	ref
NaOH	113.2 <sup>25</sup>	27	NaCl	35.91 <sup>25</sup>	27
KOH	112 <sup>20</sup>	28	KCl	34.7 <sup>20</sup>	12
NH <sub>4</sub> OH	soluble	12	NH <sub>4</sub> Cl	39.5 <sup>25</sup>	27
Mg(OH) <sub>2</sub>	0.0009 <sup>18</sup>	12	MgCl <sub>2</sub>	54.25 <sup>20</sup>	12
Ca(OH) <sub>2</sub>	0.162 <sup>20</sup>	27	CaCl <sub>2</sub>	81.9 <sup>25</sup>	27
Pb(OH) <sub>2</sub>	0.0155 <sup>20</sup>	12	PbCl <sub>2</sub>	1.08 <sup>25</sup>	27
NaNO <sub>3</sub>	91.79 <sup>25</sup>	27	NH <sub>4</sub> HSO <sub>4</sub>	288 <sup>25</sup>	29
KNO <sub>3</sub>	31.6 <sup>20</sup>	28	MgSO <sub>4</sub>	44.5 <sup>20</sup>	12
NH <sub>4</sub> NO <sub>3</sub>	192 <sup>20</sup>	12	CaSO <sub>4</sub>	0.298 <sup>20</sup>	28
Mg(NO <sub>3</sub> ) <sub>2</sub>	128.2 <sup>20</sup>	27	PbSO <sub>4</sub>	0.00425 <sup>25</sup>	12
Ca(NO <sub>3</sub> ) <sub>2</sub>	138 <sup>25</sup>	27	H <sub>2</sub> SO <sub>4</sub>	∞	12
Pb(NO <sub>3</sub> ) <sub>2</sub>	59.6 <sup>25</sup>	27	HNO <sub>3</sub>	∞	12
Na <sub>2</sub> SO <sub>4</sub>	27.8 <sup>25</sup>	27	HCl	69.4 <sup>25</sup>	18
NaHSO <sub>4</sub>	28.6 <sup>25</sup>	12	HBr	198 <sup>20</sup>	28
K <sub>2</sub> SO <sub>4</sub>	12 <sup>25</sup>	12	NaBr	90.5 <sup>20</sup>	28
KHSO <sub>4</sub>	51.4 <sup>20</sup>	28	KBr	65.2 <sup>20</sup>	28
(NH <sub>4</sub> ) <sub>2</sub> SO <sub>4</sub>	76.9 <sup>25</sup>	27	NH <sub>4</sub> Br	97 <sup>25</sup>	12
MgBr <sub>2</sub>	101.5 <sup>20</sup>	12	PbBr <sub>2</sub>	0.85 <sup>20</sup>	28
CaBr <sub>2</sub>	142 <sup>20</sup>	12			

<sup>a</sup> For example, 0.131<sup>10</sup> means a solubility of 0.131 g/100 g of H<sub>2</sub>O at 10 °C.

Clarke and Washington's (15) average composition of igneous rocks. Using the measured aerosol SiO<sub>2</sub> concentrations and the appropriate metal oxide-to-SiO<sub>2</sub> ratios calculated from Clarke and Washington's analysis, one can calculate the amounts of CaO, Na<sub>2</sub>O, MgO, and K<sub>2</sub>O. The calculated K<sub>2</sub>O concentrations agree within 6% of measured K<sub>2</sub>O concentrations, whereas the calculated and measured CaO, MgO, and Na<sub>2</sub>O concentrations differ by greater than 40%. Thus, it seems that K<sub>2</sub>O originates from soil dust and that the CaO, MgO, and the Na<sub>2</sub>O come from preferentially enriched sources, i.e., sea salt, cement dust, or fly ash. In light of the possibility that Pb, Ca, Na, K, and Mg are in either the glass and metal oxide or electrolytic phases, the metal oxide and glasses mass balance can be written as

$$\sum_i \sum_j [M_iO_j] = (1 - x_{Pb}) \frac{M_{PbO}}{M_{Pb}} [Pb] + (1 - x_{Ca}) \frac{M_{CaO}}{M_{Ca}} [Ca] + (1 - x_{Mg}) \frac{M_{MgO}}{M_{Mg}} [Mg] + (1 - x_K) \frac{M_{K_2O}}{M_K} [K] + (1 - x_{Na}) \frac{M_{Na_2O}}{M_{Na}} [Na] + \frac{M_{Fe_2O_3}}{2M_{Fe}} [Fe] + \frac{M_{Al_2O_3}}{2M_{Al}} [Al] + \frac{M_{SiO_2}}{M_{Si}} [Si] \quad (3)$$

where  $M_A$  is the molecular weight of species A and  $x_{Pb}$ ,  $x_{Ca}$ ,  $x_K$ ,  $x_{Na}$ , and  $x_{Mg}$  are the fractions of Pb, Ca, K, Na, and Mg, respectively, in the ionic-solid or electrolytic form. Determination of  $x_{Pb}$ ,  $x_{Ca}$ ,  $x_K$ ,  $x_{Na}$ , and  $x_{Mg}$  could be based on a chemical-source balance. Even if the source signature is known, determination of the chemical form may be difficult. For example, Pb resulting from automobile exhaust may either be electrolytic or not depending on the fraction of Pb emitted as PbO or Pb vs. halogenated forms. In our analysis

we will examine the two extremes:  $x_{Pb} = x_{Ca} = x_K = x_{Na} = x_{Mg} = 1$ , and  $x_{Pb} = x_{Ca} = x_K = x_{Na} = x_{Mg} = 0$ .

**Electrolytes.** An expression for the electrolyte mass of the atmospheric aerosol, i.e., ionic species dissolved in water, is

$$\sum_i [E_i] = [SO_4] + [Cl] + [NO_3] + [NH_4] + [Br] + x_{Pb}[Pb] + x_{Ca}[Ca] + x_K[K] + x_{Na}[Na] + x_{Mg}[Mg] + [H] + [OH] \quad (4)$$

The [H] or [OH] must be calculated on the basis of electro-neutrality. If the aerosol is acidic, then [OH] may be neglected and

$$[H] = M_H[2[SO_4]/M_{SO_4} + [Cl]/M_{Cl} + [NO_3]/M_{NO_3} - [NH_4]/M_{NH_4} + [Br]/M_{Br} - x_{Na}[Na]/M_{Na} - x_K[K]/M_K - 2x_{Pb}[Pb]/M_{Pb} - 2x_{Ca}[Ca]/M_{Ca} - 2x_{Mg}[Mg]/M_{Mg}] \quad (5)$$

If [H] < 0 from eq 5, then [OH] =  $-M_{OH}[H]/M_H$ . Of course, eq 5 is an expression for the net acidity. Actually, the tropospheric aerosol would likely contain a mixture of acidic and basic particles (16).

**Water.** Ho et al. (17) have shown that the aerosol water content varies diurnally. Since the ACHEX chemical composition measurements were time-averaged, the aerosol water concentrations as measured by the waterometer were time-averaged. Since the average aerosol water concentrations were determined by integrating waterometer measurements, no assumptions were made concerning the amount of water on the filter material; i.e., the aerosol water is not assumed to be equal to the unaccounted mass on the filter as is typically done.

**Carbonaceous Material.** The carbonaceous fraction of the total aerosol mass must typically be estimated since carbo-

naceous aerosol concentration measurements are very limited. Interpretation of existing carbonaceous-material measurements is complicated by the different organic carbon extraction efficiencies of solvents and the mutual extraction of inorganic nitrates by polar solvents (18, 19). Therefore, a calculation procedure must be devised that utilizes existing data to obtain values reflective of the actual carbonaceous-material loading.

Pierson and Russell (20) calculated for Denver a linear relation between the aerosol carbon, [C], and lead, [Pb], concentrations.

$$[C] = (5.84 \pm 0.34)[Pb] - 0.85 \pm 0.97 \mu\text{g m}^{-3} \quad (6)$$

In Figure 2 this correlation is compared to data for aerosol lead and carbon measurements. The Los Angeles and Denver trends are similar except that, as [Pb] → 0, the Los Angeles data approach 10 μgC m<sup>-3</sup>. The combined Los Angeles, San Jose, and Los Alamitos data indicate that eq 6 overpredicts the aerosol-carbon loading at high lead concentrations.

An additional correlation between total carbonaceous material and lead can be derived by utilizing data of Grosjean et al. (23), who reported an average noncarbon-to-carbon ratio of 0.37 in the organic aerosol fraction for 2 days in 1973 at Pasadena, CA. (The noncarbon material is nitrogen, oxygen, and hydrogen associated with carbon in organic molecules.) Thus, the total carbonaceous aerosol mass loading, Σ<sub>i</sub>[CM<sub>i</sub>], can be approximated by multiplying the Pierson and Russell correlation by 1.37

$$\sum [CM_i] = (8.02 \pm 0.47)[Pb] - 1.17 \pm 1.33 \mu\text{g m}^{-3} \quad (7)$$

In Figure 3 this correlation is compared with ACHEX aerosol lead and carbonaceous-material estimates using the data of Appel et al. (6). The CH<sub>3</sub>OH-CHCl<sub>3</sub> extractables were corrected for the solubilization of ammonium nitrate by assuming that all of the nitrate measured was ammonium nitrate and subtracting the value obtained from the CH<sub>3</sub>OH-CHCl<sub>3</sub> extractables. Subsequently, the CH<sub>3</sub>OH-CHCl<sub>3</sub>-extracted carbon value was subtracted from the total CH<sub>3</sub>OH-CHCl<sub>3</sub>-extractable mass. This procedure led to negative mass concentrations in 7 out of 11 cases. To check the extreme case, we subtracted the sum of the nitrate and CH<sub>3</sub>OH-CHCl<sub>3</sub>-extractable carbon loadings from the total CH<sub>3</sub>OH-CHCl<sub>3</sub>-extractable mass. This procedure led to negative values in 3 out of 11 cases. Therefore, either all of the nitrate must not

have solubilized in the CH<sub>3</sub>OH-CHCl<sub>3</sub> solution or some measurement error must have been present. Thus, the points plotted in Figure 3 represent the minimum aerosol carbonaceous material. As can be seen, the Los Angeles data are not well correlated with eq 7.

The correction for aerosol nitrate in the CH<sub>3</sub>OH-CHCl<sub>3</sub>-extractable mass is significant and can be shown by the following approximation:

$$[NO_3] = (M_{NO_3}/M_{NH_4NO_3}) \times [\text{CH}_3\text{OH-CHCl}_3\text{-extractable mass}] \times (1 - [\text{carbon fraction}][\text{carbon} + \text{noncarbon fraction}] / [\text{carbon fraction}])$$

$$[NO_3] = {}^{62}/_{80} [\text{CH}_3\text{OH-CHCl}_3\text{-extractable mass}] \times (1 - 1.37[\text{carbon fraction}]) \quad (8)$$

assuming nitrate is present as ammonium nitrate and that the CH<sub>3</sub>OH-CHCl<sub>3</sub>-extractable mass has the same noncarbon-to-carbon ratio as that measured by Grosjean et al. (23) for the organic aerosol fraction in Pasadena. The total noncarbon-to-carbon ratio of Grosjean is similar to those measured by Cukor et al. (24) and Ciacco et al. (25) in New York City. Based on their data for chloroform, 2-propanol, and methanol extractions, calculated noncarbon-to-carbon ratios varied between 1.36 and 1.49. Therefore, the total organic noncarbon-to-carbon ratio of Grosjean should approximate that in the CH<sub>3</sub>OH-CHCl<sub>3</sub>-extractable mass. In Figure 4 nitrate

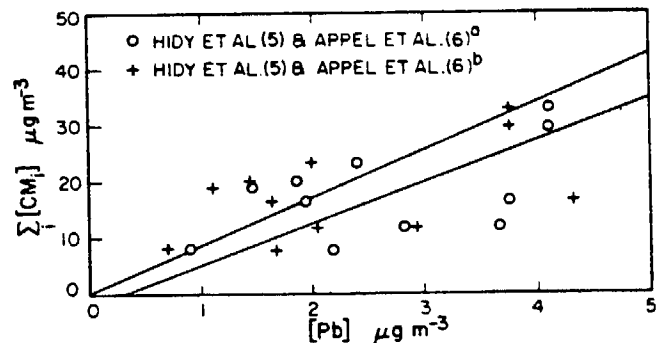


Figure 3. Relation between aerosol carbonaceous material and aerosol lead: (a) Pb from Whatman 41 high-volume filter; (b) time-averaged Pb from 47-mm Gelman GA-1 filters.

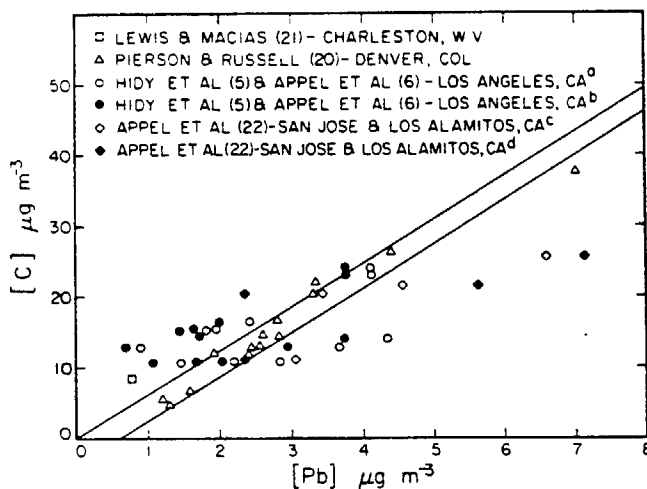


Figure 2. Relation between aerosol carbon and aerosol lead: (a) Pb from Whatman 41 high-volume filter; (b) time-averaged Pb from 47-mm Gelman GA-1 filters; (c) Pb from 47-mm Fluoropore filter; (d) Pb from Spectrograde high-volume filter. Solid lines: minimum and maximum of Pierson and Russell (20) correlation.

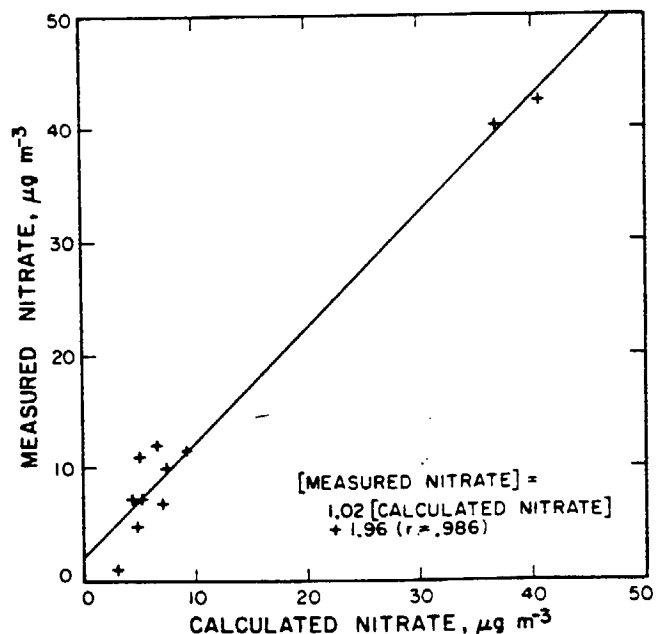


Figure 4. Measured nitrate vs. calculated nitrate. Solid line: linear least-squares fit to data.

values calculated from eq 8 are compared with the measured values of Hidy et al. (5).

Mueller et al. (26) measured aerosol carbonate carbon in Pasadena, CA, and determined it to be consistently less than 5% of the total carbon present. In light of the previously discussed inaccuracies, the carbonate fraction of the aerosol will be assumed to be negligible.

In summary, the total carbonaceous aerosol concentration can be estimated from the sum of the benzene- and  $\text{CH}_3\text{OH}-\text{CHCl}_3$ -extracted mass minus nitrate as ammonium nitrate plus the estimate for the maximum elemental carbon aerosol loading of Appel et al. (6). The carbonaceous aerosol concentration as calculated by the above procedure should generally reflect the atmospheric carbonaceous-material loading and is the best obtainable using the existing data.

#### Aerosol Mass Accounting

Table II presents a summary of the data used for the mass accounting calculation. The calculated and measured total-mass data are summarized in Table VI. In Table VI,  $M_1$  is the total mass calculated by assuming  $x_{\text{Pb}} = 0$ ,  $x_{\text{Ca}} = 0$ ,  $x_{\text{K}} = 0$ ,  $x_{\text{Na}} = 0$ , and  $x_{\text{Mg}} = 0$ , and  $M_2$  is that when  $x_{\text{Pb}} = 1$ ,  $x_{\text{Ca}} = 1$ ,  $x_{\text{K}} = 1$ ,  $x_{\text{Na}} = 1$ , and  $x_{\text{Mg}} = 1$ .  $M_3$  is the calculated total mass assuming that the total mass is the sum of the measured species. Thus, no assumptions are made concerning chemical speciation in the calculation of  $M_3$ .

All three mass calculation procedures ( $M_1$ ,  $M_2$ ,  $M_3$ ) yield similar values but disagree with the total-mass concentrations calculated from the  $\beta$  gauge, total filters, and high-volume filters. To evaluate the trend among these seven variables,  $M_1$ ,  $M_2$ ,  $M_3$ ,  $\bar{\beta}$ ,  $\overline{\text{TF}}$ ,  $\overline{\text{TV}}$ , and HVM, we performed a least-squares analysis between all pairs (see Table VII). ( $\overline{\text{VJ}}$  was omitted from the least-squares analysis since a  $\overline{\text{TV}}$  measurement was not performed.) All measured and calculated total suspended mass techniques correlated significantly. A notable feature

seen in the results in Table VII is that the  $\beta$ -gauge measurements are consistently lower than the other calculated and measured total-mass concentrations. (Possibly the instrument gain was set too low.)

The mass ratio,  $S$ , of electrolytic material to water can be calculated by

$$S = \left( \sum_i [\text{E}_i]/\overline{\text{H}_2\text{O}} \right) \times 100 \text{ g}/100 \text{ g of H}_2\text{O} \quad (9)$$

Calculated values of  $S$  are listed in Table VIII for the two extreme cases of the distribution of Pb, Ca, K, Na, and Mg between the metal oxide-glass subset and the electrolyte subset. The values calculated for  $S$  and  $S'$  are within the typical range of solubilities of electrolyte materials listed in Table V. Since the calculated mass ratios vary between 50 and 125 g/100 g of  $\text{H}_2\text{O}$ , it can be inferred that the electrolyte portion of the atmospheric aerosol at these sampling locations is dominated by soluble sulfates, nitrates, and chlorides. The chemical analysis summary shows the dominance of nitrate and sulfate (Table II). Ochs and Gatz (30) recently measured the fraction of water-soluble material in particles of  $>4.6\text{-}\mu\text{m}$  radius as  $\sim 0.3$ . Using data from Tables II and VI, we compute the soluble fraction in the Los Angeles aerosol to lie between 0.15 and 0.35. Older Los Angeles aerosol data of Cadle (31) list water and volatile organics as 0.15 of the total aerosol mass, with a water-soluble fraction of 0.15.

The ionic strength of the aerosol solution can be calculated by

$$I = (1000/2\overline{\text{H}_2\text{O}}) \left( \sum_i z_i^2 [\text{E}_i]/M_i \right) \quad (10)$$

where  $M_i$  is the molecular weight and  $z_i$  is the charge of species  $i$ . Calculated values of  $I$  are listed in Table VIII for the two extreme cases of the distribution of Pb, Ca, K, Na, and Mg. The range of ionic strengths at each sampling location is compared with the ionic-strength dependence of water activity

Table VI. Calculated and Measured Total Mass ( $\mu\text{g m}^{-3}$ ) (5)

sample	$M_1$	$M_2$	$M_3$	$\bar{\beta}$	$\overline{\text{TF}}$	$\overline{\text{TV}}$	HVM
WK	146.6	144.5	133.8	105.7	113.5	127.7	148
WL	91.2	92.4	82.4	77.7	101.5	107.5	114
VJ	115.6	115.1	96.0	85.8	160.9		211
TC	209.8	207.4	192.0	173.1	210.9	215.4	241
TD	168.3	165.0	153.9	137.8	176.9	176.0	194
TE	93.6	92.5	82.3	87.1	101.0	113.4	123

Table VII. Least-Squares Analysis of Measured and Calculated Total Mass

	$M_1$	$M_2$	$M_3$	$\bar{\beta}$	$\overline{\text{TF}}$	$\overline{\text{TV}}$	least squares parameters <sup>a</sup>
HVM	0.974	0.975	0.972	0.999	0.986	0.997	$r$
	0.929	0.905	0.867	0.738	0.933	0.870	$m$
	-10.4	-8.1	-13.3	-4.8	-12.3	5.4	$b$
$\bar{\beta}$	0.976	0.977	0.974	1.00	0.981	0.995	$r$
	1.26	1.23	1.18	1.00	1.26	1.18	$m$
	-4.6	-2.4	-7.9	0.0	-5.5	-11.4	$b$
$\overline{\text{TF}}$	0.935	0.936	0.933	0.981	1.00	0.995	$r$
	0.941	0.918	0.879	0.766	1.00	0.918	$m$
	9.4	11.1	5.1	8.5	0.0	18.9	$b$
$\overline{\text{TV}}$	0.955	0.956	0.952	0.995	0.995	1.00	$r$
	1.04	1.02	0.974	0.842	1.08	1.00	$m$
	-12.5	-10.2	-15.2	-8.3	-19.0	0.0	$b$

<sup>a</sup>  $r$  = correlation coefficient;  $m$  = slope;  $b$  = intercept.

### Calculated Electrolyte-to-Water Mass Ratios and Ionic Strengths for Los Angeles Aerosol \*

s	s'	l	l'
3.4	91.3	18.6	22.2
3.7	121.3	14.2	25.9
3.5	83.8	8.0	16.5
3.2	80.1	13.4	15.4
1.7	64.4	10.0	11.5
1.3	92.3	11.6	18.3

Mass ratio when  $x_{\text{H}_2\text{O}} = 0$ ,  $x_{\text{Ca}} = 0$ ,  $x_{\text{Na}} = 0$ ,  $x_{\text{K}} = 0$ , and  $x_{\text{Mg}} = 0$ .  
 s' = calculated mass ratio when  $x_{\text{H}_2\text{O}} = 1$ ,  $x_{\text{Ca}} = 1$ ,  $x_{\text{Na}} = 1$ ,  $x_{\text{K}} = 1$ ,  $x_{\text{Mg}} = 1$ , g/100 g of H<sub>2</sub>O. l = ionic strength when  $x_{\text{H}_2\text{O}} = 0$ ,  $x_{\text{Ca}} = 0$ ,  $x_{\text{Na}} = 0$ ,  $x_{\text{K}} = 0$ , and  $x_{\text{Mg}} = 0$ , mol/1000 g of H<sub>2</sub>O. l' = ionic strength when  $x_{\text{H}_2\text{O}} = 1$ ,  $x_{\text{Ca}} = 1$ , and  $x_{\text{Mg}} = 1$ , mol/1000 g of H<sub>2</sub>O.

Electrolytes at 25 °C in Figure 5. All of the calculations are in the region where the relative humidity variation is strongest, indicating the prevailing relative humidity and the aerosol water content are determining the atmospheric aerosol water

pH was calculated for both extreme discharges of Ca, K, Na, and Mg (see Table II). Samples VJ and TE were the only ones that were definitely acidic. Samples VJ and TE could be basic or acidic. All other samples (4) measured net basic aerosol pHs in Los Angeles and those reported in ACHEX (5) using quite different experimental techniques and different cutoff diameters. Since the coarse mode is basic and the fine mode acidic, a lower cutoff diameter would give a lower net pH. Combining the coarse and fine mode data would give a lower net pH.

Combining the coarse and fine mode data would give a lower net pH. Combining the coarse and fine mode data would give a lower net pH. Combining the coarse and fine mode data would give a lower net pH.

Combining the coarse and fine mode data would give a lower net pH. Combining the coarse and fine mode data would give a lower net pH.

### Measurement Techniques

Several experimental questions need to be considered when comparing the total suspended mass measurements using glass-fiber filters, cellulose filters, and the  $\beta$  gauge: (1) Does the  $\beta$  gauge respond to suspended particles and not exhibit interference? (2) Do filtration-efficiency significant influence on total-mass measurements? (3) What effect does equilibrating the filters at 25 °C have on the water adsorbed on the filter material and the water contained in the filter? (4) How important is filter artifact in prejudicing sulfate measurements?

Landis reported a large positive interference in  $\beta$ -gauge measurements at high relative humidity (>75%). Data from Yamamoto (38) do not show this interference. Thermodynamically predicted absorption coefficients for NaCl and (NH<sub>4</sub>)<sub>2</sub>SO<sub>4</sub> aerosols as a function of relative humidity is increased above the deliquescence point. ACHEX data using the  $\beta$  gauge do not agree with the saturation during times of high relative humidity as predicted by Landis' measurements.

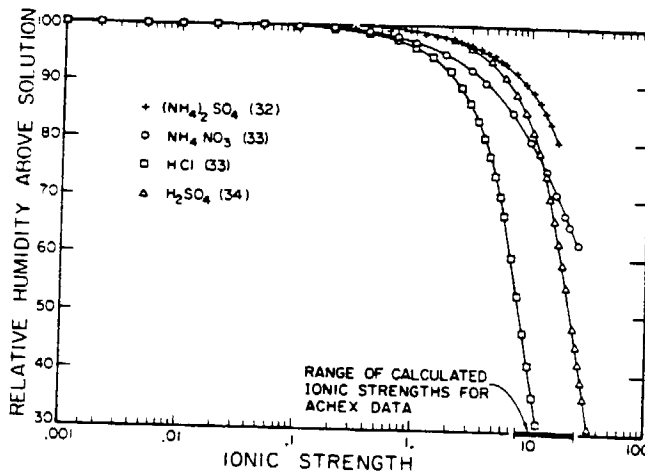


Figure 5. Water activities for typical electrolytes as a function of ionic strength ( $T = 25$  °C).

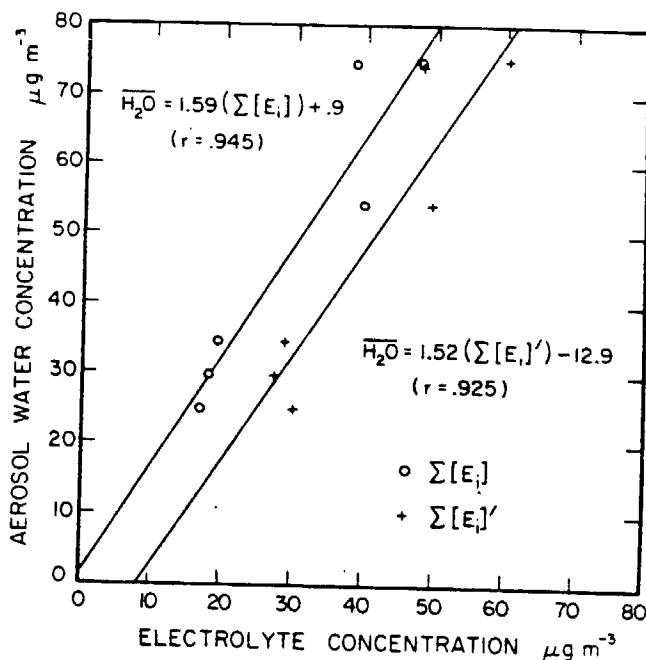


Figure 6. Aerosol water vs. electrolyte concentration. Solid lines: linear least-squares fits to data.

Landis' Figure 3 shows that  $\beta$ -gauge measurements are consistently lower than or equal to the total filter measurements. If the instrument responded to high relative humidity and had a response greater than the manufacturer's calibration for atmospheric aerosol, the filter-sample data should be less than the  $\beta$ -gauge measurements. Since the measured effect is the opposite of the calibration results, some inconsistency exists. Therefore, the  $\beta$ -gauge measurements were not considered in error and have been compared here to other mass measurement techniques.

Shown in Figure 7 is the initial filtration efficiencies of different filter materials vs. face velocity. The most recent data of John et al. (39) show that the efficiencies of Gelman GA-1 and Gelman A should be greater than 99% over the operating range of interest for a polydisperse room aerosol. Even though the data indicate higher efficiencies than those found by Appel et al. (40), the maximum discrepancy would account for an error of only 5%. The data for Whatman 41 filters do not agree as well with the other data in Figure 7. These differences can result from filter maturation, material construction variation, and different particle concentration measurement techniques. Since the filtration efficiency curves for Whatman

water. If the water is unaccountable, only the loosely adsorbed water removed by the saturated solution method is existing data.

The fate of the water removed was not predicted to be somewhat an artifact of the calculation. (22). The maximum sulfate and nitrate would be 3(g) concentration) measured sulfate concentration is only above 2  $\mu\text{g m}^{-3}$ ,  $\mu\text{g m}^{-3}$  (see Table II). It could be more accurate if the data were corrected to be quantitatively (46) indicates that this is not correct, making correc-

several important consequences of electrolytic

to accurately measure mass balance obtained from measurements of Ca, K, Ca, Fe, Mg, Al, Si, carbonaceous material, and glasses was assigned. The effect of oxide forms to the total mass is important, since metal ions "free" water would

be limited, the aerosol mass can be estimated. The data examined and does not agree with aerosol data (Figure 2). The aerosol carbon concentration, oxygen, nitrogen, and sulfur is important. As indicated by Gordon and Bryan (3), Cl<sub>2</sub>-extractable mass is a correction to this would improve future

distributed between the aerosol mass, the aerosol relative humidity, and the temperature during sampling. The mass is distributed between the aerosol and the gas phase, i.e., NH<sub>3</sub>, g continuous data, one must be careful between the gas and aerosol phases due to volatilization, and the temperature. Since mass is redistributed during sampling, care must be taken in the total suspended particulate that the filters are used. Ideally, filter weight and relative humidity and temperature should be recorded at several relative hu-

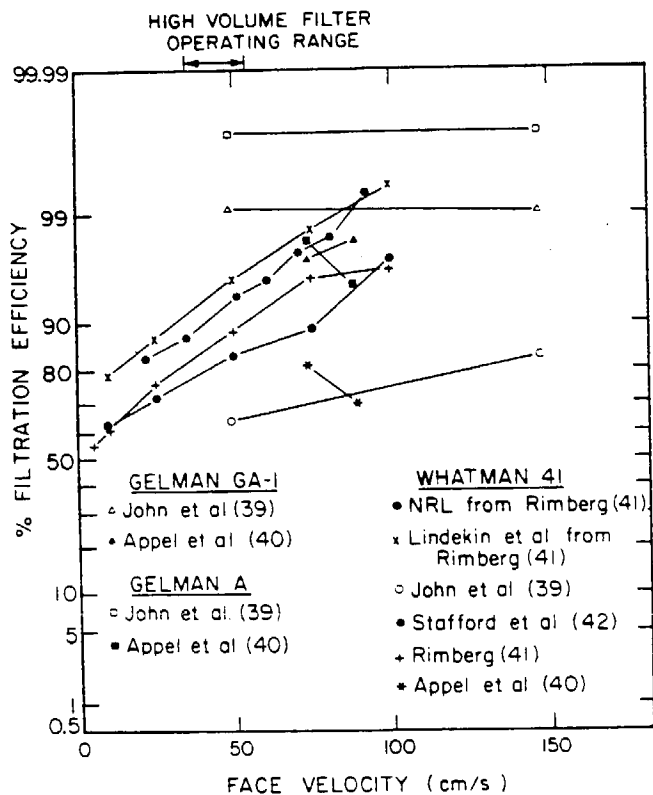


Figure 7. Filtration efficiencies for Whatman 41, Gelman A, and Gelman GA-1.

41 are lower than the curves for Gelman GA-1 and Gelman A, the effect of filtration loss must be evaluated. Lindeken et al. (43) and Stafford et al. (42) measured the increase in filter efficiency for Whatman 41 as a function of time. Using their data and making very conservative estimates, one can estimate the maximum error due to the initial filter inefficiencies as 1% for all samples. When one considers that the average standard deviation error of the three filter total suspended mass measurement techniques is 8%, initial filtration inefficiency differences cannot be the major source of error.

Shown in Figure 1 are the time-averaged normalized aerosol volume distributions for four sampling periods. Also, shown in Figure 1 are the sampler cutoffs for sampling in stagnant air (1). The value for the high-volume sampler is a more recent one than that reported in ACHEX (i.e., 60  $\mu\text{m}$ ). Wedding et al. (2) measured the sampling effectiveness of a high-volume sampler perpendicular to a 10.2 mi/h wind. Figure 1 shows that the presence of wind can significantly affect the fraction of the coarse mode sampled. Since the wind effect on the sampling efficiency of the total filter setup or the  $\beta$  gauge has not been measured, it is assumed that wind affects all samplers similarly. Thus, the ambient aerosol should not be significantly preferentially measured by any sampler.

The filters used in ACHEX were equilibrated to 55% relative humidity and 25  $^{\circ}\text{C}$  as prescribed by NASN procedures. Tierney et al. (44) and Demuyck (45) showed that glass-fiber filters lose their adsorbed or absorbed water when equilibrated to NASN conditions. Demuyck demonstrated that Whatman 41 cellulose filters irreversibly absorb water. When Demuyck's data and the ratio of filter surface areas are used, this interference would amount to 107  $\mu\text{g m}^{-3}$  for a 24-h high-volume filter. In Table VI,  $\overline{\text{HVM}}$  is consistently higher than  $\overline{\text{TV}}$ , verifying the irreversible absorption of water by Whatman 41. The cellulose triacetate filters did not irreversibly absorb water, as seen by comparing  $\overline{\text{TF}}$  and  $\overline{\text{TV}}$  values in Table VI. Whether the filter drying process removed water from the aerosol is very important. Table II and VI show that

the aerosol contains between 20 and 45% water. If the water is removed, then 20–45% of the aerosol mass is unaccountable. This fraction is unreasonably high; therefore, only the loosely held absorbed water on the filter surface is removed by the initial drying. Whether the aerosol is a supersaturated solution or more dilute cannot be determined from existing data.

Corrections for artifact nitrate and sulfate were not performed since assigning a correction would be somewhat arbitrary with current knowledge. Maximum artifact values can be calculated from the results of Appel et al. (22). The maximum artifact sulfate would be  $\sim 2 \mu\text{g m}^{-3}$  and nitrate would be  $\sim 26 \mu\text{g m}^{-3}$  (10 ppb 24-h average  $\text{HNO}_3(\text{g})$  concentration) for Whatman 41 high-volume filters. The measured sulfate values used in this study were consistently above  $2 \mu\text{g m}^{-3}$ , whereas the nitrate values were below  $26 \mu\text{g m}^{-3}$  (see Table II). Thus, the sulfate data are presumed to be more accurate than the nitrate data, but no measured values were corrected since assignment of corrections could not be quantitatively performed. Recent work by Appel et al. (46) indicates that positive and negative nitrate artifacts exist, making corrections even more difficult to assign.

### Conclusions

The foregoing analysis demonstrates several important points concerning mass accounting, the presence of electrolytic solutions, and aerosol pH.

**Mass Accounting.** A reasonably accurate mass balance for the Los Angeles aerosol has been obtained from measurements of  $\text{SO}_4$ , Cl, Br,  $\text{NO}_3$ ,  $\text{NH}_4$ , Na, K, Ca, Fe, Mg, Al, Si, Pb, carbonaceous material, and aerosol water, the predominate species being  $\text{SO}_4$ ,  $\text{NO}_3$ ,  $\text{NH}_4$ , Si, carbonaceous material, and aerosol water. Chemical speciation was assigned, and the presence of oxygen in metal oxides and glasses was accounted for. The addition of metal oxide and glass oxygen to the mass balance did not have a significant effect on the total-mass correlations. The assignment of oxide forms to certain elements is, however, physically important, since metal oxides tend to be water insoluble. Thus, no "free" water would be associated with these oxides.

Since aerosol carbon measurements are limited, the aerosol carbon concentration typically must be estimated. The Pierson and Russell (20) correlation was examined and does not seem to apply to the Los Angeles aerosol data (Figure 2). In addition to quantification of the aerosol carbon concentration, determination of the associated oxygen, nitrogen, and hydrogen in the carbonaceous material is important. As indicated by Appel et al. (6), Grosjean (18), Gordon and Bryan (19), and this work, the  $\text{CH}_3\text{OH}-\text{CHCl}_3$ -extractable mass contains considerable nitrate. Thus, a correction to this measurement for dissolved inorganics would improve future mass accounting calculations.

Since certain chemical species are distributed between the gas and aerosol phases, the total aerosol mass, the aerosol water concentration, the relative humidity, and the temperature should be continuously monitored during sampling. Ideally, other volatile species that are distributed between the gas and aerosol phases should also be monitored, i.e.,  $\text{NH}_3$ ,  $\text{HNO}_3$ , HCl, and organics. By analyzing continuous data, one can determine the distribution of material between the gas and aerosol phases and the possibility of aerosol alteration between sampling and measurement due to volatilization, uptake of water, or displacement reactions. Since mass is reversibly distributed between the gas and aerosol phases, care must be taken when determining the total suspended particulate mass from filter samples such that the filters are equilibrated with a known relative humidity and temperature at the time of weight measurement. Ideally, filter weight measurements should be performed at several relative humidities.

**Presence of Electrolyte Solutions.** The calculated electrolyte-to-aerosol water mass ratios are typical of atmospherically significant electrolyte solutions near saturation (Tables V and VIII). By assigning valences to the electrolyte species, we have calculated the ionic strength. From the ionic strengths calculated and compared with typical ionic-strength dependence of water activities in binary electrolyte solutions, the electrolyte material appears to be present in highly concentrated solutions and/or ionic solids. The amount of water in the aerosol phase is very dependent on the chemical nature of the electrolytes and the prevailing relative humidity (Figure 5). Since the aerosol water and electrolyte concentrations are interdependent, a correlation between electrolyte mass and aerosol water was evaluated. The significant correlation between electrolyte mass and aerosol water highlights an important point, namely, that electrolyte material can cause greater visibility reduction per unit mass than organics or metal oxides because of hygroscopicity.

**Aerosol pH.** The fraction of electrolyte material for Ca, Pb, K, Na, and Mg must be determined to perform an accurate chemical mass and acidity balance. Biggins et al. (11) and Reiter et al. (13) recognized the importance of differentiating between water-soluble and -insoluble Pb and Ca. Depending on the assumptions of chemical speciation for Ca, Pb, K, Na, and Mg, metal oxide vs. electrolyte, the net aerosol pH may be basic or acidic (Table II). Knowing the net aerosol pH would improve the aerosol mass balance because an additional variable would exist to check chemical speciation assumptions or measurements. Recent aerosol data include aerosol pH measurements but do not have detailed chemical analyses and aerosol water measurements to perform a mass balance (3, 47). An additional factor important to determining the net aerosol pH is the upper cutoff of the aerosol sampler. This point is graphically illustrated by Figure 1.

#### Acknowledgment

We extend appreciation to Bruce Appel for his helpful comments.

#### Literature Cited

- (1) National Research Council, Subcommittee on Airborne Particles "Airborne Particles"; University Park Press: Baltimore, MD, 1979; Chapter 1.
- (2) Wedding, J. B.; McFarland, A. R.; Cermack, J. E. *Environ. Sci. Technol.* 1977, 11, 387.
- (3) Tanner, R. L.; Cederwall, R.; Garber, R.; Leahy, D.; Marlow, W.; Meyers, R.; Phillips, M.; Newman, L. *Atmos. Environ.* 1977, 11, 955.
- (4) Liljestrand, H. M. Ph.D. Thesis, California Institute of Technology, Pasadena, CA, 1980.
- (5) Hidy, G. M., et al. "Characterization of Aerosols in California", Rockwell International Report, California Air Resources Board, ARB Contract No. 358, 1975.
- (6) Appel, B. R.; Colodny, P.; Wesolowski, J. J. *Environ. Sci. Technol.* 1976, 10, 359.
- (7) Stelson, A. W.; Friedlander, S. K.; Seinfeld, J. H. *Atmos. Environ.* 1979, 13, 369.
- (8) Macias, E. S.; Blumenthal, D. L.; Anderson, J. S.; Cantrell, B. K. "Size and Composition of Visibility-Reducing Aerosols in Southwestern Plumes", presented at the Conference on Aerosols: Anthropogenic and Natural-Sources and Transport, New York Academy of Sciences, New York, Jan 9-12, 1979.
- (9) Bryers, R. W. "Influence of the Distribution of Mineral Matter in Coal on Fireside Ash Deposition", ASME Paper No. 78-WA/CD-4, 1978.
- (10) Henry, W. M.; Knapp, K. T. *Environ. Sci. Technol.* 1980, 14, 450.
- (11) Biggins, P. D. E.; Harrison, R. M. *Environ. Sci. Technol.* 1980, 14, 336.
- (12) Weast, R. C., Ed. "Handbook of Chemistry and Physics", 54th ed.; CRC Press: Cleveland, OH, 1973.
- (13) Reiter, R.; Sladkovic, R.; Pözl, K. *Atmos. Environ.* 1976, 10, 841.
- (14) Pettijohn, F. J. "Sedimentary Rocks"; Harper and Brothers: New York, 1957; Chapter 11.
- (15) Mason, B. "Principles of Geochemistry"; Wiley: New York, 1966; Chapter 3.
- (16) Brosset, C. *Atmos. Environ.* 1978, 12, 25.
- (17) Ho, W.; Hidy, G. M.; Govan, R. M. *J. Appl. Meteorol.* 1974, 13, 871.
- (18) Grosjean, D. *Anal. Chem.* 1975, 47, 797.
- (19) Gordon, R. J.; Bryan, R. J. *Environ. Sci. Technol.* 1973, 7, 645.
- (20) Pierson, W. R.; Russell, P. A. *Atmos. Environ.* 1979, 13, 1623.
- (21) Lewis, C. W.; Macias, E. S. *Atmos. Environ.* 1980, 14, 185.
- (22) Appel, B. R.; Tokiwa, Y.; Wall, S. M.; Hoffer, E. M.; Haik, M.; Wesolowski, J. J. "Effect of Environmental Variables and Sampling Media on the Collection of Atmospheric Sulfate and Nitrate"; Final Report, California Air Resources Board, ARB Contract No. 5-1032, 1978.
- (23) Grosjean, D.; Friedlander, S. K. *J. Air Pollut. Control Assoc.* 1975, 25, 1038.
- (24) Cukor, P.; Ciaccio, L. L.; Lanning, E. W.; Rubino, R. L. *Environ. Sci. Technol.* 1972, 6, 633.
- (25) Ciaccio, L. L.; Rubino, R. L.; Flores, J. *Environ. Sci. Technol.* 1974, 8, 935.
- (26) Mueller, P. K.; Mosley, R. W.; Pierce, L. B. In "Aerosols and Atmospheric Chemistry"; Hidy, G. M., Ed.; Academic Press: New York, 1972.
- (27) West, C. J., Ed. "International Critical Tables of Numerical Data, Physics, Chemistry and Technology"; McGraw-Hill: New York, 1933; Vol. IV.
- (28) Lange, N. A., Ed. "Handbook of Chemistry", 5th ed.; Handbook Publishers: Sandusky, OH, 1944.
- (29) Tang, I. N.; Munkelwitz, H. R. *J. Aerosol Sci.* 1977, 8, 321.
- (30) Ochs, H. T., III; Gatz, D. F. *Atmos. Environ.* 1980, 14, 615.
- (31) Cadle, R. D. "Particles in the Atmosphere and Space"; Reinhold: New York, 1966; Chapter 2.
- (32) Wishaw, B. F.; Stokes, R. H. *Trans. Faraday Soc.* 1954, 50, 952.
- (33) Hamer, W. J.; Wu, Y. C. *J. Phys. Chem. Ref. Data* 1972, 1, 1047.
- (34) Robinson, R. A.; Stokes, R. H. "Electrolyte Solutions; The Measurement and Interpretation of Conductance, Chemical Potential and Diffusion in Solutions of Simple Electrolytes", 2nd ed. (revised); Butterworths: London, 1959.
- (35) Brosset, C. "Possible Changes in Aerosol Composition Due to Departure from Equilibrium Conditions during Sampling"; Swedish Water and Air Pollution Research Laboratory; Goteborg, 1978; PB-298 947.
- (36) Landis, D. A. *Atmos. Environ.* 1975, 9, 1079.
- (37) Husar, R. B. *Atmos. Environ.* 1974, 8, 183.
- (38) Macias, E. S.; Husar, R. B. In "Fine Particles. Aerosol Generation, Measurement, Sampling, and Analysis"; Liu, B. Y. H., Ed.; Academic Press: New York, 1976.
- (39) John, W.; Reischl, G. *Atmos. Environ.* 1978, 12, 2015.
- (40) Appel, B. R.; Wesolowski, J. J. In "The Character and Origins of Smog Aerosols; A Digest of Results from the California Aerosol Characterization Experiment (ACHEX)"; Hidy, G. M., Mueller, P. K., Grosjean, D., Appel, B. R., Wesolowski, J. J., Eds.; Wiley: New York, 1980.
- (41) Rimberg, D. *Am. Ind. Hyg. Assoc. J.* 1969, 30, 394.
- (42) Stafford, R. G.; Ettinger, H. J. *Am. Ind. Hyg. Assoc. J.* 1971, 32, 319.
- (43) Lindeken, C. L.; Morgin, R. L.; Petrock, K. F. *Health Phys.* 1963, 9, 305.
- (44) Tierney, G. P.; Conner, W. D. *Am. Ind. Hyg. Assoc. J.* 1967, 28, 363.
- (45) Demuyneck, M. *Atmos. Environ.* 1975, 9, 523.
- (46) Appel, B. R.; Tokiwa, Y.; Haik, M. *Atmos. Environ.*, 1981, 15, 283.
- (47) Stevens, R. K.; Dzubay, T. G.; Russwurm, G.; Rickel, D. *Atmos. Environ.* 1978, 12, 55.

Received for review May 16, 1980. Accepted February 17, 1981. This work was supported by U.S. Environmental Protection Agency grant R806844 and by State of California Air Resources Board contract A7-169-30.